جامعة أبو بكر بلقايد
UNIVERSITÉ DE TLEMCEN

Pan African University
Institute of Water and Energy Sciences

Institute of Water and Energy Sciences (Including Climate Change)

ASSESSMENT OF CLIMATE CHANGE IMPACT ON HYDROLOGY OF LOWER AWASH SUB BASIN, ETHIOPIA

Endalkachew Yeshewas Muche

Date: 05/09/2017

*Master in **Water, Engineering track***

President: Prof. Masinde Wanyama

Supervisor: Dr. Tirusew Asefa, P.E., D.WRE

External Examiner: Prof. Thameur Chaibi

Internal Examiner: Prof. Mohammed Habi

Academic Year: 2016-2017

CERTIFICATION OF APPROVAL

As thesis research supervisor, I hereby certify that I have read and evaluated this thesis prepared, under my guidance, by Endalkachew Yeshewas MUCHE, entitled: **ASSESSMENT OF CLIMATE CHANGE IMPACT ON HYDROLOGY OF LOWER AWASH SUB BASIN, ETHIOPIA** and I recommend for acceptance by the Pan African University in partial fulfilment for the requirements of the Master of Science in Water Engineering.

August 1st, 2017

Prof. Dr. Tirusew Asefa

(Supervisor)

DECLARATION

I Endalkachew Yeshewas MUCHE, hereby declare that this thesis represents my personal work, realized to the best of my knowledge. I also declare that all information, material and results from other works presented here, have been fully cited and referenced in accordance with the academic rules and ethics.

Date: 05/09/2017

Endalkachew Yeshewas Muche

Abstract

This thesis research focusing on assessing the impact of climate change on hydrology over Lower Awash Sub Basin using downscaled climate projection from GCM product outputs of HadCM3. The Statistical Down Scaling Model (SDSM) was used to downscale the GCM data from A2 and B2 emissions scenarios for future climate predictions. The output generated from the statistical downscale model (precipitation and temperature) were used to derive a hydrological model (Soil and Water Assessment Tool, SWAT). SWAT was calibrated and was used to assess the hydrological response over Lower Awash Sub Basin due to climate change.

SWAT hydrological model simulation was run for the baseline and three future scenarios (2020s, 2050s, and 2080s) to understand climate change impact on hydrological climate variable by keeping constant calibrated non-climate variables of soil and land use and some climate variables such as windspeed, sunshine hour and relative humidity. The average water balance components of A2 and B2 scenario for three-time slices of 2020s, 2050s and 2080s were compared with the baseline hydrological variables.

The performance of SWAT model in simulating the stream flow was shown to be good with a coefficient of determination (R^2) 0.92 and 0.77 and the Nash and Sutcliffe efficiency (NSE) of 0.88 and 0.75 for calibration and validation periods, respectively.

A simulation study of climate change impact on the basin demonstrates that the hydrology of the basin is very sensitive to climate change with decreased surface runoff 6.85, 7.86 and 7.73% by 2020s, 2050s and 2080s respectively for A2 scenario and about 6.66, 8.25 and 5.29% for 2020s, 2050s and 2080s respectively for B2 scenario. Temperature, rainfall and lateral flow are likely to be increased towards end of century over the study area. Increasing temperature decreased the surface runoff, water yield and increased evapotranspiration for future scenarios. The basin is less sensitive to precipitation as compared to temperature changes. Generally, the projected minimum and maximum temperatures in two scenarios is within the range projected by IPCC which reported average temperature will increase in future.

Keywords: Climate Change; Hydrology; Lower Awash Basin; SDSM; SWAT; HadCM3

Résumé

Cette recherche de thèse axée sur l'évaluation de l'impact du changement climatique sur l'hydrologie sur le sous bassin inférieur de l'Awash en utilisant des projections climatiques réduites à partir des résultats de produits GCM de HadCM3. Le modèle de réduction de l'échelle statistique (SDSM) a été utilisé pour réduire les données GCM des scénarios d'émissions A2 et B2 pour les futures prévisions climatiques. La production générée à partir du modèle de réduction de l'échelle statistique (précipitation et température) a été utilisée pour dériver un modèle hydrologique (Outil d'évaluation du sol et de l'eau, SWAT). Le SWAT a été calibré et utilisé pour évaluer la réponse hydrologique sur le sous bassin inférieur de l'Awash en raison du changement climatique.

La simulation du modèle hydrologique SWAT a été organisée pour la ligne de base et trois futurs scénarios (2020, 2050 et 2080) pour comprendre l'impact du changement climatique sur la variable climatique hydrologique en maintenant constantes des variables non climatiques calibrées du sol et de l'utilisation des terres et certaines variables climatiques telles que la vitesse du vent, l'heure du soleil et l'humidité relative. Les composantes moyennes de l'équilibre hydraulique du scénario A2 et B2 pour les tranches triennales des années 2020, 2050 et 2080 ont été comparées aux variables hydrologiques de base.

La performance du modèle SWAT dans la simulation du flux d'eau s'est démontrée bonne avec un coefficient de détermination (R^2) 0,92 et 0,77 et l'efficacité de Nash et Sutcliffe (NSE) de 0,88 et 0,75 pour les périodes d'étalonnage et de validation, respectivement.

Une étude de simulation de l'impact des changements climatiques sur le bassin démontre que l'hydrologie du bassin est très sensible au changement climatique avec une diminution du ruissellement superficiel 6,85, 7,86 et 7,73% pour 2020, 2050 et 2080 respectivement pour le scénario A2 et environ 6,66, 8,25 et 5,29 % pour 2020, 2050 et 2080 respectivement pour le scénario B2. La température, les précipitations et les débits latéraux sont susceptibles d'augmenter jusqu'à la fin du siècle sur la zone d'étude. L'augmentation de la température a diminué le ruissellement de la surface, le rendement de l'eau et une évapotranspiration accrue pour les scénarios futurs. Le bassin est moins sensible aux précipitations par rapport aux changements de température. Généralement, les températures minimales et maximales projetées

dans deux scénarios sont dans la fourchette projetée par le IPCC, ce qui indique que la température moyenne augmentera à l'avenir.

Mots-clés : Changement climatique ; Hydrologie ; Bassin inférieur de l’Awash ; SDSM ; SWAT ; HadCM3

Acknowledgment

Above all I thank the almighty of GOD for his mercy and grace upon me during all my works and in all my life.

I would like to express my profound gratitude to my supervisor Dr. Tirusew Asefa for his valuable advice, guidance and for his friendly approach throughout the work of this thesis.

I would like to extend to thank Dr. Elisabeth van den Akker, for offering me an internship and for her kindness and her valuable support throughout the program.

I would like to thank PAUWES for offering me a postgraduate scholarship to do my masters studies. I also pay my sincere thanks to all PAUWES technical staff and administrative staff for their support, tolerance and encouragement.

Finally, a particular thank to my family and my friends, who supported me to conduct this thesis work.

Table of Contents

List of Tables

List of Figures

List of Abbreviations

AOGCM	Atmospheric-Ocean General Circulation Model
ARS	Agricultural Research Service
CN	Curve Number
CN-AMC	Curve Number-Antecedent Soil Moisture Condition
DD	Dynamical Downscaling
DEM	Digital Elevation Model
ENMSA	Ethiopian National Metrological Service Agency
ET	Evapotranspiration
GCM	Global Climate Models
GHG	Green House Gases
GIS	Geographic Information System
HadCM3	Hadley Center Climate Model Version 3
HRU	Hydrologic Response Units
IPCC	Inter-Governmental Panel on Climate Change
ITCZ	Inter Tropical Convergence Zone
MoWR	Ministry of Water Resources, Ethiopia
NCEP	National Center for Environmental Prediction
RCM	Regional Climate Model
RCP	Representative Concentration Pathways
SCS	Soil Conservation Service
SD	Statistical Downscaling
SDSM	Statistical Down Scaling Model
SRES	Special Report on Emissions Scenarios
SUFI2	Sequential Uncertainty Fitting
SWAT	Soil and Water Assessment Tool
SWAT-CUP	Soil and Water Assessment Tool-Calibration and Uncertainty Program
UNEP	United Nations Environment Program
USDA	United States Department of Agriculture
WMO	World Metrological Organization

Chapter 1. INTRODUCTION

1.1. Background

IPCC (2007), defines climate change as significant change of climate which directly or indirectly disturb the natural ecosystems, and the human economies and cultures and which is in addition to natural climate variability recorded over a long period of time. climate is often described by the statistical interpretation of precipitation and temperature data observed over a comparable period of time for a given region or location (NAPA, 2007).

Climate pattern such as temperature, precipitation, humidity, wind and seasons play a fundamental role in shaping the natural ecosystems, and the human economies and cultures that depend on them. Changes in climate and their impacts are now visible in various places around the globe and are expected to become more evident in the coming decades (Kevin, 2012). Climate experts and researchers agree that climate change is expected to have adverse ecological, socio-economic development impacts of all nations (Matthews, 2012). However, the degree of the impact varies across the nation.

According to IPCC fifth assessment report, on the key messages for Africa stated that Africa's climate is already changing and the impacts are already being left. Further climate change is inevitable in the coming decades in the continent. Correspondingly the report stated that Ethiopia is one of the many developing countries which will be vulnerable to climate change (IPCC, 2007).

The country national association report (2007) indicated that very high dependence on rein fed agriculture, low water resources development, high population growth rate, low economic development level, weak institutions, and lack of awareness make the country vulnerable to climate variability and change (NAPA, 2007). Hence, assessing vulnerability to climate change and preparing adaptation strategies to mitigate the dire consequences of extreme hydrological events is crucial for the country.

1.2. Problem Statement

IPCC (2014) report revealed that, there will likely be more heavy rainfall over the region with high certainty and more extremely wet days by the mid-21st century. There will also likely be an increase in the frequency of hot days in the future. Correspondingly, the maximum and minimum temperatures over East Africa will rise and that there will be more warmer days compared to the baseline by the middle and end of this century. An increase in average temperature event may cause extreme climatological event (Matthews, 2012). This is expected to have a potential impact on sea-level rise and change in precipitation pattern. Any changes in precipitation pattern will have an impact on river flow (Berhane, 2011).

The Change on temperature and precipitation pattern can cause significant impacts on water resources by resulting in changes in the hydrological cycle. The hydrological cycle change can have a direct consequence on the quantity of evapotranspiration, quantity and quality of the runoff components (Alemu, 2011). Although, the spatial and temporal water resource availability can be significantly affected by hydrological cycle changes, which clearly amplifies its impact on agriculture, industry and urban development sectors are not exceptions.

The Awash basin is one of the most important river basins in Ethiopia, and intensively utilized river basin due to its strategic location, access roads, available good land and water resources. According to the country water resources report the basin has an estimated irrigation potential of 206,000 ha (Belete Berhanu, 2013). However, this potential area faces an environmental degradation threat. The environmental degradation has been revealed in deforestation, high erosion, water logging and flood storms. This environmental degradation has caused persistent food insecurity and absolute poverty in the basin (Balcha, 2001).

The River Awash rises in Oromia Region and terminates in Lower Awash Sub Basin at Lake Abe on the border with Djibouti. Lower Awash Sub-Basin is labeled by the name of the main river of the sub-basin, Awash River. The Lower Awash Sub Basin is found in Afar region and has been chosen as a study area for this project. Afar is a lowland region of eastern Ethiopia. It is a home of 1.5 million people, most of the Afar population depends on livestock farming (Akker, 2015). The Afar pastoralist region have been characterized by frequent drought, flash flood, low rainfall, sparse arable land and limited access to water (SDR-ASAL, 2014). Drought has been, and still is a prominent factor in Afar pastoralist. Failed rains and poor rainfall affect pastoralist

through shortfall of fodder and water. Drought has been recurring in these areas since the early 1970s (Fasil et al, 2001).

The Lower Awash Sub Basin (Afar region) suffer from frequent drought and floods, phenomena which require a thorough initial understanding of meteorological characteristics for subsequent water use and management. Some high intensity rainfall could produce local floods, but most heavy runoffs come from upland humid regions of Awash basin causing lowland inundation and sedimentation in the Lower Awash Sub basin. Although, the Lower Awash Sub Basin is now under infrastructure development, but its conditions under future climate change has not been investigated at the local scale. Projecting the hydrologic response of the sub basin using climate change inputs and hydrological model is an important first step towards sound planning and management of the Awash Basin. This study demonstrated the hydrologic response of the Lower Awash Sub Basin respond to climate change and variability how they are affected today and how they might respond in the future if the climate condition changes.

1.3. Research Objective

The objective of this research is to assess the impacts of climate change on hydrological climate variables over Lower Awash Sub Basin using downscaled climate projection from GCM products outputs of HadCM3 in the future 2100 year.

The specific objectives of the study are as follows: -

- To generate fine resolution climate change scenarios using statistical downscaling model at sub basin level;
- To project the variability in temperature and precipitation for selected climate change scenarios for a period of (2020s, 2050s and 2080s) at local climate station;
- To study possible effect of climate change on the hydrology of Lower Awash Sub Basin based on the downscale climate scenario data using SWAT hydrological model.

1.4. Scope of the Research

The study focuses on the impact of climate change on hydrology over Lower Awash Sub Basin using downscaled climate projection products. The IPCC scenarios A2 (medium-high emission scenario) and B2 (medium-low emission scenario) scenarios reveal a reliable projection of a reasonable future climate condition at the regional scale. Thus, applicability of A2 and B2

scenarios in estimating the impacts of climate change at sub-basin level was investigated in this research. A regional climate change scenario using these emissions was statistically downscaled to derive a sub-basin level hydrological model.

Soil and Water Assessment Tool (SWAT) is used to simulate the hydrological response of a catchment. SWAT was Calibrates and Validated using observed climate and hydrological data for baseline (**1988-2010**) period. The statistical downscaling model (SDSM) is used to downscale the GCM data from A2 and B2 emissions scenarios for future climate prediction. The output generated from the statistical downscale model (precipitation and temperature) is used as input to the hydrological model (SWAT). The calibrated SWAT model was subsequently used to assess the hydrological response over Lower Awash Sub Basin due to climate change.

1.5. Research Question

Specific objective	**Research question**
To generate fine resolution climate change scenarios using statistical Downscaling Model at Sub Basin level	What are the downscaling techniques to generate finer resolution climate data at the Sub Basin level?
To project the variability in temperature and precipitation for selected climate change scenarios for a period of (2020s, 2050s and 2080s) at local climate stations;	What are the changes in mean of precipitation and temperature over the historical and future climate data and how this is reflected in local stations?
To study possible effect of climate change on the hydrology of Awash Sub Basin based on the downscale climate scenario data using SWAT hydrological model.	What are the expected changes in hydrologic variables on the Sub Basin level? How does the hydrologic looks like?

Chapter 2. LITERATURE REVIEW

2.1. Climate Change Impact on Water Availability

Climate is usually defined as the average weather in a place. It includes patterns of temperature, precipitation, humidity, wind and seasons. Climate play an important role in shaping a natural ecosystem and it's a key factor for water resources planning (Adem et al., 2016). The Change in precipitation and temperature specifically incredibly impacts the measure of water coursing through the hydrologic cycle and therefore, water availability. The higher the precipitation the more water is available and, hence, accessible to beneficiary use; the lower precipitation decrease the water availability and could potential results in drought. Similarly, the higher the temperature the more water is lost from the land surface because of evapotranspiration. The lower temperature the lower evapotranspiration; the more water that could be available for beneficial use for a given precipitation.

Understanding the respond of climate change and variability requires knowledge of how the current system is operating, how they are affecting water availability today and how they might respond to changes in the future. Climate and hydrologic recorded data over a long period of time help one understand the relationship between climate change and the available water in a given region or location.

2.2. Climate Change Impact in Ethiopia

According to IPCC (2007), Ethiopia is one of many developing countries which will be vulnerable to climate change. This is primarily a result of low level of socio-economic development, inadequate infrastructure, lack of institutional capacity and higher dependency on natural resources base that make the country more vulnerable to climate factors.

Vulnerability of Ethiopia to climate variability and change primarily attributed to very high dependence on rainfed agriculture which is very sensitive to climate variability and change, under-development of water resources, high population growth rate, low economic development level, low adaptive capacity, weak institutions, and lack of awareness. (NAPA, 2007)

The most common adverse impacts of climate change that affect Ethiopia are drought and floods. The country faces a challenge in food insecurity arising from occurrences of drought and floods;

land degradation due to heavy rainfall; damages in road and other infrastructure by floods (ADSWE, 2012).

For more than three decades, Ethiopia has experienced recurrent deadly droughts including those of the 1972/73, 1984, 2002/03, 2015/2016 that are typically associated to the onset of El Nino.

2.3. Global Circulation Model

Global or General Circulation Models (GCM) are large scale numerical models of the atmosphere and ocean circulation. They use hydrodynamic (Navier-stokes equations on Rotating sphere) with thermodynamics (radiation and latent heat) coupled together with atmospheric, ocean and other modeled aspects of climate system to form a global climate model or earths system model.

GCMs simulates the Earth's climate system over time to compute atmospheric water vapor, ocean temperatures, greenhouse gas concentrations, annual and daily solar heating and describe how these components interact with each other to create complex climate variability and change (ARCC, 2014).They are the main tools used to provide reasonably accurate representation of global and continental scale climate information on average daily, monthly, seasonal, annual and longer time scales used for forecast and projection of impacts of anthropogenic greenhouse gases (GHGs) and aerosols on future climate.

2.4. Downscaling

GCM divides the earth's surface into many grid cells, typically having a horizontal resolution of about 250 to 600 kilometers, with 10 to 20 vertical layers in the atmosphere and 10 to 30 layers in the oceans. Their spatial resolution is very coarse, they cannot account finer scales of processes.

Many physical processes, such as mountains, water bodies, infrastructure, land-cover characteristics, and components of the climate systems such as convective clouds and coastal breezes, have scales that are much finer than 250-600 kilometers (ARCC, 2014). Those climate systems that occur at smaller scale cannot be properly modeled in GCMs and the outputs do not provide valuable information for impact studies and for decision makers who need the information at fine-scales of 10-50km. Therefore, there is a need to derive the fine-scale climate

information from large scale modeled or observation data through downscaling process so that finer scale impact studies can be conducted.

The downscaling technique is based on the assumption that a significant interaction and relationship exist between large-scale and fine-scale climatic factors. The method used to downscale large to fine-scale climate can be done at temporal and spatial features of climate projections. Spatial downscaling refers to the derivation of climate information at finer spatial resolution from coarser spatial resolution GCM output (e.g., 20 km resolution from 500km grid cell GCM output). Temporal downscaling refers to the derivation of fine-scale temporal data from coarser-scale temporal GCM output information (e.g., daily data from monthly or seasonal information) (ARCC, 2014).

Downscaling procedures can be grouped in to two approaches (Choux, 2005): Dynamical downscaling (DD) and Statistical downscaling (SD).

2.4.1. Dynamic downscaling

Dynamic downscaling approach is a method of extracting the local information from the GCM outputs by the means of limited area models or regional climate models (Choux, 2005). The procedure is to nest a regional climate model (RCM) with the coarse GCM data as boundary conditions. The main advantage of RCMs is their capability of detail description of smaller scale atmospheric processes; in order to generate realistic climate information at a spatial resolution approximately 20-50 kilometers (ARCC, 2014). Evidently, the use of dynamically downscale RCMs output can resolve smaller scale atmospheric process of orographic precipitation than the GCM host (Pharasi, 2006). However, the major limitation of RCM technique is their considerable computational cost as GCMs. This is because RCMs involve the explicit solving of dynamics of the atmospheric system, using fundamental conservation laws of mass, energy and momentum. Furthermore, RCMs outputs are subjects to systematics errors and cannot correct the discrepancies of the nesting GCM variables used at the boundaries, often they require a bias correction or further downscaling to a higher resolution.

2.4.2. Statistical downscaling

Statistical downscaling (SD) techniques are based on the principle that local climate is largely a function of the large scale atmospheric state. The statistical relationships or transfer function is described as R=F(L), where R represents the local-scale predictand climate variable (e.g., daily

precipitation) to be downscaled, L is the set of large-scale climate predictor variables (e.g., atmospheric circulation indices) (Amorim, 2014). The function is typically established by time independent training and validation procedures using observations (e.g., stations, reanalysis) (Amorim, 2014). This downscale approach applies the information from GCMs to the region by using a series of equations to relate variations in global climate to variations in local climate (Matthews, 2012).

The statistical downscaling process contains the following inherent assumptions (Amorim, 2014):

i. The predictor-predictand relationship should be physically plausible;
ii. The predictor must be adequately represented by the GCM on a range different timescale;
iii. Predictor must reflect the climate change signal;
iv. The predictor-predictand relationship is assumed to be time-invariant (stationary) even under future non-stationary of the climate.

In addition, a reliable statistically downscaling model should be based on representative observational time series. Particularly due to stationarity issues which are potentially more series for statistically techniques than for dynamical models (Amorim, 2014).

Statistical downscaling can produce site specific climate projections, which RCMs cannot provide because computationally limited to a 20-50 km spatial resolution (ARCC, 2014). These approaches require less computational effort than dynamic downscaling, it tests scenarios for longer timeframes (decades or centuries) rather than the brief (shorter timeframes) of the downscaling approach (Matthews, 2012). This allows the users to develop a large number of different climate simulations and thus investigate the statistical characteristics of downscaled variable. Moreover, SD methods allow talking weather data available at the study site into account. However, this approach relies on the critical assumption that the relationship between present large scale atmospheric circulation and local climate remains valid under different forcing conditions of possible future climates.

The SD method can be classified in to three categories (Pharasi, 2006) ; weather typing approach, stochastic weather generators and regression based method.

Weather Typing Approach

Weather typing based downscaling method involve relating the observed local-scale metrological data such as precipitation to a subjectively or objectively derived weather classification scheme (Choux, 2005).

The frequency distributions of local or regional climate are obtained by weighting the local climate states with the relative frequencies of the weather classes. Regional climate projections are then estimated by evaluating the frequency distribution of weather classes simulated by the GCM. The main advantage of weather typing that large scale atmospheric patterns are likely to remain its influence on local climate as climate varies and changes. On the other hand, the method is inadequate for simulating extreme events and, as all statistical models, entirely dependent on stationary relationships (IPCC 2007). Moreover, there is a lack of systematic studies evaluating the performance of GCMs in reproducing weather patterns and in some cases, the changes in the frequency of observed weather patterns are consistent with GCM simulations (Amorim, 2014).

Stochastic Weather Generation

Stochastic weather generators are similar in many aspects to the circulation-based downscale approaches, but differ in how they are applied to future climate conditions. Instead of being conditioned by circulation patterns, stochastic models simulate all surface weather variables such as precipitations conditional on the precipitation occurrence.

The main advantage of stochastic weather generation is that it can exactly reproduce many observed climate statistics, such as the mean, median and interquartile range. However, since these models do not incorporate secondary variables in the calibration phase such as humidity and atmospheric circulation, accurate linkages to the host GCMs cannot be achieved. In addition, stochastic generators provide a weak reproduction of precipitation extreme and have systematic problems with modeling variability and outliers (Pharasi, 2006).

Regression Based Method

The regression based methods rely on the empirical statistical relationships between large scale predictors and local scale parameters for instance the statistical downscaling model (SDSM)

model, (Choux, 2005). The predictor-predictand relationship can described using different functions (Choux, 2005). These techniques are generally simple and less computationally demanding in comparison to other downscaling methods, but their application is limited to local sites where accurate predictor-predictand relationships can be found.

Table 2.1 Comparisons on dynamic and statistical downscaling *(ARCC, 2014).*

	Dynamical downscaling	Statistical downscaling
provides	• 20-50 km grid cell information • Information at sites with no observational data • Daily time-series • Monthly time series • Scenarios for extreme events	• Any scale to station-level information • Daily time-series (only some methods) • Monthly time-series • Scenarios for extreme events (only some methods) • Scenarios for any consistently observed variable
Requires	• High computational resources and expertise • High volume of data inputs • Reliable GCM simulations	• Medium/low computational resources • Medium/low volume of data inputs • Sufficient amount of good quality observational data • Reliable GCM simulations
Advantages	• Based on consistent, physical mechanism • Resolves atmospheric and	• Computationally inexpensive and efficient, which allows

	surface processes occurring at sub-GCM grid scale • Not constrained by historical record so that novel scenarios can be simulated • Experiments involving an ensemble of RCMs are becoming available for uncertainty analysis.	for many different emissions scenarios and GCM parings. • Methods range from simple to elaborate and are flexible enough to tailor for specific purposes • The same method can be applied across regions or the entire globe, which facilitates comparisons across different case studies • Relies on the observed climate as a basis for driving future projections • Can provide point-scale climate variables for GCM-scale output • Tools are freely available and easy to implement and interpret; some method capture extreme events
Disadvantages	• Computationally intensive • Due to computational demands, RCMS are typically driven by only one or two GMC/emission	• High quality observed data may be unavailable for many areas or variables

	scenario simulations • Limited number of RCMS available and no model results for many parts of the globe • May require further downscaling and bias correction of RCM outputs • Results depend on RCM assumptions; different RCMs will give Different results • Affected by bias of driving GCM	• Assumes that relationships between large and local-scale processes will remain the same in the future (stationary assumptions) • The simplest methods may only provide projections at a monthly resolution
Applications	• Country or regional level assessments with significant government support and resources • Future planning by government agencies across multiple sectors • Impact studies that involve various geographic areas	• Weather generators in widespread use for crop-yield, and other natural resource modeling and management • Delta or change factor method can be applied for most adaptation activities

2.5. Climate Change Scenarios

A scenario is a coherent, internally consistent and plausible description of possible future state of the world conditions produced to inform decision makers under uncertainty (Reza, 2014). The IPCC developed a set of scenarios to represent the range of driving forces and emissions in the scenario to reflect the current understanding and knowledge about underlying uncertainties. The four narrative storylines were developed and released by IPCC in 2000 are published in Special Report on Emissions Scenarios (SRES) to describe the relationship between the driving force of greenhouse gas and aerosols emissions and their evolution in the next century. Each scenario

represents a specific quantitative interpolation of one of the four storylines. These scenarios are labeled as A1, A2, B1 and B2. Each storyline represents different demographic, social, economic, technological, and environmental developments (Matthews, 2012).

The storylines are outlined in the IPCC Special Report on Emission Scenarios (SRES).

A1 scenario: - according to the IPCC, the A1 scenario and storyline family describes the world of very rapid economic growth, global population that peaks in mid-century and declines thereafter and the rapid introduction of efficient technologies. Major focuses are convergence among regions, capacity building, and increased cultural and social interactions, with a substantial reduction in regional difference in per capital income (IPCC, 2007). A1 scenario is developed into three groups that describe alternative directions of technological change in the energy system. These three groups: A1F1-fossil intensive, A1T-non-fossil energy sources and/or A1B-balance across all sources. In A1 scenario, population will be increasing to 8.7 billion in 2050 and decline towards 7 billion people by end of the century (IPCC, 2007).

A2 scenario (Medium-High Emissions scenario): - the IPCC states that, it is a scenario with higher rates of greenhouse gas emission in combination with higher sulphate and other aerosol emissions. It represents a differentiated world and describes the world in a various economic region in which the income gap between developed and developing countries is not narrow. Regions with abundant energy and mineral resources evolve more resource-intensive economies. In this scenario, global environmental concerns are relatively weak but regional and local pollutions are planned to mitigate. A2 scenario is constructed based on the different economy growth rate and efficiency of technology dependent on the regional scale in which population reaches to 15 billion people in year 2100 and will be increased after 2100 (IPCC, 2007).

B1 scenario: - it describes a future based on the high level of environmental approach and a balanced economic development. B1 scenario focuses on global environmental protection and gains in improved efficiency of resources use. The best measures are taken to reduce material wastage by maximizing recycling and enhancing energy saving lead to reductions in pollution. B1 scenario has some major push toward post-fossil technologies. Population is the same as A1 scenario but slower rate (IPCC, 2007).

B2 scenario (Medium-Low Emission Scenario): - according to the IPCC, B2 scenario is a lower rate of emissions that assumes the world is more committed to solving global and local environmental. It designed based on the world emphasizes on local solutions to economic, social, and environmental sustainability. Increasing in population is assumed at a lower rate than A2 scenario. B2 scenario focuses on intermediate levels of economic development, less rapid technological development compared to B1 and A1 scenarios. However, it focuses towards environmental protections and social equity at the local and regional scale. In B2 scenario, population reaches to 10 billion in 2100 and increasing with slower development rate of technology compared to A1 and B1 scenarios.

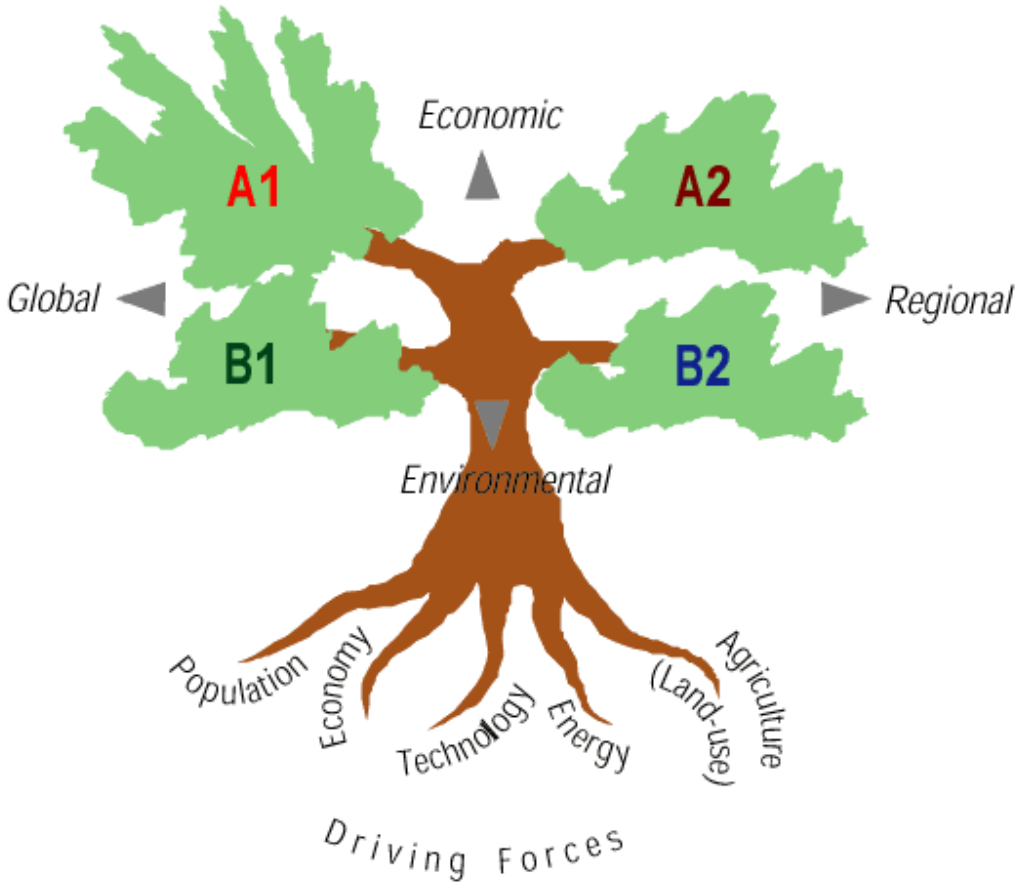

Figure 2.1 The four IPCC SRES scenario storylines *(Carter, 2007)*

2.6. Climate Change Models and Emission Scenario

The inter government panel on climate change (IPCC) is the leading international body for the assessment of climate change. It was established in 1998 by the United Nations Environment Program (UNEP) and the World Metrological Organization (WMO) to provide the world with a clear scientific view on the current state of knowledge in climate change and its potential environmental and socio-economic impacts and adaptation assessment. currently 194 countries are members of the IPCC.

The IPCC developed a set of emissions scenarios to represent the range of driving forces and emissions in the scenario to reflect the current understanding and knowledge about underlying uncertainties.

Future levels of global GHG emissions are the products of a very complex, less-understood dynamic system, driven by forces such as population growth, socio-economic development and technological progress thus, to predict emissions accurately is virtually impossible.

Given the uncertainties in both emissions models and our understanding of key driving forces, scenarios are an appropriate tool for summarizing both current understanding and current uncertainties.

Table 2.2 History of scenarios *(Bjornaes, 2014)*

Year	Name	Used
1990	SA90	First Assessment Report
1992	IS92	Second Assessment Report
2000	SRES-Special report on Emissions and Scenarios	Third and Four Assessment Report
2009	RCP-Representative Concentration Pathways	Fifth Assessment Report

Representative Concentration Pathways (RCP)

The Representative Concentration Pathways (RCP) is the latest generation of scenarios that provide input to climate models (Bjornaes, 2014). RCPs are time and space dependent

trajectories of concentrations of greenhouse gases and pollutants resulting from human activities, including changes in land use. RCPs provide a quantitative description of concentrations of the climate change pollutant in the atmosphere over time, as well as their radiative force in 2100 (e.g., RCP 6 achieves an overall impact of 6watt per square meter by 2100) (Bjornaes, 2014). The word representative signifies that each RCP provides only one of many possible scenarios that would lead to specific radiative forcing pathway. Radiative force is the measure of the additional energy taken up by the earth system due to increases in climate change pollution by greenhouse effect; and expressed as Watts per square meter.

The four RCPs are consistent with certain socio-economic assumptions. These will later be replaced by the shared socio-economic pathways which provide flexible description of possible future within each RCP (Bjornaes, 2014).

Table 2.3 Representative concentration pathways *(Bjornaes, 2014)*

	Developed by	Radiative force	IA Model	Description
RCP 8.5	International Institute for Applied System Analysis in Austria	Rising radiative forcing pathway leading to 8.5 Watt/m^2 in 2100.	MESSAGE	**High emissions: -** consistent with a future with no policy changes to reduce emissions. Comparable SRES scenario: A1 F1
RCP 6	National institute for Environmental Studies, Japan	Stabilization without overshoot pathways to 6 Watt/m^2 at Stabilization after year 2100	AIM	**Intermediate emissions: -** consistent with the application of a range of technologies and strategies for reducing greenhouse gas emissions. Comparable SRES scenario: B2

RCP 4.5	Pacific Northwest National Laboratory, USA	Stabilization without overshoot pathway to 4.5 at Stabilization after year 2100	GCAM (MiniCAM)	**Intermediate emissions: -** consistent with a future with relatively ambitious emissions reductions. Comparable SRES scenario: B1
RCP 2.6	PBL Netherlands Environmental Assessment Agency	Peak in radiative forcing reaches 3.1 Watt/m2 before it turns to 2.6 Watt/m2 by 2100 and decline	IMAGE	**Low emissions**: - In order to reach such forcing levels, ambitious greenhouse gas emissions would be required over time.

2.7. Hydrologic Model

Hydrologic models are simplified, conceptual representation of a part or parts of the hydrologic cycle. The structure of a hydrological model is represented as a set of equations linking the inputs and outputs with its center acting as a system transformer. Hydrological models use mathematical and empirical expressions that define quantitative relationships between inputs (e.g. temperature, precipitation) and outputs (e.g. discharge) for water resource studies (Berhane, 2011).

Hydrological modeling is a great method of understanding of the hydrologic process and how changes affect these processes for the planning and development of water resources management. The purpose of using a model is to establish baseline characteristics whenever data is not available and to simulate long-term impacts that are difficult to calculate.

Hydrologic models can be used in two ways: to assess the existing hydrology and water quality conditions of a water resource, and to predict future hydrology, which may develop as a result of changes in land use, climate or any other physical alteration to the environment.

2.7.1. Hydrological model classification

The classification of hydrological model classified to different criteria from various classification systems based on process description, timescale, space scale, techniques of solutions or model use. Classification are generally based on the method of representation of the hydrological cycle or a component of hydrological cycle.

Hydrological model can be classified as:

1. **Statistical models:** they are purely a mathematically construct where a process that produce results are not considered. They fit regression curves to observed data. Predictions of future events are made from enough previous observation (such as flood frequency, rating curve). Though these models are simple and easy to understand and convey information, they do not include process information and they may not be valid beyond the range of historical information that was used to construct them (Berhane, 2011).
2. **Numerical models:** they use mathematical and empirical relationships to represent complex physical and dynamical processes within the earth systems. They are useful to analyze project alternatives and predict the effects of future changes, such as urban development, land use change, climate change, etc. numerical models can be generally divided into three (Berhane, 2011):

    a) **Lumped models:** these empirically based models integrate over some time and space scales. The high non-linear response of watersheds appears linear (such as Rational Method, HEC-1, etc.). Though they are conceptually simple and easy to program and apply, they require substantial calibration data and they are not useful outside of the range of calibration.

    b) **Semi-distributed models:** these semi-distribute (simplified distributed) model are partially allowed to vary in space by dividing the basins into a number of smaller sub basins. They are mixture of empirical and physics based approaches. They lie between lumped and distributed models. They have the advantage of increased spatial resolution and better process descriptions over simple lumped parameter models. They also maintain the computational advantage over fully distributed, physics based models (such as SWAT, HEC-HMS, TOPMODEL).

c) **Distributed models:** these model takes account of spatial variations in all variables and parameters. The physical processes occurring in the watershed may be explicitly simulated, and then integrated to produce the watershed response (such as MIKE-SHE, ADH etc.). They can be used to analyze changing conditions such as land use changes, project alternatives, and climate change and they are extendible beyond the calibration range. However, they are data intensive and code development is difficult (Berhane, 2011).

2.7.2. Hydrologic model selection criteria

There are many criteria which can be used to choose the right hydrological model. These criteria are project dependent since every project has its own specific requirements and needs. Furthermore, some criteria are also user dependent, such as personal preference for computer operation system, input/output management and structure.

Among the various project-dependent selection criteria, the main criteria that should be considered when selecting hydrological model are: the ease of running the model and interpreting the results, availability of input data, availability of the model and support, applicability to land-use practices, applicability to broad geographic areas and accuracy of prediction.

In this study, a semi-distributed model which is the Soil and Water Assessment Tool (SWAT) is used to assess the climate change impact on the hydrology of Lower Awash Sub Basin. The choice of these models depends on the moderate input data requirement (uses readily available inputs), ability to simulate the major hydrological process and its availability. SWAT has been shown to have a good performance in simulating sub basin scale processes and has been successfully used worldwide in many applications at a watershed scale.

SWAT is selected as the hydrological model to be used in this research (Abera, 2011):

1. SWAT has been used in various studies in the global scope.
2. Compared to other models, SWAT has strengths in predicting impacts of climate change and water availability on watershed.
3. SWAT is a free and open source code model which fulfills the requirements of developing countries. Modification of the model are possible by users.

2.8. Soil and Water Assessment Tool (SWAT) Model

The Soil Water Assessment Tool (SWAT) is freely available watershed model actively supported by the United States Department of Agriculture (USDA) - Agricultural Research Service (ARS) at the Grass-land, Soil and Water Research Laboratory in Temple, Texas, USA. SWAT is a semi-physically based model that is used to predict the impact of land management practice on water, sediment and agricultural chemical yields in large complex watersheds with varying soil, land use and management conditions over long periods of time (Neitsch et al., 2005).

SWAT is a continuous time model and operates on a daily and sub-daily time steps at a watershed scale to simulate multiple hydrological processes involving water quality and quantity, including the transport and transformation process of water, sand and chemical substances. The model can be used to simulate the effect of climate and land cover changes by tuning the climate and land cover input (Berhane, 2011). The SWAT system is embedded within a geographic information system (GIS) that can integrate various spatial environmental data including soil, land cover, climate and topographic features.

SWAT is a semi-distributed parameter model where by each watershed is divided into sub-watersheds, based upon a digital elevation model. Sub-watersheds are further divided in to Hydrologic Response Units (HRU) based upon common land use, management, and soil type. SWAT assigns a single set of parameters to each Hydrologic Response Units, thereby simulating surface runoff and infiltration by lumping these processes at the HRU-scale. The model estimates relevant hydrologic components such as evapotranspiration, surface runoff and peak rate of runoff, ground water flow and sediment yield for each HRU. SWAT includes eight major modeling components: weather, hydrology, soil temperature, plant growth, nutrients, pesticides and land management and performs a mass balance on daily time step (Sawyer, 2010).

The hydrology components of SWAT partitions precipitation into four control volumes: the surface, the soil profile or root zone, the shallow aquifer and the deep aquifer. SWAT hydrologic simulations are based on the water balance equation:

$$SW_t = SW_0 + \sum_{i=1}^{t}(R_{day} - Q_{surf} - ET_a - W_{seep} - Q_{gw}) \quad (1)$$

Where, SW_t is the soil water content (mm water) at the end of time step t (days), SW_0 is the initial soil water content day *i* (mm water), R_{day} is the amount of precipitate on day *i* (mm water), Q_{surf} is the amount of surface runoff on day *i* (mm water), ET_a is the amount of evapotranspiration on day I (mm water), W_{seep} is the amount of water entering the vadose zone from the soil profile on day I (mm water), and Q_{gws} is the amount of base flow from the shallow aquifer on day *i* (mm water).

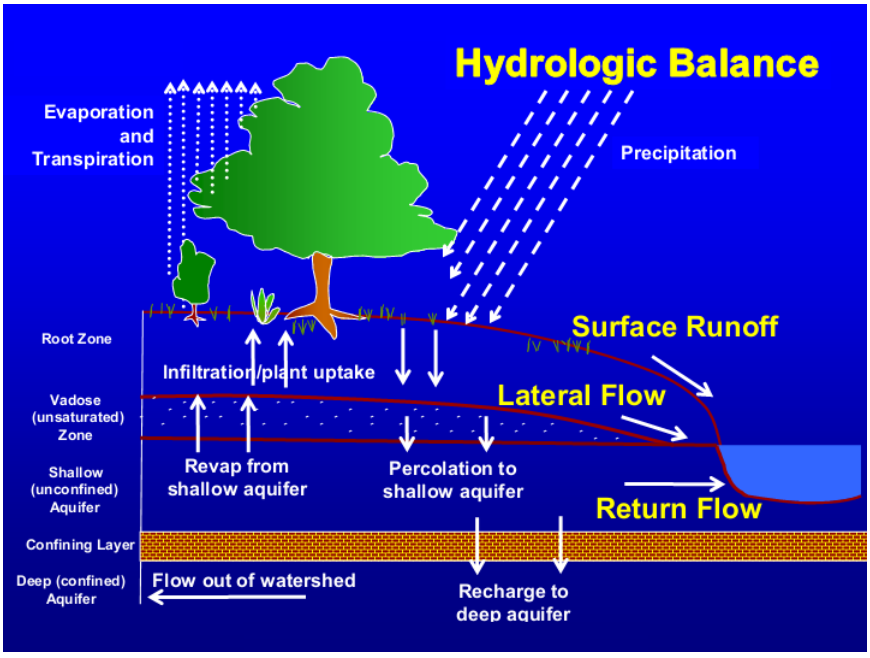

Figure 2.2 Schematic representation of the hydrologic cycle *(Neitsch et al., 2005)*

SWAT has the capability to represent multiple soil layers in the HRU water balance if increased complexity is required (Gautam, 2012). A water balance is computed for each HRU at every time step. A summary of the resulting water balance at the end of each (daily) time step can be viewed in the HRU output file (. HRU).

The contribution to streamflow from each HRU (assuming a single soil layer) can be represented by the subsequent equation:

$$Q = R_{day} - ET_a - Q_{surf} - Q_1 - W_{seep} + CR + Q_{gws} - Q_{gwd} \quad (2)$$

Where, Q is the runoff leaving the HRU on day *i* (mm water), R_{day} is the amount of precipitation on day *i* (mm water), Q_{surf} is the amount of surface runoff on day (mm), ET_a is the

amount of evapotranspiration on day (mm), W_{seep} is the amount of water percolating the underlying soil layer on day (mm), Q_{gwd} is groundwater flow lost to the deep aquifer on day (mm), Q_{gws} is the amount of base flow from the shallow aquifer on day (mm), CR is the upward movement of water from the shallow aquifer on day (mm), and Q_1 is the lateral flow on day (mm),

The total streamflow from the watershed is the summation of the Q contribution from each HRU.

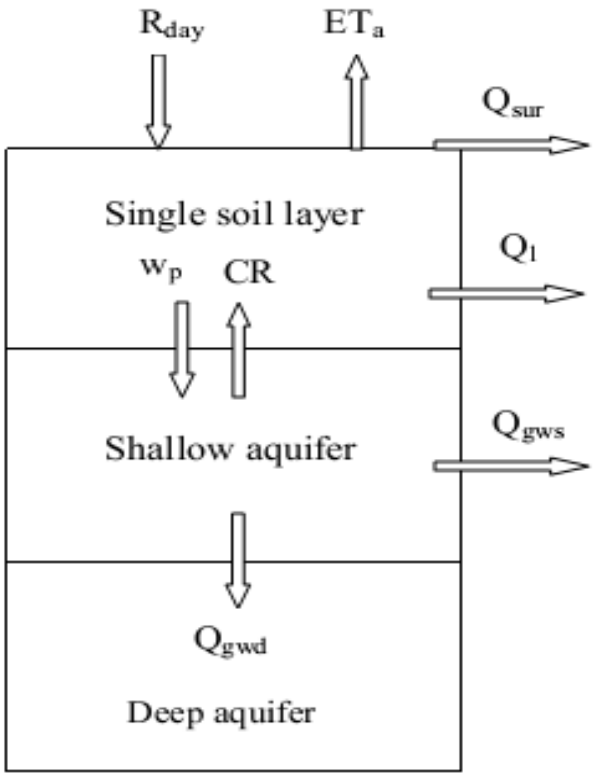

Figure 2.3 schematic representation of the water balance for a single soil layer HRU represented in SWAT *(Gautam, 2012).*

Surface Runoff

Runoff is that part of the precipitation as well as any other contribution, which appears in surface streams of either perennial or intermittent form. It is the flow collected from a drainage basin or water shade and it appears at the out let of the basin. Generally, surface runoff occurs whenever the rate of water reaching the ground surface exceeds the rate of infiltration.

SWAT provides two methods for estimating surface runoff: the SCS curve number procedure (SCS, 1972) which CN is a function of the soil's permeability, land use and antecedent soil water conditions and the Green & Ampt infiltration method (1911). In this study SCS curve number procedure was preferred over the Green & Ampt infiltration method. The Green & Ampt infiltration method assumes that there will be excess water at the surface at all times which was invalid for the study area and also this method requires sub-daily precipitation data which was the other limitation to use this method. SCS curve number method estimates the amount of runoff based on land use, soil type and antecedent moisture condition. Therefore, the SCS curve number method is simple, widely used and efficient for determining the approximate amount of runoff from a rainfall event under varying land use and soil type (Neitsch et al., 2005).

The SCS (1972) has developed a method of determining excess rain by dividing precipitation into: Direct runoff (Q) which shows up as runoff, Actual retention which is the depth of abstraction and Initial abstraction which is the depth of rain that must fall before runoff starts.

The SCS (1972) curve number equation is given by:

$$Q_{surf} = \frac{(R_{day} - I_a)^2}{(R_{day} - I_a + S)} \quad (3)$$

Where, Q_{surf} is the accumulated surface runoff (mm/day), R_{day} is the daily precipitation (mm/day), I_a is the initial abstraction which is commonly approximated as 0.2S (mm/day), and S is the retention parameter (mm/day).

Runoff will occur when R_{day}>I_a, by substituting in the above equation 0.2S for I_a the equation gives:

$$Q_{surf} = \frac{(R_{day} - 0.2S)^2}{(R_{day} - 0.8S)} \quad (4)$$

The retention parameter varies spatially due to change in soils, land use. Management and slope, and temporarily due to changes in the soil water content. The retention parameter S is given as

$$S = 25.4\,(\frac{100}{CN} - 10) \quad (5)$$

Where, CN is the curve number for the day, which is a function of soil permeability, land use and antecedent soil water condition. SWAT model defines three antecedent moisture conditions

to determine the appropriate CN for each day using CN-AMC (Curve Number-Antecedent Soil Moisture Condition) distribution based on the moisture content of the soil calculated by the model (Neitsch et al., 2005).

SCS defines three antecedent moisture conditions: I-Dry (wilting point), II- Average moisture and III-Wet (field capacity). The moisture condition I curve number is the lowest value that the daily curve number can assume in dry conditions. The curve numbers for moisture conditions II and III are calculated using the following equations:

$$CN_1 = CN_2 - \frac{20(100 - CN_2)^2}{(100 - CN_2 + \exp[2.533 - 0.0636(100 - CN_2)])} \quad (6)$$

$$CN_3 = CN_2.exp[0.00673(100 - CN_2)] \quad (7)$$

Where CN_1 is the moisture condition I curve number which is the lowest value the daily curve, number can assume, CN_2 is the moisture condition II curve number, and CN_3 is the moisture condition III curve number.

Typical curve number for moisture condition II curve number available from table are appropriate for slopes less than 5%. In areas where the slope is greater than 5%, the equation developed by Williams, 1995 is using to calculate curve number:

$$CN_{2s} = \frac{(CN_3 - CN_2)}{3}[1 - 2exp(-13.86.slp)] + CN_2 \quad (8)$$

Where CN_{2s} is the moisture condition II curve number adjusted for slope, CN_3 is the moisture condition III curve number for the default 5% slope, CN_2 is the moisture condition II curve number for the default 5% slope, and slp is the average percent slope of the basin. SWAT does not adjust curve number for slope. If the user wishes to adjust the curve number for slope effects, the adjustment must be done prior to entering the curve number in the management input file.

The **peak runoff** rate is the maximum volume flow rate passing a particular location during a storm event. SWAT calculates the peak runoff rate using a modified rational method given by:

$$q_{peak} = \frac{C.i.A}{3.6} \quad (9)$$

Where: q_{peak} is the peak runoff rate (m^3/s), i is the rainfall intensity (mm/hr) in time t_{conc} , A area is the sub basin area (Km2) and C is the runoff coefficient given by

$$C = \frac{Q_{surf}}{R_{day}} \quad (10)$$

Where: Q_{surf} is the accumulated surface runoff (mm/day), R_{day} is the daily precipitation (mm/day).

t_{conc} the time of concentration, is the time required for rain falling at the farthest point of the catchment flow to the measuring point of the river. Thus, after time t_{conc} from the commencement of rain, the whole of the catchment is taken to be contributing to the flow. The value of i, the mean intensity, assumed that the rate of rainfall is constant during t_{conc}, and that all the measured rainfall over the area contributes to the flow. The peak flow q_{peak} occurs after the period t_{conc}. Its calculated as

$$t_{conc} = t_{ov} + t_{ch} \quad (11)$$

where t_{conc} is the time of concentration for sub basin (hr), t_{ov} is the time of concentration for overland flow (hr) and t_{ch} is the time of concentration for channel flow.

The overland flow time is computed as:

$$t_{ov} = \frac{L_{sip}}{3600.v_{ov}} \quad (12)$$

Where: L_{sip} is the average sub basin slope length (m), v_{ov} is the overland flow velocity (m/s), and 3600 is a unit conversion factor.

The overland flow velocity calculated as:

$$V_{ov} = \frac{q_{ov}^{0.4} . slp^{0.3}}{n^{0.6}} \quad (13)$$

Where q_{ov} is the average overland flow rate (m^3/s), *slp* is the average slope of the sub basin (m/m) and n is the manning's roughness coefficient for the sub-basin.

Channel flow time concentration t_{ch} , can computed using the equation;

$$t_{ch} = \frac{L_c}{3.6.V_c} \quad (14)$$

Where L_C is the average flow channel length (km), V_C is the average flow velocity (m/s) and 3.6 is a unit conversion factor.

The average flow channel length is calculated as:

$$L_C = \sqrt{L.L_{cen}} \quad (15)$$

Where L is the channel length from the furthest point to the sub basin outlet (km), L_{cen} is the distance along the channel to the sub basin centroid (km).

The average velocity is estimate from Manning's equation assuming a trapezoidal channel with 2:1 side slopes and a 10:1 bottom width-depth ratio

$$V_C = \frac{0.489 * q_{ch}^{0.25} * slp_{ch}^{0.375}}{n^{0.75}} \quad (16)$$

Where V_c is the average channel velocity (m/s), q_{ch} is the average channel flow rate (m^3/s), slp_{ch} is the channel slope (m/m), and n is Manning's roughness coefficient for the channel.

In large sub basins with a time of concentration greater than one day, only a portion of the surface runoff will reach to the main channel on the day it is generated. SWAT incorporates a surface runoff storage feature to lag a portion of the surface runoff release to the main channel.

Once surface runoff is calculated with the curve number method, the amount of surface runoff released to the main channel is calculated:

$$Q_{surf} = \left(Q'_{surf} + Q_{stor,i-1}\right) * \left(1 - \exp\left[\frac{-surlag}{t_{conc}}\right]\right) \quad (17)$$

Where Q_{surf} is the amount of surface runoff discharged to main channel in a day (mm), Q'_{surf} is amount of surface runoff generated in a sub basin in a day(mm), $Q_{stor,i-1}$ is the surface runoff stored or lagged from the previous day (mm), Surlag is the surface runoff lag coefficient, and t_{conc} is the time of concentration for the sub basin (hrs).

Lateral Flow

Lateral flow will be significant in areas with soils having high hydraulic conductivities in surface layers and an impermeable or semipermeable layer at a shallow depth. In such a system, rainfall will percolate vertically until it encounters the permeable layer. The water then ponds above the impermeable layer forming a saturated zone of water, i.e. a perched water table. This saturated zone is the source of water for lateral subsurface flow.

SWAT incorporates a kinematic storage model for subsurface flow developed by Sloan (1983) and summarized by Sloan and Moore (1984).

$$Q_{lat} = 0.024 * \frac{\left[2 * SW_{ly,excess} * K_{sat} * slp\right]}{\emptyset_d * L_{hil}} \quad (18)$$

Where Q_{lat} is lateral flow, $SW_{ly,excess}$ is the drainable volume of water stored in the saturated layer in millimeters (mm) (a soil is considered to be saturated whenever the water content of the layer exceeds the layer's field capacity water content), K_{sat} is the saturated hydraulic conductivity (mm.hr), slp is the increase in elevation per unit distance equivalent to Tanαhill (where Tanαhill is the slope of the hill segment), $\emptyset_d$ is the drainable porosity of the soil layer (mm/mm), and L_{hil} is the hill slope length (m).

2.9. SWAT- Calibration and Uncertainty Program

The Soil and Water Assessment Tool-Calibration and Uncertainty Program (SWAT-CUP) is an open space interface that was developed for SWAT by using the generic interface, any calibration, uncertainty or sensitivity program can be easily linked to SWAT model. The program joins Sequential Uncertainty Fitting (SUFI2), Generalized Likelihood Uncertainty Estimation (GLUE), Parameter Solution (ParaSol), and Markov chain Monte Carlo (MCMC) (Abbaspour, 2015). In this study, SUFI-2 is used to perform calibrations and uncertainty analysis.

2.9.1. Sequential uncertainty fitting (SUFI-2)

SUFI-2 accounts parameter uncertainty for all sources of uncertainty such as uncertainty in driving variables (e.g., rainfall), conceptual model, parameters and measured data. The degree to which all uncertainties are accounts for is quantified by a measure referred to as the P-factor,

which is the percentage of measured data bracketed by the 95% prediction uncertainty (95PPU) and R-factor, which is the thickness of the 95PPU envelop (Abbaspour, 2015). These 95PPUs are the model outputs in a stochastic calibration approach. It is not representing a single signal model output, but rather expressed the good solutions by the 95PPU, generated by certain parameter ranges. Abbaspour (2005) suggested that, for P-factor a value of >70 % for discharge, while for R-factor of Round 1.5. SUFI2 uses R-factor, which is the average thickness of the 95PPU divided by the standard deviation to measure the strength of the calibration uncertainty analysis (Berhane, 2011).

$$R - factor = \frac{d_x}{\sigma_x} \tag{19}$$

$$d_x = \frac{1}{k}\sum(X_u - X_L) \tag{20}$$

Where d_x is average distance between the upper and the lower 95PPU, k is the number of observed data points, σ_x is the standard deviation of the measured variable X.

After acceptable values of R-factor and P-factor, the goodness of fit quantified by the coefficient of determination R^2 and Nash-Sutcliffe (NS) coefficient efficiency between the observation and the final result.

$$R^2 = \frac{[\sum(Q_{m,i} - \overline{Q_m})(Q_{s,i} - \overline{Q_s})]^2}{\sum(Q_{m,i} - \overline{Q_m})^2 \sum(Q_{s,i} - \overline{Q_s})^2} \tag{21}$$

$$NS = 1 - [\frac{\sum(Q_{m,i} - Q_s)^2}{\sum(Q_{m,i} - \overline{Q_m})^2} \tag{22}$$

Where R^2 is the coefficient of determination, NS is the Nash-Sutcliffe coefficient, Q_m is the measured discharge, Q_s is the simulated discharge, $\overline{Q_m}$ is the average measured discharge and $\overline{Q_s}$ is the average simulated discharge. R^2 describes the proportion of the variance in measured data explained by the model. NS indicates how well the plot of observed and simulated data fits 1:1 line. R^2 and NS ranges from 0 to 1, fact that for R2 and NS they larger they are the better they are (Abbaspour, 2015).

2.10. Statistical Downscaling Model (SDSM)

The Statistical Downscaling Model (SDSM), developed by Robert L. Wilby and Christian W. Dawson (Wilby & Dawson, 2007). SDSM is the well-recognized statistical downscaling tool that facilitates the rapid and low-cost development of multiple single site projections of daily surface climate variables under current and future climate forcing.

The SDSM combines two statistical downscaling techniques linear regression and a stochastic weather generator. More precisely, predictors are linked to the local predictand through linear relationships, minimize the root mean squared error. In addition, the variance of the downscaled daily data is stochastically adjusted in order to better reproduce the observed time-series (Wilby & Dawson, 2007).

The SDSM permits the spatial downscaling of daily predictor-predictand relationships using multiple linear regression techniques. The predictor variables provide daily information concerning the large-scale state of the atmosphere, while the predictand describes conditions at the site scale which could be used as input for hydrological models.

The SDSM software reduces the task of statistically downscaling daily weather series into seven discrete steps (Wilby & Dawson, 2007) :

1. **Quality control and data transformation**: Few metrological stations have 100% complete and fully accurate data sets. Handling of missing and imperfect data is necessary for most practical situations. Simple quality control checks enable the identification of the gross data error, specification of missing data codes and outliers prior to model calibration.
2. **Screening of the predictor variables**: Identifying empirical relationships between gridded predictors (such as mean sea level pressure) and single site predictand (such as station precipitation) is central to all statistical downscaling methods. The main purpose of screening variables operation is to assist the user in the section of appropriate downscaling predictor variables.
3. **Model calibration**: The “Calibrate” model operation takes a user-specified predictand along with a set of predictor variables, and components the parameters of multiple regression equation.

4. **Weather generator**: The weather generator operation generates ensembles of synthetic daily weather series given observed or National Center for Environmental Prediction (NCEP) re-analysis atmospheric predictor variables. The procedure enables the verification of calibrated models (using independent data) and the synthesis of artificial time series for present climate conditions.
5. **Data analysis**: SDSM provides means of interrogating both downscaled scenarios and observed climate data with the **Summery Statistics** and **Frequency Analysis** screens.
6. **Graphical analysis**: Three options for graphical analysis are provided by **SDSM 5.2** through the **Frequency Analysis, Compare Results and the Time Series Analysis** screens.
7. **Scenario generations:** The scenario generator operation produces ensembles of synthetic daily weather series given atmospheric variables supplied by a climate model.

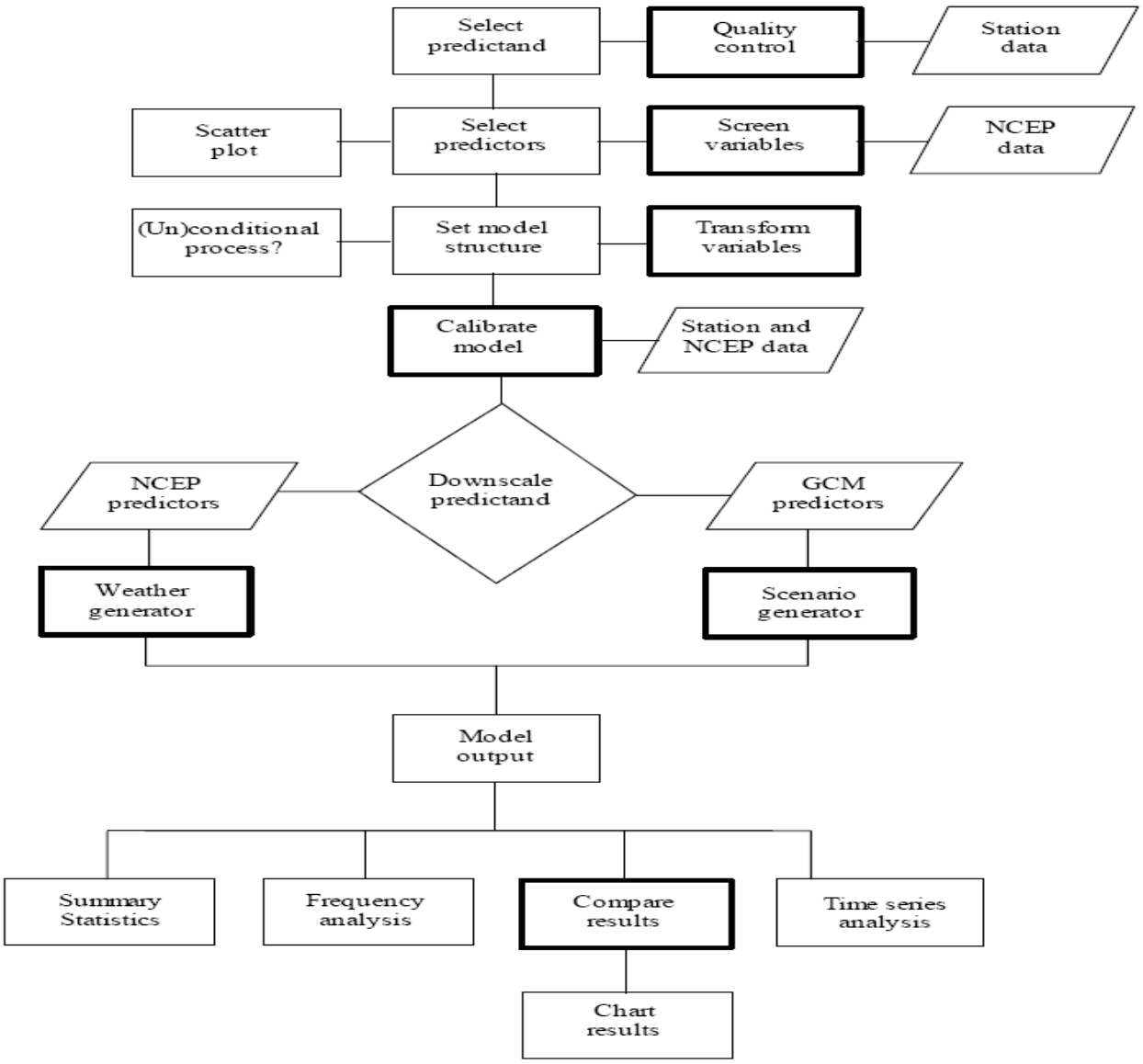

Figure 2.4 SDSM version 4.2 climate scenario generation *(Wilby & Dawson, 2007)*

Advantage of using SDSM in downscaling climate parameters as stated by (Reza, 2014):

- It has been widely used in many watershed scales over arrange of different climatic condition in the world by producing reliable results.
- It is user friendly and freely available software which can be downloaded from (http://co-public.lboor.ac.uk/cocwd/SDSM/).
- It generates ensembles which enable the user to implement uncertainty analyses.

2.10.1. NCEP/NCAR predictor data

National Center for Environmental Prediction (NCEP) is a joint product with the National Center for Atmospheric Research (NCAR). It has all the gridded predictor variables to use in calibration and validation in SDSM. The horizontal grid resolution in NCEP atmospheric predictors is 2.5° latitude by 2.5° longitude (Reza, 2014). NCEP/NCAR provided a 40-year record of global analysis of atmospheric predictors. The 26 predictor variables are produced by state-of-art assimilation of all available observed weather data into a global climate forecasting model that produces interpolated grid output of many weather variables (Reza, 2014). The data can be obtained from (http://www.cics.uvic.ca/scenarios/sdsm/select.cgi).

Table 2.4 large scale predictor variable NCEP available in SDSM *(Wilby & Dawson, 2007)*

NO	Predictor variable	Predictor description	NO	Predictor variable	Predictor description
1	ncepmslpaf	Mean sea level pressure	14	ncepp5zhaf	500hpa divergence
2	ncepp_faf	Surface airflow strength	15	ncepp8_faf	850hpa airflow strength
3	ncepp_uaf	Surface zonal velocity	16	ncepp8_uaf	850hpa zonal velocity
4	ncepp_vaf	Surface meridional velocity	17	ncepp8_vaf	850hpa meridional velocity
5	ncepp_zaf	Surface velocity	18	ncepp8_zaf	850hpa vorticity
6	ncepp_ thaf	Surface wind direction	19	ncepp850af	850hpa geopotential height
7	ncepp_zhaf	Surface divergence	20	ncepp8thaf	850hpa wind direction
8	ncepp5_faf	500hpa airflow strength	21	ncepp8zhaf	850hpa divergence
9	ncepp5_uaf	500hpa zonal velocity	22	ncepr500af	Relative humidity at 500hpa
10	ncepp5_vaf	500hpa a meridional velocity	23	ncepr850af	Relative humidity at 850hpa
11	ncepp5_zaf	500hpa vorticity	24	nceprhumaf	Near surface relative humidity
12	ncepp500af	500hpa geopotential height	25	ncepshumaf	Surface specific humidity
13	ncepp5thaf	500hpa wind direction	26	nceptempaf	Mean temperature at 2m

2.10.2. HadCM3 model

In this study, the Hardley Center Couple Model, Ver.3.0 (HadCM3) Model is used for the GCM downscaling, which is a coupled oceanic-atmospheric general circulation model. Wilby and Dawson (2007) reported that the techniques and HadCM3 model is a coupled atmosphere-ocean general circulation model (AOGCM) which is composed of the atmospheric model, HadAM3, and the ocean model, HadOM3. The horizontal resolution of atmospheric component is 2.5° by 3.75° while the oceanic component's resolution is 1.25° by 1.25°. the simulation of HadCM3 assumes year length in 360-day calendar which 30 days per month. The model was developed in

1999 and was the first coupled atmosphere-ocean which did not require flux adjustments (IPCC, 2007). The adjustments have to be done artificially by the other climate change models to prevent them from drifting unrealistic climate states (Reza, 2014). The highly quality of current climate simulation using HadCM3 model, made it one of the most efficient and reliable model in climate change studies. HadCM3 ranks highly compared to other models and was used extensively in IPCC through the third and fourth assessment. It has the capability to capture the time dependent fingerprint of climate change in response to natural and anthropogenic (Reza, 2014) which has made it a particularly useful tool in studies of climate changes.

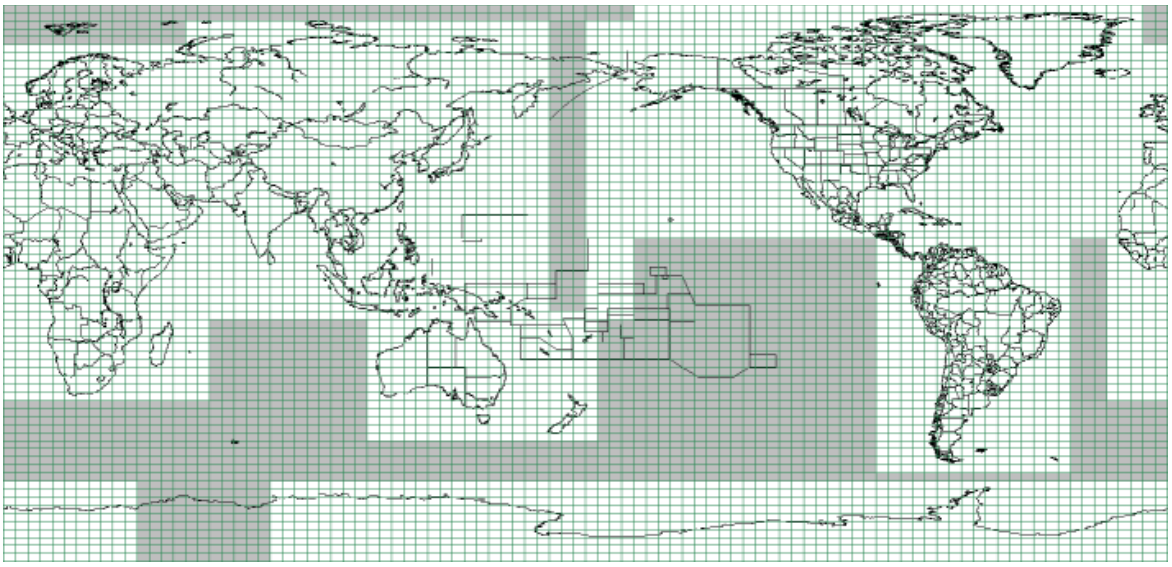

Figure 2.5 Data grid box for HadCM3 model (http://www.cccsn.ec.gc.ca/?page=pred-hadcm3)

The horizontal atmosphere resolution produces a total grid of 96 × 73 grid cells for the whole world which the surface resolution varies from 417 km × 278 km at the Equator to 295 km × 278 km at 45° of latitude (Reza, 2014). The HadCM3 data can be downloaded from IPCC and also the Canadian Climate Impact Scenarios and CCIS provides all the NCEP and HadCM3 data in the grid box based on the value of latitude /longitude of the study area so that the grid box provides a zip file contains three directories: NCEP-1961-2001, H3A2a-1961-2099 and H3B2a-1961-2099.

NCEP-1961-2001: It contains all the observed predictor data produced from NCEP/NCAR. There is a difference in the resolution in grid cells of NCEP and HadCM3, all the 41 years of

daily observed predictor data were interpolated to the same grid as HadCM3 and then the data were normalized.

H3A2a-1961-2099: It contains 139 years of daily GCM predictor data assuming a characteristic of scenarios with higher rate of GHG emissions in combination with higher sulphate and other aerosol emissions. HadCM3 A2a data was normalized over the 1961-1990 period.

H3B2a-1961-2099: This directory contains 139 years of daily GCM predictor data assuming a characteristic of scenarios with higher rates of GHG emissions in combination with lower rate of sulphate and other aerosol emissions. HadCM3 B2a data normalized over the 1961-1990 period.

The normalization is done by dividing each time slice of future (2011-2040, 2041-2070 and 2071-2099) to the current period (1961-1990).

2.10.3. Setting the model parameter

The **Year length** is set to the normal calendar year (366) which allows 29 days in February every fourth year (i.e. leap year) is used whenever dealing predictand and NCEP predictor whereas the year length of 360 days which allows 30 days in every month is used in the scenario generation part since HadCM3 uses model years consisting of 360 days.

The **Event Threshold** is set to zero for temperature and 0.1mm/day for precipitation to treat trace rain days as dry days. Missing data identifier is the code assigned to missing data in all input with the code (-999) the value will be skipped. Negative values allowed unconditional processes in the downscaling model such as for minimum temperature.

The **Model Transformation** is applied to the predictand in conditional models. The default (None) is used for the predictand that is normally distributed as in the case of daily temperature. The alternatives Fourth root, Natural log and Inverse Normal are used for precipitation since the model is conditional and the data is skewed.

Variance inflation controls the magnitude of variance inflation in the downscaled daily weather variables. This parameter can be adjusted during the calibration period to force the model replicate the observed data. The default value produces approximately normal variance inflation prior to any transformation and is applied to maximum and minimum temperature. Larger values

increase the variance of downscaled properties. Variance inflation is de-activated by setting the parameter to zero.

Bias correction compensates for any tendency to over or under estimate the mean of conditional processes by the downscaling model. The default value is 1, indicating no bias correction.

2.10.4. Screening of downscaling predictor variable

The purpose of the screen variables option is to assist in the choice of appropriate downscaling predictor variables for model calibration. The choice of predictor variables is one of the most influential steps in the development of statistical downscaling procedure. Identifying empirical relationships between gridded predictors such as station mean sea level pressure and single site predictands such as station precipitation is central to all statistical downscaling. SDSM performs three supporting tasks: seasonal correlation analysis, partial correlation analysis and scatterplots. The approach is done by choosing all predictors and run the explained variance on a group of twelve at a time. Out of the groups, those predictors which have high explained variance are selected. Then partial correlation analysis is done for selected predictors to see the level of correlation with each other. There could be a predictor with a high explained variance but it might be very highly correlated with another predictor. This means that it is difficult to tell this predictor will add information to the process and therefore it will be dropped from the list. Finally, the scatterplot indicates whether this result is due to a few outliers or it is a potentially useful downscaling relationship.

2.10.5. Model calibration

The Calibrate Model process constructs downscaling models based on multiple regression equations, given daily weather data the predictand and regional scale, atmospheric predictor variables. The model structure for calibration can be specified by selecting the process either unconditional or conditional. In conditional process, there is an indirect link assumed between the data and the predictors and local weather such as local precipitation amounts depend on wet/dry day occurrence. Whereas the unconditional process assumed a direct link to the predictors. The model structure is set to unconditional for maximum and minimum temperature and conditional for precipitation. The model type determines whether individual downscaling models will be calibrated for each calendar months, climatological season or entire year. The model is structured as a monthly model for both precipitation and temperature downscaling, in

which case twelve regression equations are derived for twelve months using different regression parameters for each month equation. Finally, the data period should be set in order to specify the start and end date of the analysis.

2.10.6. Weather and scenario generator

The Weather Generator operation produces ensembles of synthetic daily weather series given observed or NCEP re-analysis atmospheric predictor variables and regression model weights produced by the calibrate model operation. It enables the verification of calibrated models by assuming the availability of independent data as well as the synthesis of artificial time series representative of present climate conditions. It can also be used to reconstruct predictands or to infill missing data.

The Scenario Generation operation produces ensembles of synthetic daily weather series given the regression weight produced during the calibration process and the daily atmospheric predictor supplied by a GCM (either under the present or the future greenhouse gas forcing). Twenty ensembles of synthetic daily time series were produced for the two emission scenarios (HadCM3 A2s & B2a) for a period of 139 years (1961 to 2099). Finally, the mean of twenty ensembles for the specified period is produced for the maximum and minimum temperature and precipitation.

2.11. Review of Previous Study

The major problems that restrains development in the awash river basin are recurrent large-scale flooding and drought (Tessema, 2011). The basin faces an occurrence of drought on average, once every two years and causes a great deal of damage to crop and livestock (Tessema, 2011).

The effect of climate change i.e. frequent droughts, flash flood and erratic rainfall combined with rapid population growth are contributing to a shortage of natural resources, thereby threating the traditional way of life in the region (SDR-ASAL, 2014). Commonly annual rainfall is low in arid and semi-arid regions (Akker, 2015). Some high intensity rainfall could produce local floods, but most torrential runoffs come from upland humid regions of Awash basin causing lowland inundation and sedimentation.

As various documents have indicated that in Afar, including the study area, the rainfall patterns have changed over the past decades, particularly in terms of timing and duration. The frequency

of drought is increasing particularly over the past two decades. According to Hare (1983), in areas with coefficient of variation greater than 30% the rainfall is highly variable, and the areas are vulnerable to drought. This type of situation is very common in the pastoral and agro-pastoralist communities including the study area (Hare, 1983).

The arid and semi-arid parts of Africa including Afar pastoralist region have been characterized by frequent droughts with high animal mortality followed by famine and high death rates in the human population (Fasil et al, 2001).

Hailemariam (1999) evaluated the impacts of climate change on water resources of the Awash River Basin in Ethiopia using the outcomes of general circulation models (GCMs) of the Canadian Climate Center (CCCM) and the Geophysical Fluid Dynamics Laboratory (GFD3), for a doubling of CO_2 condition, and from the Geophysical Fluid Dynamics Laboratory (GFDL) models GF01, GF4, AND GF7, for a transient increase of CO_2, for the projection of awash river runoff in the future. Their study shows that runoff decreases significantly in warmer and drier scenarios over the whole basin. A 20% decrease in rainfall coupled with a 2^o C increase in temperature showed in a 41% decrease in the annual runoff. A temperature increase of 2^o C without precipitation change showed in a 9% decrease in annual runoff. Likewise, an increase in precipitation by 10% showed a 2 to 4^o C increase in temperature and result in a surplus of runoff ranging from 4 to 12%. Hailemariam (1999) noted that the CCCM and GFD3 models for a doubling of CO_2 projected a temperature increase of 2.4 and 3.0^o C, respectively. GFD3 showed a 5% increase in precipitation, while CCCM indicates a 2% decrease with doubling of CO_2. They also found out that the result of the GCM scenarios for change in runoff decrease in a ranging from 10 to 34% for CCCM, GFD3, GF4, GF7, and GF01. They noted that the Awash River Basin significantly affected by the changed climate that considerably result water deficit in the basin. They suggested that global warming would result in a general increase in dryness, which would decrease water availability in the basin.

Chapter 3. DESCRIPTION OF THE STUDY AREA

3.1. Description of The Study Area

3.1.1. Location

Awash River rises on the high plateau in Ethiopia and flows along the rift valley into the Afar triangle, and terminates in Lower Awash Sub Basin at Lake Abbe on the border with Djibouti. Lower Awash Sub-Basin is labeled by the name of the main river of the sub-basin, Awash River. Geographically Lower Awash Sub Basin is located between 10^0 34' to 12^0 21' North latitude and 39^0 52' to 41^0 49' East longitude with an altitude range of 214.54 to 1537.57 meters above sea level. Lower Awash Sub Basin extends to 2302670 hectares limited within the Afar region, it, however, borders with, Amhara Region in the west, and Somali Region in the south east of the sub basin. The sub-basin inscribes three administrative zones, coded 01, 04 and 05 and nine districts, labeled Dubti, Assaita, Afambo, Mile, Adear, Dewe, Telalak, Chifra and Ewa, and the regional capital Semera-Logia city administration.

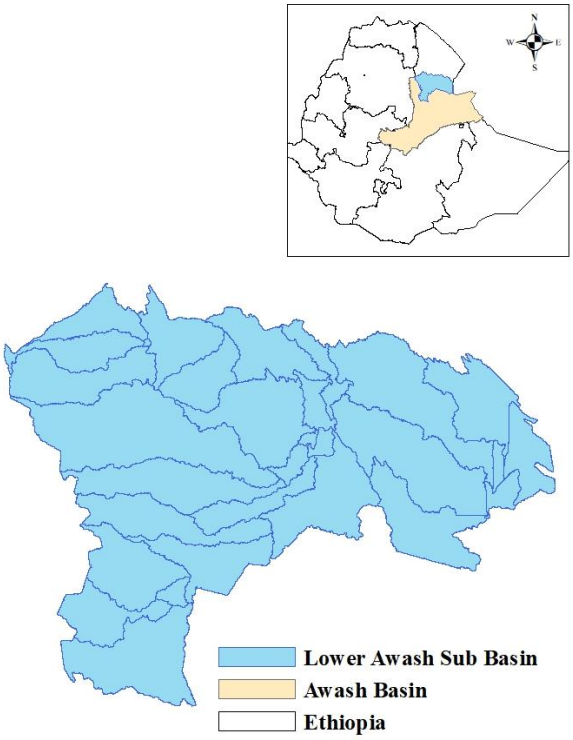

Figure 3.1 Location map of Lower Awash Sub-basin

3.1.2. Topography

The lower awash sub basin consists of various land forms, all slope classes: undulating plain, rolling plain, hilly and mountain. Dewe, Telalak, Adear and Mille weredas are characterized dominantly with hills and mountain land forms, with patches of rolling plain and flat land units. These hills and mountain ridges are geologically weathered rocks covered by scattered to dense shrubs. Whereas Chifra, Ewa, Dupti, Asaita and Afambo weredas are characterized dominantly with lowland flat lands.

The elevation of the project area ranges from 214 up to 1537.57meters above sea level. The highest elevation within the sub basin is 1537.57 metres and the elevation at the lowest point of the sub basin is 214 meters above sea level. Dewe, Telalak, Chifra and Ewa weredas contribute a little high altitude, bordering Amhara Region. However, high lands account only 0.01% of the area of the sub basin. Almost all, 99.99%, of the sub basin is lowland; Addar, Mille, Dubti, Aysaita and Afambo lay at lower altitude, relatively than the rest Districts, of the sub basin, below 500 meters, except few isolated hills mountain ridges. The difference in altitude and therefore of climate conditions have provided the scene for a wide variety of cropping patterns in agriculture.

3.1.3. Slope

Slopes within the sub basin range from flat to very steep, in excess of 0-3 percent in the more lowland areas; the land escape of the watershed is characterized by flat plain, which constitutes 62.10 % of the sub basin area (ADSWE, 2012). Rolling plain land forms also constitute the second significant land form next to flat plain lands contributing 12.76%, mainly distributed starting from middle to the upper part of the watershed. Usually the rolling plains follow immediately after the foot of the hill. Hill and mountain land forms, contribute respectively only 5.31 and 1.65 percent of the sub-basin area (ADSWE, 2012).

3.1.4. Drainage

The relief of the sub basin is mainly rolling plain, which is the dominant landform. The physiographical characteristics of a watershed influence in great measure its hydrological response and especially the flow regime during floods and periods of drought. The concentration time, which characterizes the speed and intensity of the sub basin's reaction to a stress (rainfall),

is influenced by the morphologic characteristics. The shape of the sub basin is somewhat short from south to north with relatively large width east to west.

The drainage pattern has something to do with erosion hazard and sediment yield. The River Awash River rises in Oromia Region and terminates in Lower Awash Sub Basin at Lake Abe. The river passes through a number of districts along its route in the sub basin. The drainage pattern of the sub basin is ordered by this main river, to which all other drainage lines are tributaries. Most of the tributaries of the main river Awash are long; joining to the main river channel in much kilometer's travel rise from different parts of Amhara Region. This indicates that all parts of the watershed don't contribute runoff to the main channel of the river simultaneously and significantly affect the flood flow characteristics of the sub basin.

3.1.5. Climate

The Lower Awash Sub Basin receives bi-modal type of rainfall pattern. The main rainy season occurs from June to September when the Inter Tropical Convergence Zone (ITCZ) is in the north. During this season, the south west equatorial westerlies from the Atlantic Ocean cause higher rainfall over Ethiopia. Most of this relief rain is received in the South West Highlands, decreasing to the north east and east, when the air stream descends. Thus, the study area is the lee ward side of this wind pattern since it is found in the eastern part of Ethiopia. The small rainy season occurs in March and April when the ITCZ lies across southern Ethiopia. During this period, the moist easterly and southerly winds from Indian Ocean gives rain to the east including the project area (ADSWE, 2012).

Rainfall data was obtained from the meteorological stations in and near the sub basin. The mean annual precipitation ranges from 150.63-1000 mm. The mean areal precipitation of the study area is 424.71 mm. The mean annual maximum temperature varies in the study area from 29.7 to 36°C and the mean annual minimum temperature from 14.5 to 22.7°C. The annual daily average sunshine duration ranging from 7 to.8 hours. The average daily mean wind speed in the study area ranging from 0.9 to 2.91m/s. The relative humidity value ranges from 47 to 65%. The evapotranspiration (PET) of the basin increases from western part towards the eastern part of the project area. Its average annual PET range is 1501.03-2012.67mm.

The study area has three distinct seasons: the small rainy season from March to April and the main rainy season from July to September with the rainfall peak occurring in July and August and the remaining months are dry season. Based on the aridity index which considers the balance between rainfall and potential evapotranspiration, the project area is classified as arid (47%), semi-arid (48.2%) and dry sub-humid (4.8%). Thus, the total area of the project is considered as dry land (ADSWE, 2012).

3.1.6. Land Use/ Cover

The farming system in the watershed was dominantly livestock rearing, which was centuries old system. Accordingly, the major land use types of the sub basin, constituted over 40% of the sub basin area, were expected to grazing and browsing land, covered by shrubs, bushes and grass. The second dominant land cover, constituted 49.02%, was exposed surfaces, rocks and soils.

3.2. Data Availability

3.2.1. Metrological data

Metrological data for Lower Awash River Basin were collected from the Ethiopian National Metrological Service Agency (NMSA) at Addis Ababa office. The daily metrological data collected were precipitation, maximum and minimum temperature, relative humidity, wind speed and sunshine hours. This Metrological data used for purpose of downscaling the GCM data using Statistical Downscaling Model (SDSM) and used as input to the SWAT model to develop the hydrological model.

Table 3.1 List of stations name, location and meteorological variables

Station Name	Elevation	Latitude	Longitude	Year
Adayitu	507	11.11	40.783	1983-2015
Assaita	430	11.53	41.5298	1983-2015
Dubti	376	11.723	41.01	1983-2015
Logiya	393	11.65	41	1983-2015
Mille	487	11.4256	40.77	1983-2015

3.2.2. Hydrological data

Monthly stream flow data for Lower Awash River Basin were sourced from Hydrology Directorate of the Ministry of Water, Irrigation and Electricity. The stream flow data were collected for period of 1990-2015 at the hydrological gauging station of the basin of Dubti Outlet. This stream flow data used for calibrate and validating the SWAT model simulation.

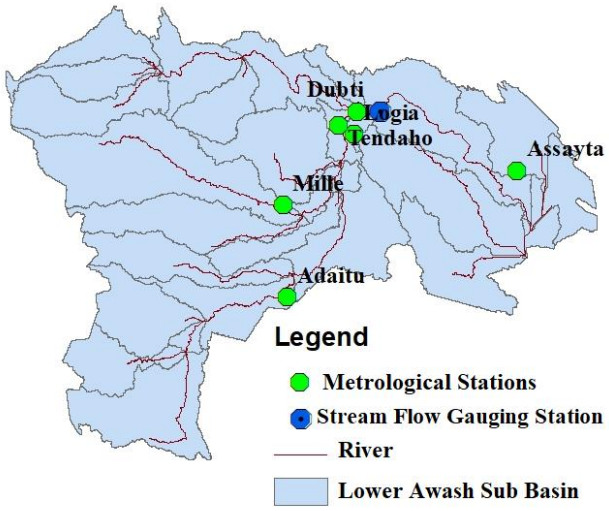

Figure 3.2 Hydrological and Meteorological stations of Lower Awash Sub Basin

3.2.3. Spatial data

The Digital Elevation Model (DEM) for this area was downloads from Open Topography high-resolution topography data and tools (www.opentopography.org), which provides the NASA Satellite Radar Topographic Mission (SRTM) at a raster resolution of 30m Digital Elevation Data for the entire world. The DEM provide the spatial framework for the SWAT model. The data is a basic input of the catchment delineations, stream flow networks, flow accumulation, slope and other variables.

Land use /land cover used for model were sourced from Ministry of Water, Irrigation and Electricity, GIS department at Addis Ababa office, which was extracted from Awash basin master plan study between 1999 and 2000.

Soil map of Ethiopia published at 1:1,000,000 scales (FAO, 1998), were used to classify different types soil properties for SWAT model and its sourced from Ministry of Agriculture, GIS department at Addis Ababa office.

3.2.4. Global climate data

Climate scenario data used for Statistical Downscaling Model (SDSM) were obtained from the Canadian institute for climate studies for model output of HadCM3 of two special report on emissions scenarios A2 and B2 produced by greenhouse gas, sulphate aerosol, and solar forcing. Observed and modelled predictors come respectively from the National Center for Environmental Prediction (NCEP) reanalysis and the Hardley Center Couple Model (HadCM3). From the Canadian institute for climate studies website (http://www.cics.uvic.ca) the NCEP and HadCM3 data downloaded in the grid box based on the value of latitude and longitude in the study area. The grid box provides a zip file contains three directories: NCEP-1961-2001, H3A2a-1961-2099 and H3B2a-1961-2099.

Chapter 4. METHODOLOGY

General Methodology

The general methodology for this study can be described by the following flow chart;

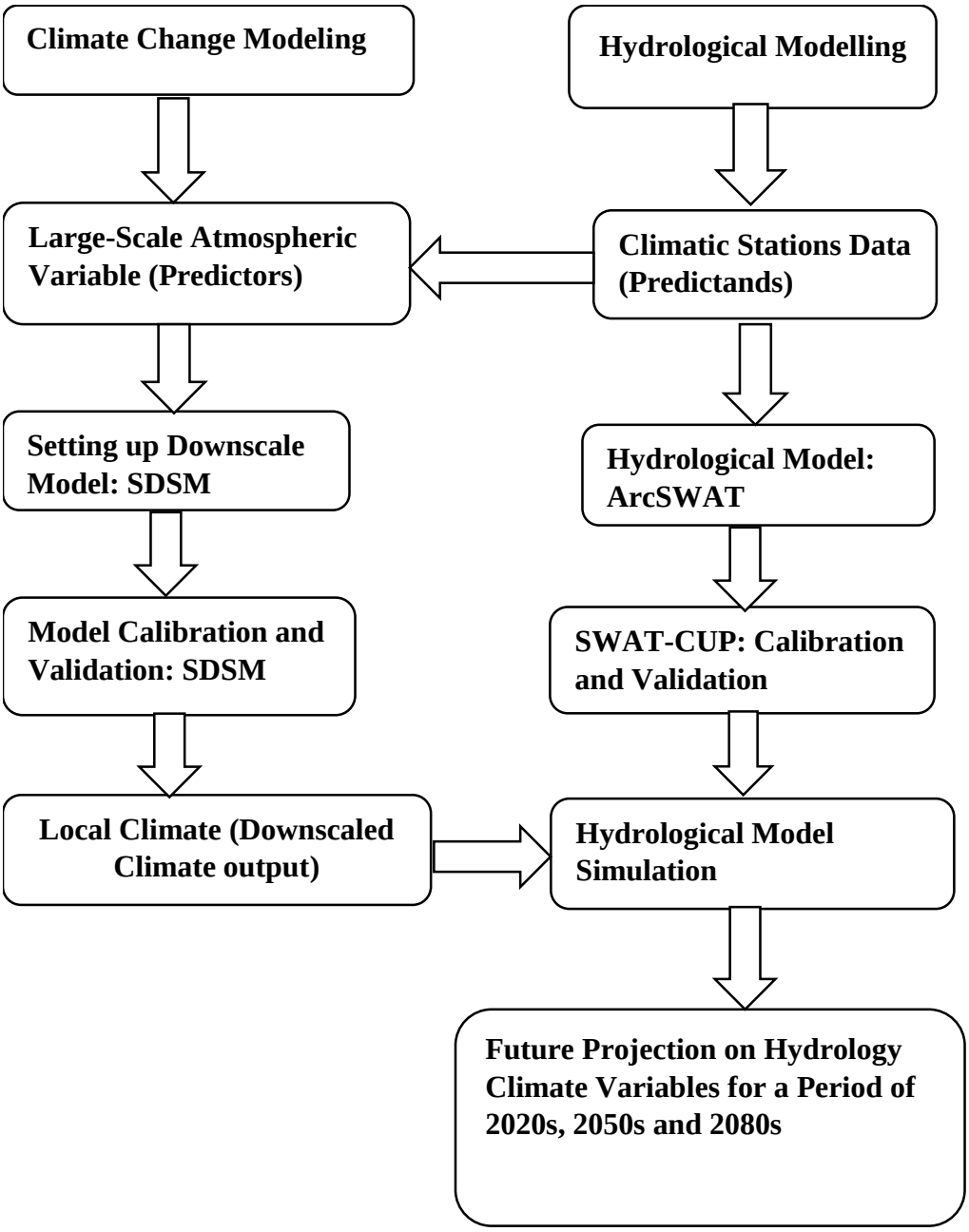

Figure 4.1 general methodology flow chart

4.1. Climate Change Downscaling

The Statistical Downscaling Model (SDSM Ver.4.2), developed by Robert L. Wilby and Christian W. Dawson (Wilby & Dawson, 2007) was used in this study to construct climate change scenarios for Lower Awash Sub Basin in Ethiopia. SDSM uses a multi linear regression method to link large scale climate variables (predictors) as provided by Global Climate Models (GCMs) simulations with daily climatic data at local site (predictands) (Wilby & Dawson, 2007). The predictor variables provide daily information concerning the large-scale state of the atmosphere, while the predictand describes conditions at the site scale which could be used as input for hydrological models.

The three rain gauge stations chosen for the spatial downscaling were based on temporal and spatially coverage along with completeness and quality of data at each location. Daily time series data are used for all the variables to run the statistical downscaling in Statistical Downscaling Model (SDSM).

4.1.1. Data used in SDSM

The data used for the climate change downscaling contain daily climatic parameters (precipitation, maximum and minimum temperature) as predictand variables at a local scale of Lower Awash Sub Basin. The Hardley Center Couple Model, Ver.3.0 (HadCM3) Model was used for the GCM downscaling. HadCM3 Model is a coupled atmosphere-ocean general circulation model (AOGCM) developed at the Hadley Centre in the United Kingdom. It is widely used for climate change impact studies and can be easily downscaled using SDSM. The predictor variables contain the historical NCEP data with the specific climate change scenarios H3A2a (medium-high) and H3AB2a (medium-low) inside the spatial grid cell of the large-scale climate change GCM-HadCM3 model (Kabiri, 2014).

4.1.2. Climatic stations data (Predictands)

Predictand daily time series data precipitation and temperature are used for Lower Awash Sub Basin study area. Data missing may affect the result of SDSM and it is important to run statistical downscaling with reliable data. Thus, linear interpolation regression was used to fill missing data for the whole stations. Four rain gage stations found inside the project area but one of the stations (Mille) did not have sufficient data to downscale. As a result, the three rain gauge stations (Assaita, Dubti and Logiya) were selected to downscale the variables by using SDSM

downscaling. The Assaita and Dubti stations was used to downscale daily precipitation, maximum and minimum temperature by using SDSM downscaling. Unlike the two stations, only daily precipitation data were used for Logiya Stations to downscale Precipitation by using SDSM. The selected stations for downscaling are listed in table 4.1.

Table 4.1 stations used for downscaling in Lower Awash Sub Basin.

Station Name	Elevation	Latitude (degree)	Longitude (degree)	Period (year) PCP	Period (year) TempMax	Period (year) TempMin
Assaita	430	11.53	41.53	1985-20016	1985-2016	1985-2015
Dubti	376	11.72	41.01	1983-2015	1983-2016	1987-2015
Logiya	393	11.65	41.00	1983-2016	no data	no data

4.1.3. Large scale atmospheric variable (Predictors)

Observed and modelled predictors come respectively from the National Center for Environmental Prediction (NCEP) reanalysis and the Hardley Center Couple Model (HadCM3). The Canadian Institute for climate studies website provides all the NCEP and HadCM3 data and it can be downloaded from (http://www.cics.uvic.ca/scenarios/sdsm/select.cgi) in the grid box based on the value of latitude and longitude of the study area. The grid box provides a zip file contains three directories: NCEP-1961-2001, H3A2a-1961-2099 and H3B2a-1961-2099.

Observed large scale NCEP reanalysis data are prepared by the Canadian Institute for climate studies under Canadian Climate Impact Scenarios (CCIS) project. NCEP data contains 26 predictor daily atmospheric variables which are extracted from the grid box covering the predictands. The grid box (30X, 11Y) for Dubti and Logiya and grid box (30X, 12Y) for Assaita consist of large scale predictor (NCEP, H3A2a and H3B2a) used for this study area.

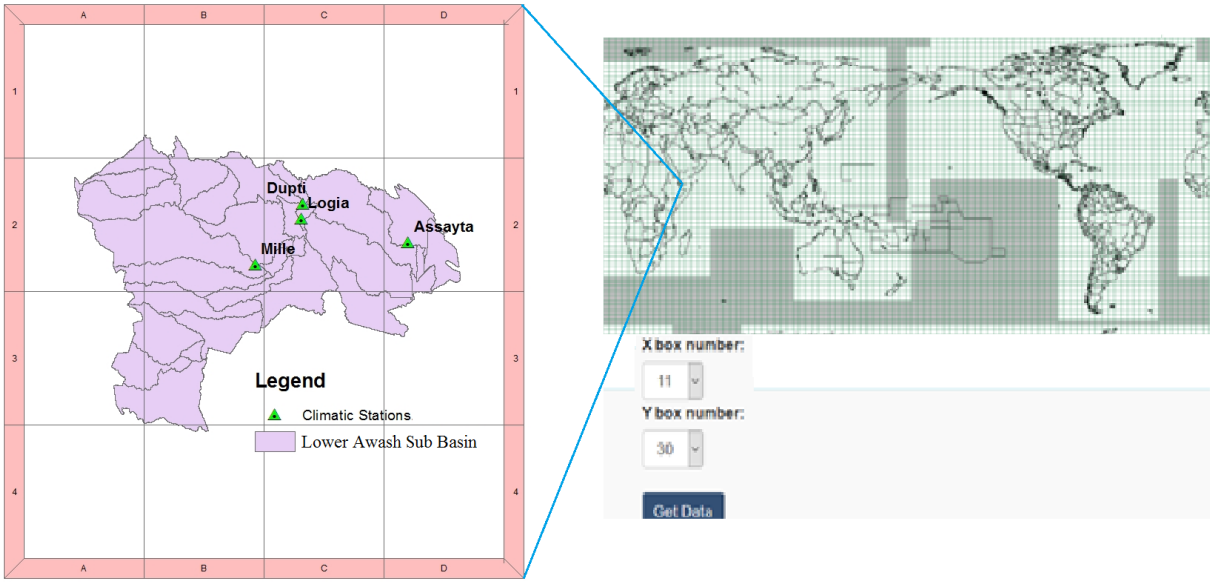

Figure 4.2 The Grid box large scale predictor (NCEP, H3A2a and H3B2a) data used for this study area.

4.1.4. SDSM for lower awash sub basin

Precipitation and maximum and minimum temperature as predictand data are downscaled for this study area. SDSM needed to be set up for the various predictands to get a reliable result. This task run quality control checks of the observed daily climate data to identify the gross data error and missing data. It also transforms a fourth root model function to normalize the distribution and make it less skewed to low precipitation values. The forth root transformation is used as distribution of data is skewed.

Setting the Model Parameter

The **Year length** is set to the normal calendar year (366) which allows 29 days in February every fourth year (i.e. leap year) is used whenever dealing predictand and NCEP predictor whereas the year length of 360 days which allows 30 days in every month was used in the scenario generation part since HadCM3 uses model years consisting of 360 days.

The **Event Threshold** is set to zero for temperature and 0.3mm/day for precipitation to treat trace rain days as dry days. Missing data identifier is the code assigned to missing data in all input with the code (-999) the value will be skipped. Negative values allowed unconditional processes in the downscaling model such as for minimum temperature.

The **Model Transformation** is applied to the predictand in conditional models. The default (None) was used for the predictand that is normally distributed as in the case of daily temperature. The Fourth root transformation is applied for precipitation as distribution of data is skewed.

Variance inflation controls the magnitude of variance inflation in the downscaled daily weather variables. This parameter can be adjusted during the calibration period to force the model replicate the observed data. The default value (i.e. 12) produces approximately normal variance inflation prior to any transformation and is applied to maximum and minimum temperature. Whereas for precipitation this parameter adjusted during the calibration process and set to 18.

Bias correction compensates for any tendency to over or under estimate the mean of conditional processes by the downscaling model. The default value (i.e. 1), is applied to maximum and minimum temperature for the whole station. However, during downscaling Assaita Station daily precipitation data this parameter was adjusted in order to match the mean of the conditional process and set to 0.85 accordingly.

4.1.5. Screening predictor variable

The purpose of the **Screen Variables** option is to assist in the choice of appropriate downscaling predictor variables for model calibration. The choice of predictor variables is one of the most influential steps in the development of statistical downscaling procedure. Identifying empirical relationships between gridded predictors and single site predictands is central to all statistical downscaling. SDSM performs three supporting tasks: seasonal correlation analysis, partial correlation analysis and scatterplots. The approach is done by choosing all predictors and run the explained variance on a group of twelve at a time. Out of the groups, those predictors which have high explained variance are selected. Then partial correlation analysis is done for selected predictors to see the level of correlation with each other.

The application of these empirical predictor-predictand relationships of the observed climate is to downscale ensembles of the same local variables for the future climate. This is based on the assumption that the predictor-predictand relationships under the current condition remain valid under future climate conditions.

The predictors are which high correlated with the predictand ($p < 5\ \%$) have been chosen for future prediction. The selected large-scale predictors for all the local predictands are listed in table 4.2.

Table 4.2 list of selected large-scale predictor variables for predicting daily precipitation, maximum and minimum temperature

Stations	Predictands	Predictors (NCEP reanalysis data)	Predictor variable	Partial r
Assaita	PCP	Mean sea level pressure	ncepmslpaf	-0.11
		500hpa zonal velocity	ncepp5_uaf	0.109
		850hpa airflow strength	ncepp8_faf	0.127
		850hpa geopotential height	ncepp850af	-0.146
	TempMax	Mean sea level pressure	ncepmslpaf	-0.204
		500hpa airflow strength	ncepp5_faf	0.105
		500hpa geopotential height	ncepp500af	0.243
		500hpa wind direction	ncepp5thaf	0.108
		850hpa divergence	ncepp8zhaf	0.114
		Near surface relative humidity	nceprhumaf	-0.17
		Surface specific humidity	ncepshumaf	0.188
		Mean temperature at 2m	nceptempaf	0.521
	TempMin	500hpa airflow strength	ncepp5_faf	0.116
		500hpa geopotential height	ncepp500af	0.222
		850hpa vorticity	ncepp8_zaf	0.123
		Relative humidity at 850hpa	ncepr850af	0.129
		Surface specific humidity	ncepshumaf	0.172
		Mean temperature at 2m	nceptempaf	0.329
Dubti	PCP	Surface velocity	ncepp_zaf	-0.093
		500hpa airflow strength	ncepp5_faf	0.083
	TempMax	Mean sea level pressure	ncepmslpaf	-0.232
		Surface velocity	ncepp_zaf	-0.237

		500hpa geopotential height	ncepp500af	0.176
		500hpa wind direction	ncepp5thaf	0.202
		850hpa meridional velocity	ncepp8_vaf	0.118
		850hpa divergence	ncepp8zhaf	0.115
		Relative humidity at 500hpa	ncepr500af	0.109
		Surface specific humidity	ncepshumaf	0.548
		Mean temperature at 2m	nceptempaf	0.236
	TempMin	Surface velocity	ncepp_zaf	-0.223
		500hpa wind direction	ncepp5thaf	0.153
		850hpa zonal velocity	ncepp8_uaf	0.157
		Surface specific humidity	ncepshumaf	0.43
Logiya	PCP	Surface specific humidity	ncepshumaf	-0.016
		Mean temperature at 2m	nceptempaf	0.088

4.1.6. Model calibration

The **Calibrate Model** process constructs downscaling models based on multiple regression equations, given daily weather data the predictand and regional scale, atmospheric predictor variables. The model structure for calibration can be specified by selecting the process either unconditional or conditional.

The model structure is set to unconditional for maximum and minimum temperature and conditional for precipitation. Unconditional process can be established for the temperature data as a direct link to the predictor assumed. In a conditional process, there is an indirect link assumed between the data and predictors, hence some local parameters of precipitation would estimate such as wet/dry day occurrences.

In order to run the calibration in SDSM, the NCEP-Re analysis data set is used in compliance with the specified year period for each predictand to identify the empirical linear regression of the large-scale predictors with the local sites. The historical data of predictands are split into two parts: the first part is used for calibration and the second part of the data is used for the validation

as an independent dataset. A best performed calibration results are obtained with correlation and standard errors for every month. Table 4.3. shows the calibration and validation period length for variety of predictands used in SDSM.

Table 4.3 Time series for calibration and validation in SDSM downscaling

Station name	**predictands**	**Available data period (year)**	**Calibrated period (year)**	**Validated period (year)**
Assaita	PCP	01/01/85-12/31-16	1985-2001	1995-2001
	TempMax	01/01/85-12/31/16	1985-2001	1995-2001
	TempMin	01/01/85-08/25/15	1985-2001	1995-2001
Dubti	PCP	01/01/83-03/28/15	1983-2001	1995-2001
	TempMax	01/01/83-03/31/15	1983-2001	1995-2001
	TempMin	12/11/87-03/31/15	1983-2001	1995-2001
Logiya	PCP	01/01/83-12/28/16	1983-2001	1995-2001

4.1.7. Weather generator

The **Weather Generator** operation produces ensembles of synthetic daily weather series given observed or NCEP re-analysis atmospheric predictor variables and regression model weights produced by the **Calibrate Model** operation. It enables the verification of calibrated models by assuming the availability of independent data as well as the synthesis of artificial time series representative of present climate conditions. It can also be used to reconstruct predictands or to infill missing data. Twenty ensembles of synthetic daily time series were produced for the NCEP re-analysis normalized period (as specified in table 4.3). Finally, the mean of twenty ensembles for the specified period is produced for the precipitation and maximum and minimum temperature. The results of downscaling indicate that the model run is satisfactorily validated between simulation data and observed data.

Precipitation (Assaita)

The downscaled precipitation value at the Assaita stations could not replicate the observed value compared to maximum and minimum temperature. Given the fact that, daily precipitation

amounts at individual sites are relatively poorly resolved by regional scale predictions. According to Trope (2005) rainfall prediction has a larger degree of uncertainty than those for temperature. Rainfall is highly variable in space and so the relatively coarse spatial resolution of the current generation of climate model is not adequate to fully capture that variability. Bate (2008) stated that, climate model simulation of precipitation has improved over time but it is still a problematic. The total mean annual precipitation downscaled value at the Assaita stations shows a 1.3% difference compared to observed value. The model highly overestimated in some months specially at the month of November, December and January and underestimates in some other months. The result however, can be taken as satisfactory.

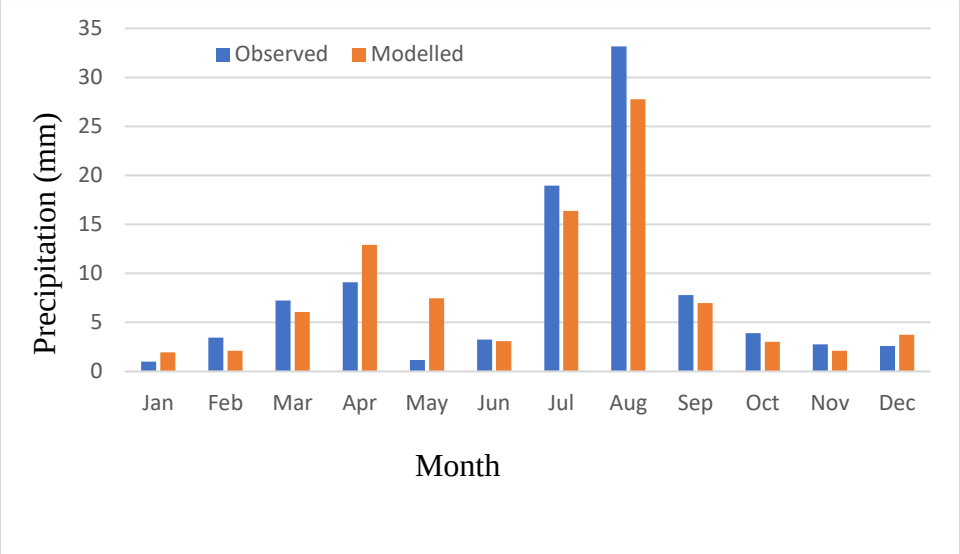

Figure 4.3 Daily mean precipitation between observed and calibrated at Assaita station

Maximum Temperature (Assaita)

The results of downscaling maximum Temperature at the Assaita station indicate that there is satisfactory agreement between simulation data and observed data. As shown in Figure 4.4, observed and downscaled values show similar pattern. The model in downscaling the annual mean maximum temperature shows a slightly decrease of 0.01%. The monthly downscaled temperature shows slightly lower value from the months of October to January by 0.07-0.16% and from the months of June to September by 0.04-0.22 % and slightly higher for the months of February to May by 0.01- 0.26%.

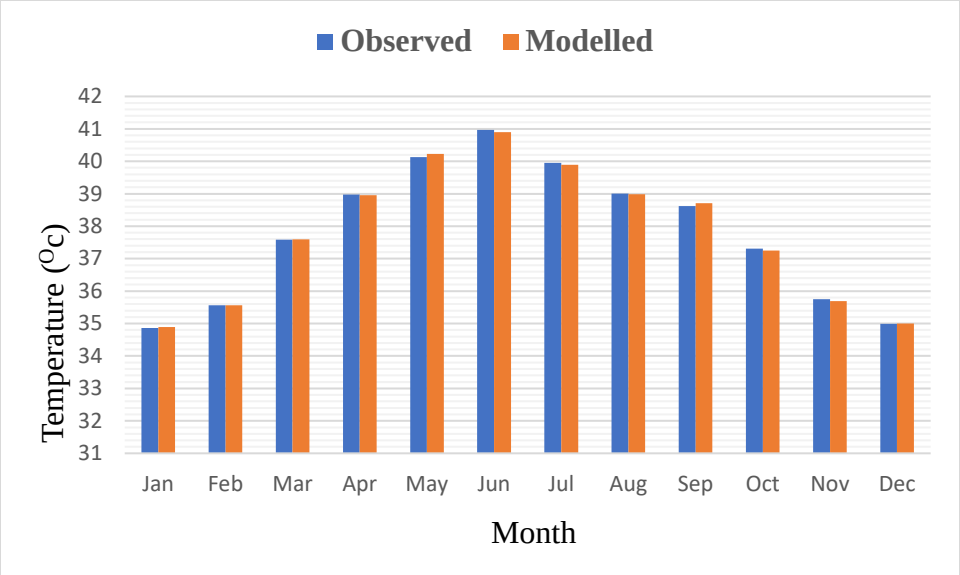

Figure 4.4 Daily mean maximum temperature between observed and calibrated at Assaita station

Minimum Temperature (Assaita)

The results of downscaling minimum Temperature at the Assaita station indicate that there is satisfactory agreement between simulation data and observed data. As shown in Figure 4.5, observed and downscaled values show similar pattern. The model in downscaling the annual mean minimum temperature shows a slightly increase of 0.05%. The variability of monthly minimum temperature of observed values is well preserved in the downscaled value from October to January and June to September. From February to May the value of observed value is slightly higher than the downscaled values but the general trend for both observed and downscaled values shows a similar pattern as shown in figure.

The monthly downscaled temperature showed slightly lower value from the months of June to September by 0.01-0.13 % and slightly higher for the months of February to May by 0.07-0.34%. From the months of October to January by 0.06-0.24% the value of observed value is slightly higher than the downscaled values but the general trend for both observed and downscaled values showed a similar pattern as shown in figure.

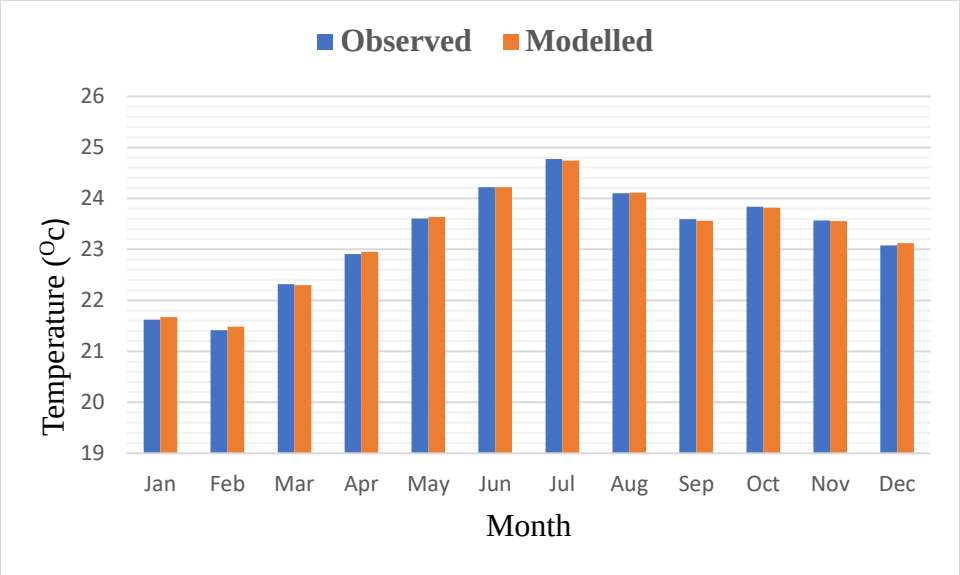

Figure 4.5 Daily mean minimum temperature between observed and calibrated at Assaita station

Precipitation (Dubti)

The downscaled precipitation value at the Dubti stations satisfactorily replicate the observed value. As shown in Figure 4.6, observed and downscaled values show similar pattern. The total mean annual precipitation downscaled value at the Dubti stations showed decrease by 0.49% compared to observed value. The model highly overestimated in some months specially at the month of October, November, and December and underestimates in months of February, March and June.

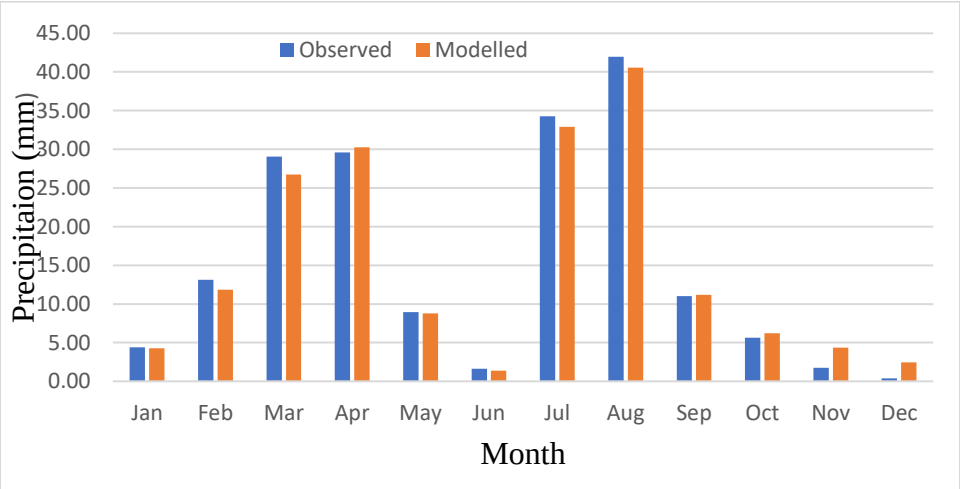

Figure 4.6 Daily mean precipitation between observed and calibrated at Dubti station

Maximum Temperature (Dubti)

The results of downscaling maximum Temperature at the Dubti station indicate that there is satisfactory agreement between simulation data and observed data. The model in downscaling the annual mean maximum temperature shows a slightly decrease of 0.02%. The monthly downscaled temperature showed slightly lower value from the months of August to January by 3.61-7.7% and slightly higher for the months of February to July by 0.12- 9.11%. However, the general trend for both observed and downscaled values shows a similar pattern as shown in Figure 4.7.

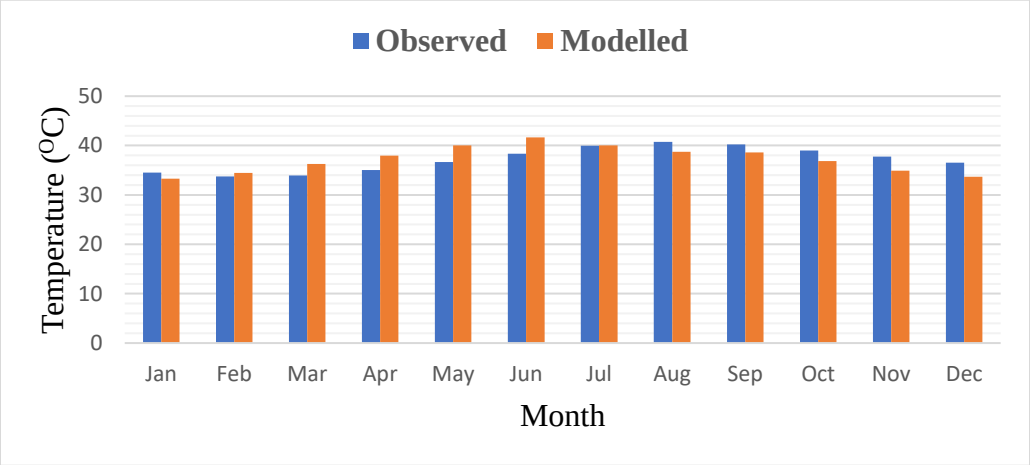

Figure 4.7 Daily mean maximum temperature between observed and calibrated at Dubti station

Minimum Temperature (Dubti)

The results of downscaling minimum Temperature at the Dubti station showed satisfactory agreement between simulation data and observed data. The model in downscaling the annual mean minimum temperature shows a slightly increase of 0.2%. The monthly downscaled temperature showed slightly higher value from the months of August to January by 0.16 – 8.75 % and slightly lower for the months of February to July by 1.54 - 4.98 %. However, the general trend for both observed and downscaled values shows a similar pattern as shown in Figure 4.8.

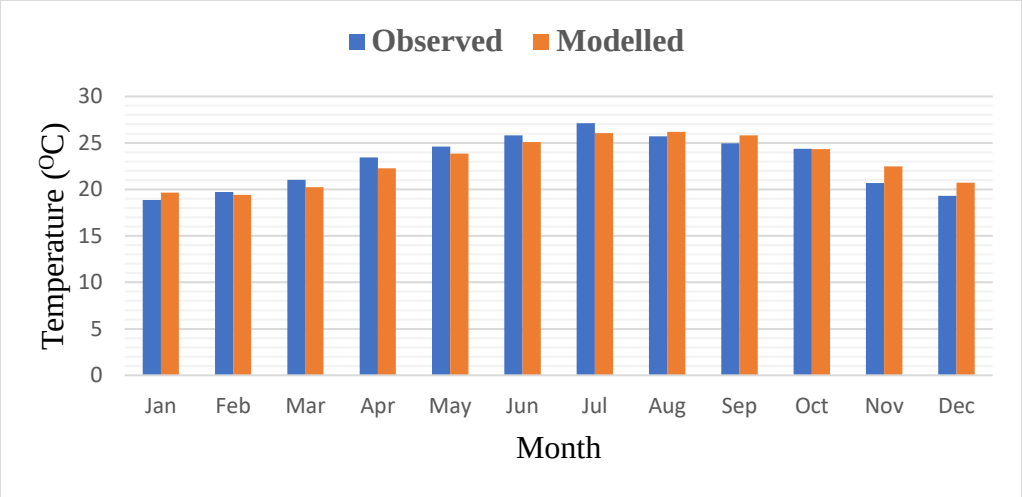

Figure 4.8 Daily mean minimum temperature between observed and calibrated at Dubti station

Precipitation (Logia)

The downscaled precipitation value at the Logia stations poorly replicate the observed value compared to Assaita and Dubti stations. Given the fact that, daily precipitation amounts at individual sites are relatively poorly resolved by regional scale predictions. The total mean annual precipitation downscaled value at the Logia stations shows a 10.43% difference compared to observed value. The model highly overestimated in some months specially at the month of April and May and underestimates in months of September, October, November and December. However, the general trend for both observed and downscaled values shows a similar pattern as shown in Figure 4.9.

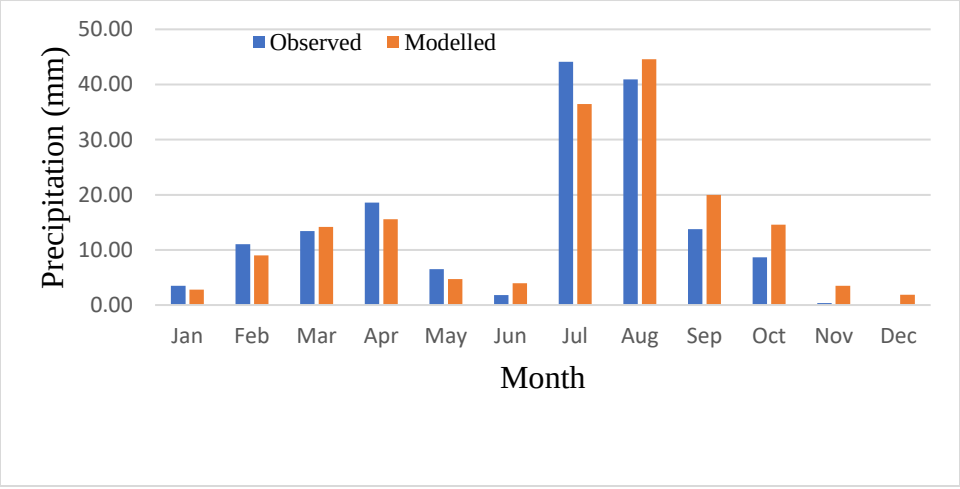

Figure 4.9 Daily mean precipitation between observed and calibrated at Logia station

4.1.8. Scenario generator

The Hardley Center Couple Model (HadCM3) is used to downscale daily future climate variables for the next century at the sub basin. The Scenario Generation operation in SDSM produces ensembles of synthetic daily weather series given the regression weight produced during the calibration process and the daily atmospheric predictor supplied by a GCM. Twenty ensembles of synthetic daily time series were produced for the two emission scenarios (HadCM3 A2s & B2a) for a period of 139 years (1961 to 2099). Finally, the mean of twenty ensembles for the specified period is produced for the maximum and minimum temperature and precipitation. The future scenarios were developed by dividing the future time series into three period time slices 2020s (2010-2039), 2050s (2040-2069) and 2080s (2070-2099). HadCM3 model simulation use 360-day calendar, where each month is 30 days. To prepare the data as input for hydrological modelling purpose this time series needed to be converted to a 366 days calendar. This was done by created additional days and calculated average of previous 30days in case of January, March, May, July, August, October, December, and considering leap years for February.

Precipitation (Assaita)

Projection of precipitation shows increasing tendency towards for all future time horizon for both A2 and B2 scenarios at Assaita stations. The precipitation expected to experience a mean annual increase by 40.17%, 76.02% and 134.41% by 2020s, 2050s and 2080s respectively for A2 scenarios and about 41.09%, 56.65%, 95.41% by 2020s, 2050s and 2080s respectively for B2 scenario. The total mean annual precipitation downscaled value 4.743, 5.956, 7.931 mm by 2020s, 2050s and 2080s respectively for A2 scenarios and 4.774, 5.3, 6.612 mm by 2020s, 2050s and 2080s respectively for B2 scenarios.

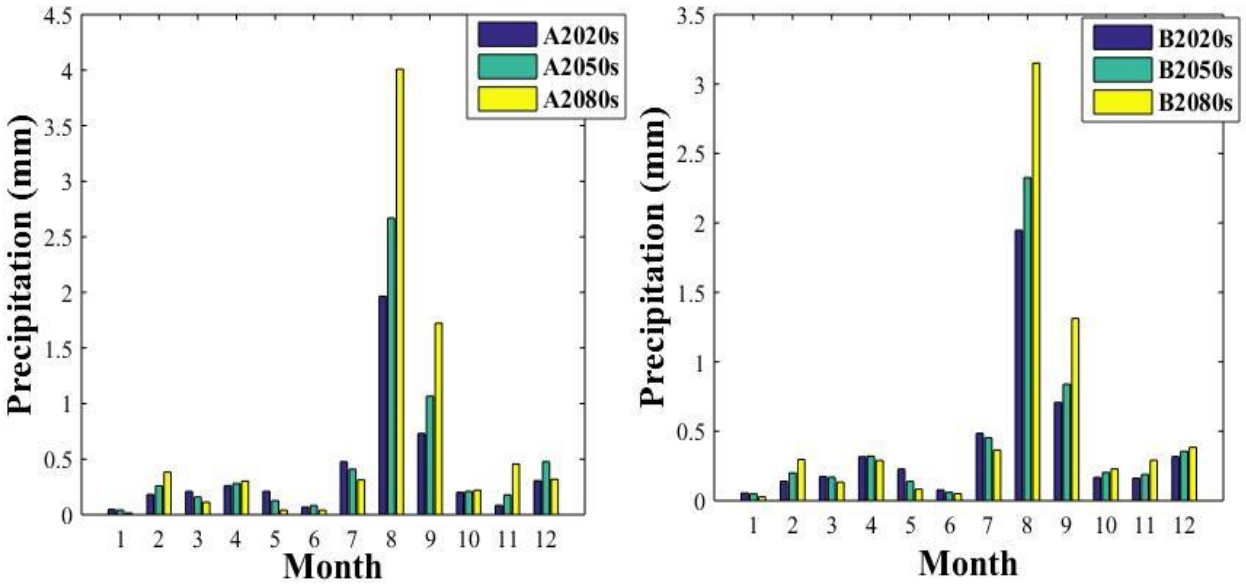

Figure 4.10 Daily mean precipitation for future scenarios at Assaita station

Maximum Temperature (Assaita)

The downscaled maximum temperature generated by the SDSM based on the HadCM3 model input has projected maximum temperature increases at Assaita Station. The projected maximum temperature for future periods for A2 and B2 scenarios are shown in Figure 4.11. The model predicts the annual maximum temperature to increase by 3.54%, 6.08%, 10.23%, for 2020s, 2050s and 2080s respectively in A2 scenarios and 3.56%, 5.18%, 7.56%, for 2020s, 2050s and 2080s respectively in B2 scenarios.

The highest maximum temperature of the seasons occurred on June whose temperature is 43.71 °C,46.39°C, 49.47°C for 2020s, 2050s and 2080s respectively in A2 scenarios and 43.76 °C,45.54°C, 47.39°C for 2020s, 2050s and 2080s respectively in B2 scenarios. The lowest maximum temperature was occurred in December and January reaches about 34.29°C, 31.9°C, 29.00°C for 2020s, 2050s and 2080s respectively in A2 scenarios and about 34.27°C, 32.8°C, 30.73°C for 2020s, 2050s and 2080s respectively in B2 scenarios.

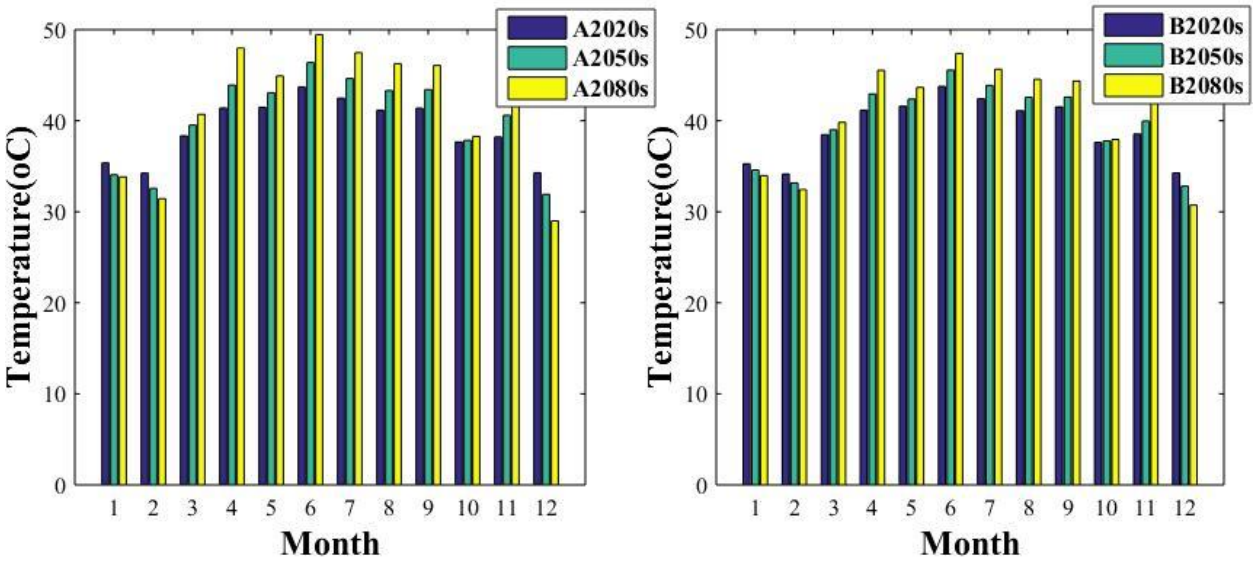

Figure 4.11 Daily mean maximum temperature for future scenarios at Assaita station

Minimum Temperature (Assaita)

The downscaled minimum temperature showed an increasing trend in all future time horizon for both A2 and B2 scenarios. The projected minimum temperature for future periods for A2 and B2 scenarios are shown in Figure 4.12.

The model predicts the annual minimum temperature to increase by 8.67%, 13.42%, 20.94%, for 2020s, 2050s and 2080s respectively in A2 scenarios and 8.55%, 11.48%, 16.04%, for 2020s, 2050s and 2080s respectively in B2 scenarios compared to the baseline minimum temperature. The highest minimum temperature of the seasons occurred on September whose temperature is 27.11°C, 30.33°C, 35.56°C by 2020s, 2050s and 2080s respectively for A2 scenarios and about 27.21°C, 29.23°C, 32.33°C by 2020s, 2050s and 2080s respectively for B2 scenarios. The lowest minimum temperature was occurred in February reaches about 19.42°C, 16.56°C, 14.34°C for 2020s, 2050s and 2080s respectively in A2 scenarios whereas about 19.31°C, 17.54°C, 16.09°C by 2020s, 2050s and 2080s respectively for B2 scenarios.

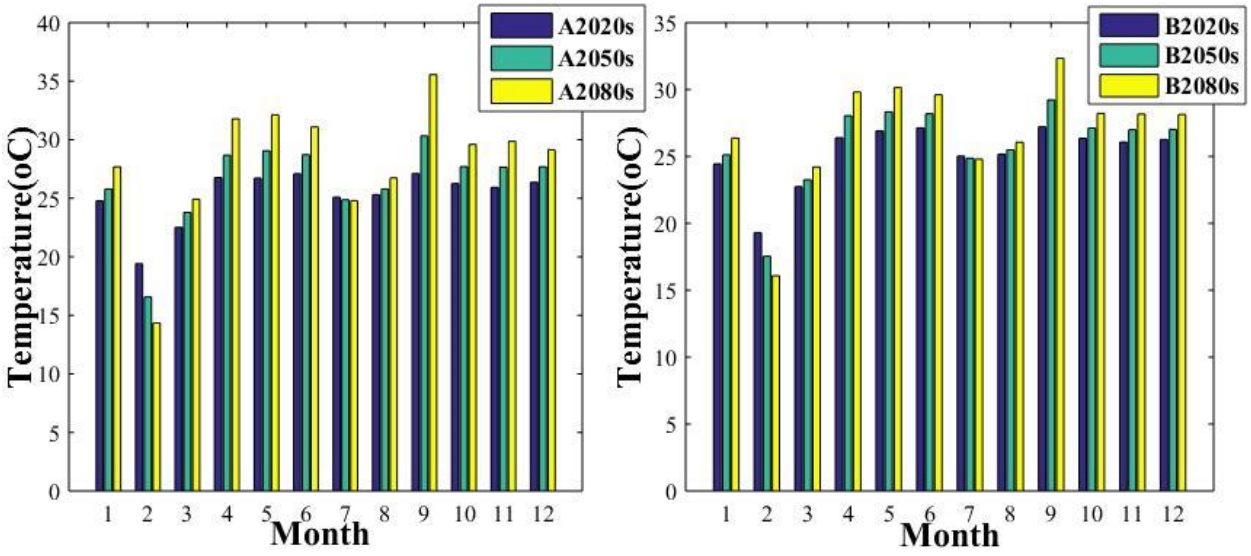

Figure 4.12 Daily mean minimum temperature for future scenarios at Assaita station

Precipitation (Dubti)

Projection of precipitation shows increasing trend towards for all future time horizon for both A2 and B2 scenarios at Dubti stations. The precipitation expected to experience a mean annual increase by 17.15%, 11.80% and 12.32% by 2020s, 2050s and 2080s respectively for A2 scenarios and about 19.5%, 11.66%, 21.53% by 2020s, 2050s and 2080s respectively for B2 scenario. The total mean annual precipitation downscaled value 6.938, 6.621, 6.652 mm by 2020s, 2050s and 2080s respectively for A2 scenarios and 7.077, 6.613, 7.198 mm by 2020s, 2050s and 2080s respectively for B2 scenarios.

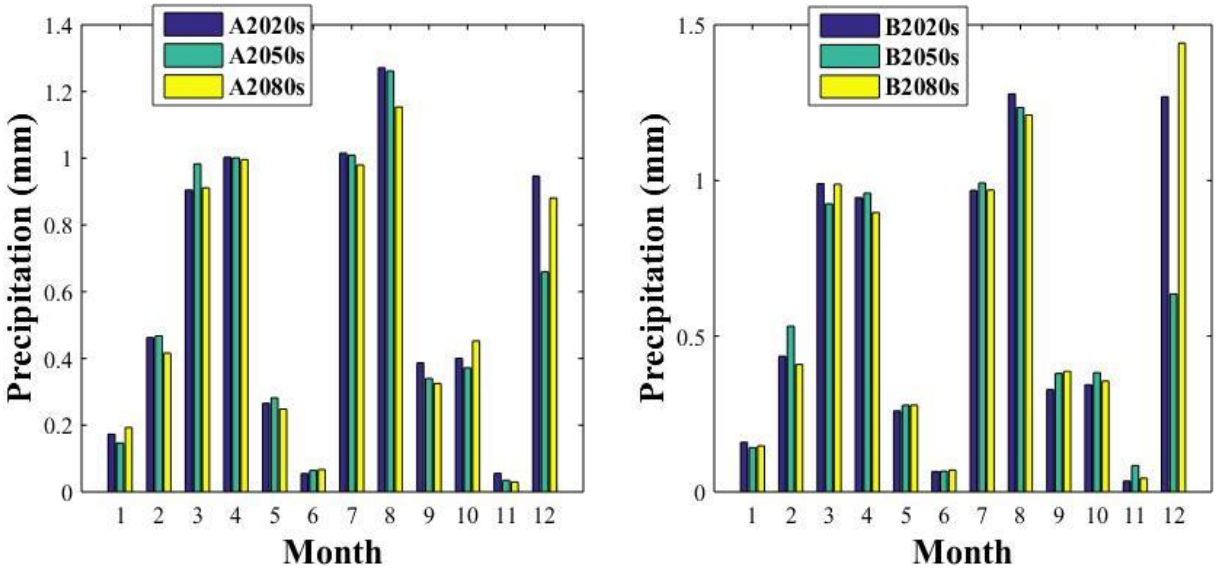

Figure 4.13 Daily mean precipitation for future scenarios at Dubti station

Maximum Temperature (Dubti)

The downscaled projected maximum temperature at Dubti station shows an increasing trend in all future time horizon for both A2 and B2 scenarios. The model predicts the annual maximum temperature to increase by 0.02%, 0.62%, 2.32%, for 2020s, 2050s and 2080s respectively in A2 scenarios and 0.14%, 0.57%, 1.49%, for 2020s, 2050s and 2080s respectively in B2 scenarios.

The highest maximum temperature of the seasons occurred on October whose temperature is 41.76 °C,42.66°C, 44.67°C for 2020s, 2050s and 2080s respectively in A2 scenarios and 41.94 °C,42.70°C, 43.71°C for 2020s, 2050s and 2080s respectively in B2 scenarios. The lowest maximum temperature occurred in January reaches about 33.66°C, 33.87°C, 34.92°C for 2020s, 2050s and 2080s respectively in A2 scenarios and about 33.56°C, 33.8°C, 34.3°C for 2020s, 2050s and 2080s respectively in B2 scenarios.

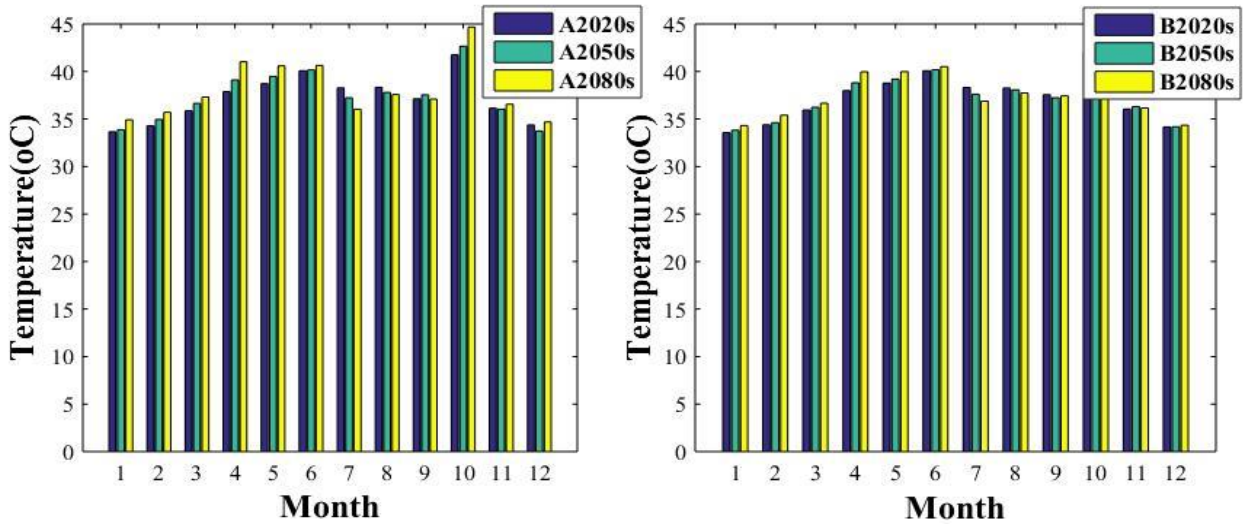

Figure 4.14 Daily mean maximum temperature for future scenarios at Dubti station

Minimum Temperature (Dubti)

Projection of annual minimum temperature at Dubti station shows decreasing trend towards the near future 2020s and 2050s and shows increasing trend towards the far future 2080s for A2 scenario. Whereas, for B2 scenario annual minimum temperature shows decreasing trend towards for all future time horizon. The model predicts the annual minimum temperature to decrease by 1.03%, 0.82%, for 2020s, 2050s respectively and increase by 0.16% for 2080s under A2 scenarios. whereas the annual minimum temperature decreases by 0.77%, 0.82%, 0.38%, for 2020s, 2050s and 2080s respectively in B2 scenarios.

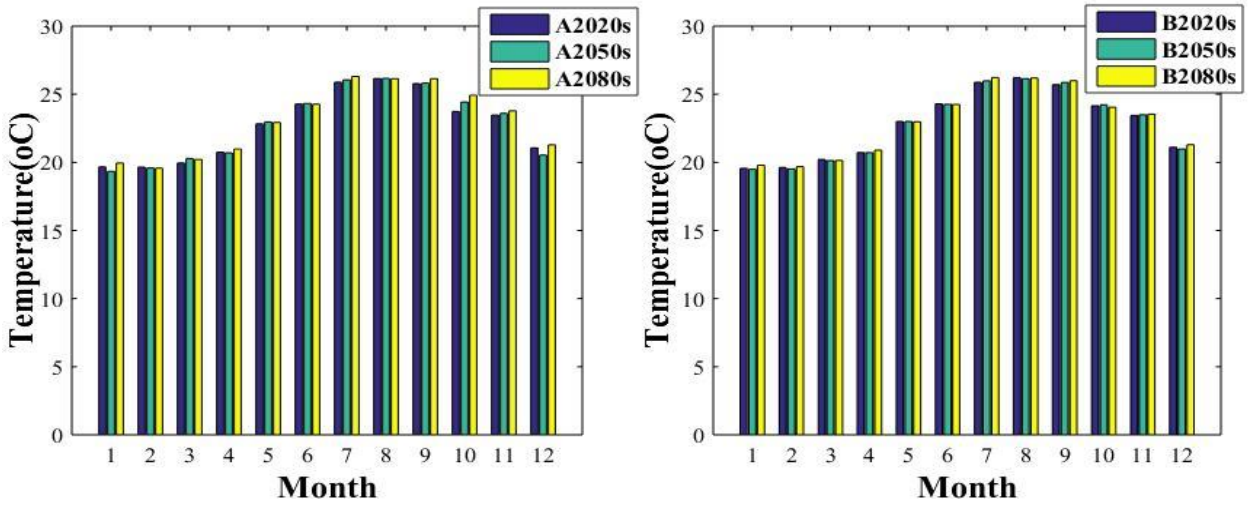

Figure 4.15 Daily mean minimum temperature for future scenarios at Dubti station

Change in Precipitation (Logia)

Projection of precipitation shows decreasing trend towards for all future time horizon for both A2 and B2 scenarios at Logia stations. The precipitation expected to experience a mean annual decrease by 3.14%, 17.73% and 31.05% by 2020s, 2050s and 2080s respectively for A2 scenarios and about 7.6%, 12.2%, 26.58% by 2020s, 2050s and 2080s respectively for B2 scenario. The total mean annual precipitation downscaled value 5.69, 4.83, 4.05 mm by 2020s, 2050s and 2080s respectively for A2 scenarios and 5.43, 5.16, 4.31 mm by 2020s, 2050s and 2080s respectively for B2 scenarios.

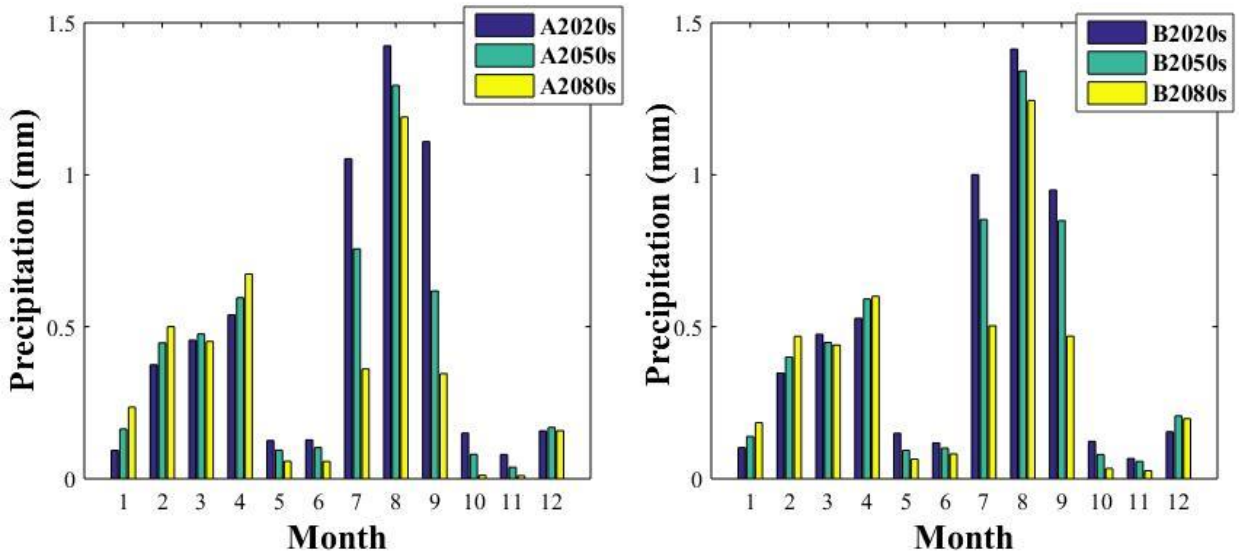

Figure 4.16 Daily mean precipitation for future scenarios at Logiya station

4.2. SWAT Hydrological Model

SWAT is a semi-distributed parameter model where by each watershed is divided into sub basins, based upon a Digital Elevation Model (DEM) provided by the user. Sub basins are further divided in to Hydrologic Response Units (HRU) which are composed of land use, slope, and soil type. SWAT assigns a single set of parameters to each Hydrologic Response Units, thereby simulating surface runoff and infiltration by lumping these processes at the HRU scale. The model estimates relevant hydrologic components such as evapotranspiration, surface runoff and peak rate of runoff, ground water flow and sediment yield for each HRU.

The weather component of the models needs input data on precipitation, daily maximum and minimum temperature, solar radiation, wind speed, and relative humidity data. The input data to the SWAT model consists of DEM, land use data, soil data, weather data and river flow for calibration and validation purpose.

The SWAT model weather generation data base has only for US only. However, development of the model input and preprocessing of the data file made for the Lower Awash River Basin in order to be used in the SWAT model. The raw data sources utilized and translation of these raw data inputs to original SWAT 2012 input files were made.

4.2.1. Digital elevation model (DEM)

A Digital Elevation Model (DEM) was used to model the geography of the study area. A DEM is a grid of square cells where each cell represents the elevation value. The DEM for this area was downloads from Open Topography high-resolution topography data and tools (www.opentopography.org), which provides the NASA Satellite Radar Topographic Mission (SRTM) at a raster resolution of 30m Digital Elevation Data for the entire world.

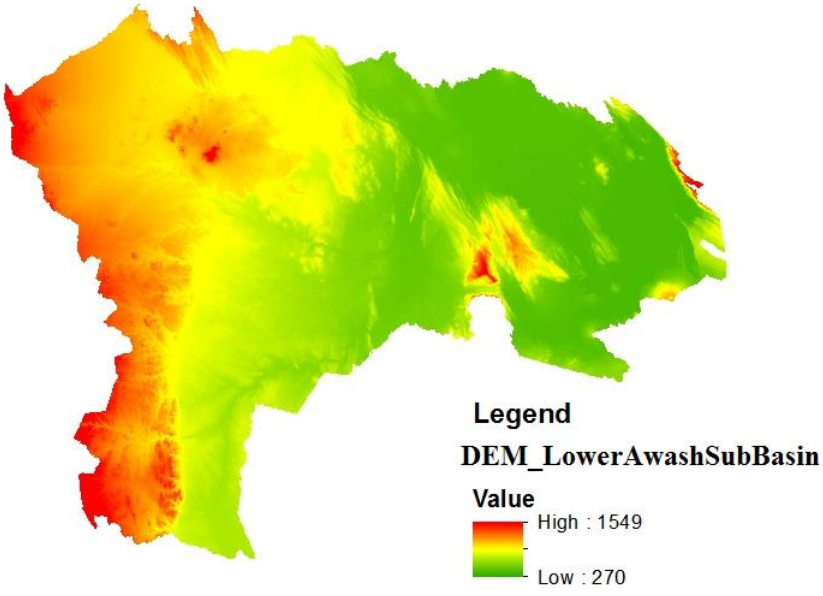

Figure 4.17 Digital elevation model for lower awash sub basin

The DEM is used at a resolution of 1 arc-second for the Lower Awash Sub Basin with an altitude range of 270 to 1549 meters above sea level.

4.2.2. Watershed delineation

The DEM was used to delineate the watershed and to analyze the drainage patterns of the land surface terrain. The sub basin parameter slope gradient and length of the terrain, and the stream network characteristics channel slope, length and width are also derived from the DEM. The spatial datasets used in the SWAT model were projected to the same Universal Transverse Mercator (UTM) projection parameters: UTM Zone 37N for the reason that SWAT requires all input files in meter units.

The watershed process requires DEM setup, stream definition, outlet and inlet definition, watershed outlet selection and definition and calculation of sub basin parameters. The SWAT automatic watershed delineator sub divides a sub watershed into areas having unique land use, soil and slope combinations. The Dubti flow is manually added at the watershed outlet and selected to finalize the watershed delineation. Finally, the sub basin delineates and covers an area of 17435.24 km2 and divided into 32 sub basins based on threshold area of 35,000 ha and 122 HRUs.

4.2.3. HRU definition

The Hydrological Response Units (HRUs) analysis tool in ArcSWAT helps to load land use and soil layers to the project. Before incorporating the land use, and soil data into SWAT land cover types reclassified made.

The land use lookup table was created to make a correspondence between SWAT land use code and each categories of land use on the map as text format table. The original Lower Awash Sub Basin land use types were reclassified into ten SWAT land use classes. The delineated watershed by ArcSWAT automatic watershed delineator and the reclassified land use overlapped 95.5 %.

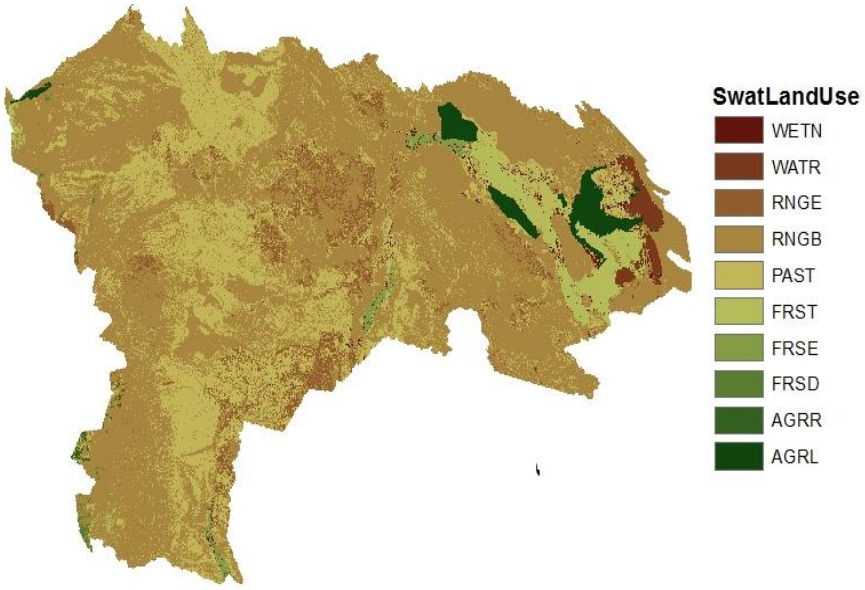

Figure 4.18 The land use types in lower awash sub basin

Table 4.4 The land use types and their aerial coverage in lower awash sub basin

Value	Area	SWAT Code	Land use
0	60.359	RNGB	Range-Brush
1	2.096	AGRL	Agricultural Land-Generic
2	0.142	AGRR	Agricultural Land-Row Crops
3	0.18	FRSD	Forest-Deciduous
4	0.743	FRSE	Forest-Evergreen
5	5.096	RNGE	Range -Grasses
6	25.583	PAST	Pasture
7	1.053	WATR	Waterbody
8	0.632	WETN	Wetland non-forested
9	4.115	FRST	Forest mixed

The Soil type lookup table was created to make a correspondence between SWAT soil database code and each categories of Soil type on the map as text format table. The FAO soil types were

reclassified into nine SWAT soil classes. The delineated watershed and the Soil map overlapped 100 %.

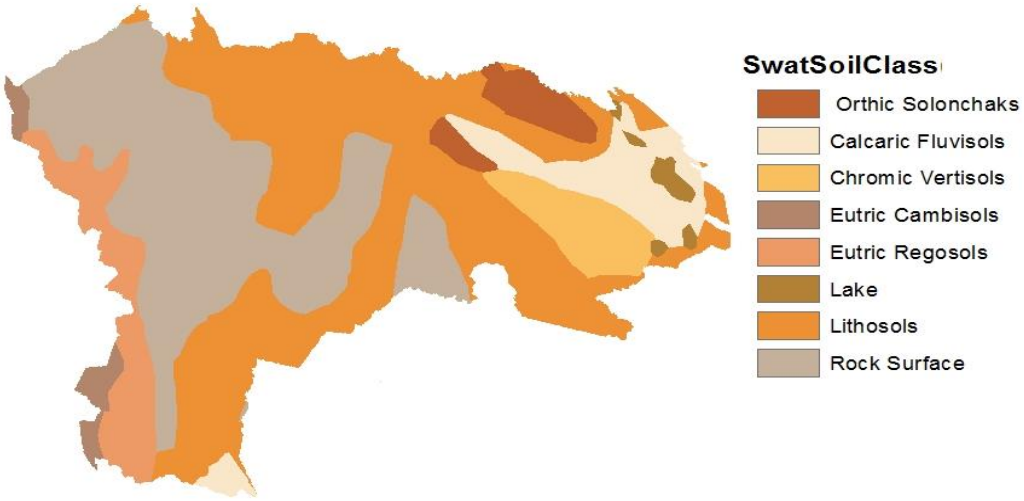

Figure 4.19 The Soil types for lower awash sub basin

Table 4.5 The Soil types and their aerial coverage in lower awash sub basin

Value	Area	SWAT Soil Class	Soil Type
0	1.795	Be9-3c-26	Eutric Cambisols
1	42.06	I-Re-3a-83	Lithosols
2	7.44	Jc6-2a-118	Calcaric Fluvisols
3	7.4	Re47-2c-239	Eutric Regosols
4	4.814	Vc7-3a-279	Chromic Vertisols
5	2.641	Xk19-2a-324	Rock Surface
6	29.4	Xk20-2a-328	Rock Surface
7	3.409	Zo12-2a-387	Orthic Solonchaks
8	1.041	WATER-1972	Lake

HRU analysis in SWAT includes divisions of HRUs by slope classes in addition to land use and soils. To define the HRUs distribution multiple HRU definition was used. As per recommended

by the SWAT user manual 20 % land use, 10% soil and 20% slope thresholds were use. Finally, 122 HRUs created for Lower Awash Sub Basin.

Figure 4.20 Land Slope for lower awash sub basin

4.2.4. Importing weather data

SWAT needs climate data for the simulation of hydrological processes. The weather data were collected from National Metrological Service Agency (NMSA) of Ethiopia at Addis Ababa office. The daily metrological data collected were precipitation, maximum and minimum temperature, relative humidity, wind speed and sunshine hours.

Table 4.6 List of stations name, location and meteorological variables

Station Name	Elevation	Latitudes	Longitudes	PCP	TempMax	TempMin	Year
Adayitu	507	11.11	40.783	√	√	√	1983-2015
Assaita	430	11.53	41.5298	√	√	√	1983-2015
Bati	1660	11.1967	40.0154	√	√	√	1983-2015
Dubti	376	11.723	41.01	√	√	√	1983-2015
Logiya	393	11.65	41	√	X	X	1983-2015
Mille	487	11.4256	40.77	√	√	√	1983-2015

SWAT needs formatting work for weather data before incorporating them into SWAT model. The weather data required by SWAT consists of daily precipitation, maximum and minimum

temperature, relative humidity, wind speed and solar radiation. Hence, due to luck of data availability and quality most of the stations they don't have weather data (relative humidity, wind speed and solar radiation) required by the SWAT model. However, by using a synoptic station and embedded the weather generator in to the SWAT model fills the data gap. Assaita metrological stations were selected as synoptic station because of data availability relative to other stations and the metrological data fulfill all input requirements for SWAT. The Assaita weather generator table was embedded in SWAT user database.

The gauge locations and the data tables formatted as text files. A gage location table indicates to the model the location of rain and temperature gauges. One precipitation gage location table was created containing 6 gauges and one temperature gauge location table with 5 weather stations.

4.2.5. Sensitivity analysis

Sensitivity analysis is the process of identifying the model parameters that exerts the highest influence on model calibration. The sensitivity analysis was carried out for the calibration a period of five years and validated for over the period of five years. A total of 8 parameters were considered for the sensitivity analysis. The flow was sensitive to the ground water parameters: the threshold depth of water in the shallow aquifer required for return flow to occur (GWQMN) in mm, baseflow alpha factor (ALPHA_BF) in days, groundwater delay (GW_DELAY) in days. The flow also found to be sensitive to soil property of available water capacity of the soil layer (SOL_AWC) in mm/mm soil depth. The flow also sensitive to channel network parameters: average slope of main channel (CH_S2), manning's "n" value for the main channel (CH_N2).

Table 4.7 List of parameters considered for the sensitivity analysis.

Parameter	Description	Input calibration range	t-Stat	P-Value
CN2	SCS runoff curve number II	± 20%	-3.449	0.002
ALPHA_BF	Baseflow alpha factor (days)	0.034-0.034	0.604	0.552
GW_DELAY	Groundwater delay (days)	0.0-50	-3.184	0.004
GWQMN	Threshold depth of water in the shallow aquifer required for return flow to occur (mm H2O)	0.0-4000	0.196	0.847
CH_N2	Manning's "n" value for the main channel	0-1	1.649	0.114
SOL_AWC	Available water capacity of the soil layer (mm /mm soil depth)	± 20%	-0.313	0.757
CH_S2	Average slope of main channel	0-10	1.080	0.292
CH_K1	Effective hydraulic conductivity in tributary channel alluvium.	0-300	-0.647	0.525

Table 4.8 SWAT flow sensitive parameters and fitted values after calibration using SUFI2 for the Lower Awash River Basin

Parameter Name	Fitted Value	Min value	Max value
1:R__CN2.mgt	-0.183333	-0.5	0.5
2:V__ALPHA_BF.gw	0.683333	0	1
3:V__GW_DELAY.gw	51	30	450
4:V__GWQMN.gw	1.233333	0	2
5:V__CH_N2.rte	0.165	0	0.3
6:R__SOL_AWC(..).sol	-0.075	-0.2	0.1
7:R__CH_S2.rte	8.49985	-0.001	10
8:R__CH_K1.sub	95	0	300

4.2.6. Flow calibration and validation

Flow calibration was performed for a period of five years from 1991 to 1995 and validation over the period from 1996-2000 at Dubti flow gage station. The SUFI-2 calibration method was used to calibrate the model using the observed stream flow. Observed daily stream flows were

converted to monthly average flows and simulations run were conducted on monthly basis to compare the modeling output with the measured monthly average discharge at the outlet of Dubti watersheds.

SWAT calibrated and validation outputs captured the historical flow quite well. As shown in the table, the calibration resulted in P-factor of 0.73 %, R-factor of 1.28, R2 of 0.92 and NS of 0.88 whereas validation resulted in R2 of 0.77 and NS of 0.75. The calibration process using SUFI2 gave the final fitted parameter. These final fitted parameter values were incorporated into the SWAT2012 model to investigate the impact of climate change in the Lower Awash Sub Basin.

Table 4.9 Calibration and validation result

	Period	P-factor	R-factor	R2	NS
Calibration	1991-1995	0.73	1.28	0.92	0.88
validation	1996-2000	0.75	1.34	0.77	0.75

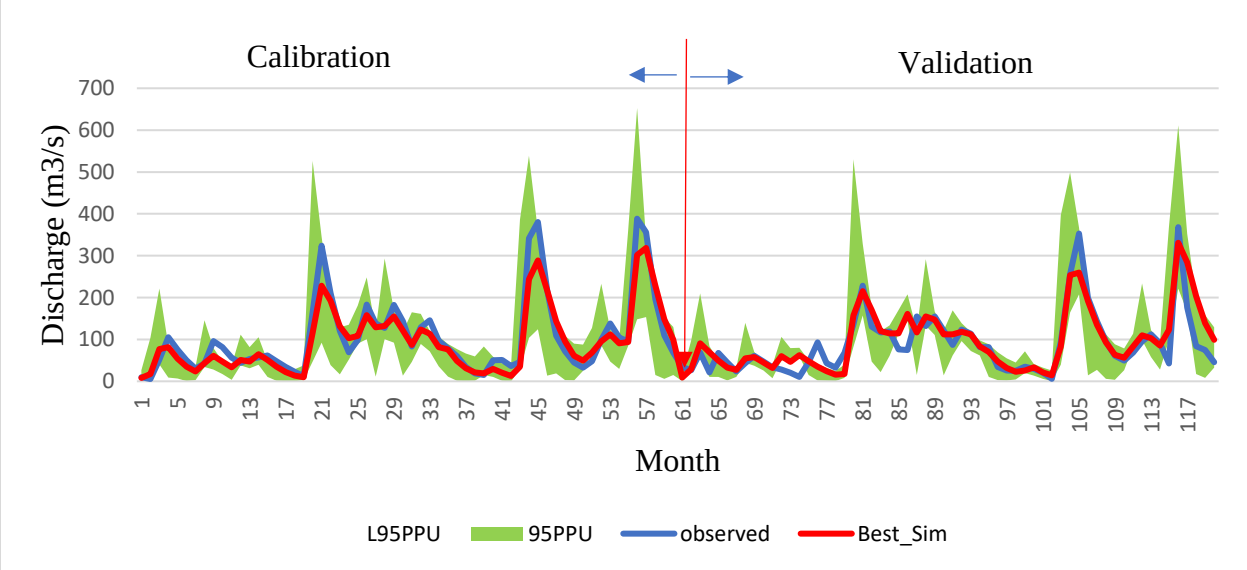

Figure 4.21 Calibration and validation

Chapter 5. RESULTS AND DISCUSSION

This chapter presents the impact of climate change on hydrology of Lower Awash Sub Basin using the hydrological model simulation run based on the statistical downscaling climate variables input. SWAT hydrological model simulation was run for the baseline and three future scenarios (2020s, 2050s, and 2080s) to understand climate change impact on precipitation and temperature by keeping constant calibrated non-climate variables of soil and land use and some climate variables such as windspeed, sunshine hour and relative humidity.

5.1. Assessment of Climate Change Impact on Hydrology

The objective of this work is to assess the impact climate change on hydrology over the study area. The simulation result of average hydrological climate variables of Precipitation, Temperature, Evapotranspiration, Surface Runoff, Lateral Flow and Water Yield for three future scenarios 2020s, 2050s and 2080s were compared with the baseline hydrological variable. The results for the analysis of each climate variables discussed in the following sections.

5.1.1. Change in Precipitation

The projected annual mean rainfall shows an increasing tendency for all future time horizon under A2 and B2 scenario. The rainfall expected to experience a mean annual increase by 1.69%, 2.34% and 4.45 % by 2020s, 2050s and 2080s respectively for A2 scenario and 1.70%, 1.67%, 3.49%, for 2020s, 2050s and 2080s respectively in B2 scenario.

The study area has three distinct seasons the small to moderate rainy season from March to April and the main rainy season from July to September with the rainfall peak occurring in July and August. Especially the highest rainfall peak is occurred in the month of August whose value 116.97, 118.87 and 127.96 mm by 2020s, 2050s and 2080s respectively for A2 scenario and 116.86,116.81, 123.24 by 2020s, 2050s and 2080s respectively for B2 scenario. The lowest rainfall is occurred in June reaches about 8.54, 9.1 and 8.23 mm by 2020s, 2050s and 2080s respectively for A2 scenario and about 8.61, 8.97 and 8.37 mm by 2020s, 2050s and 2080s respectively lowest rainfall occurred for B2 scenario.

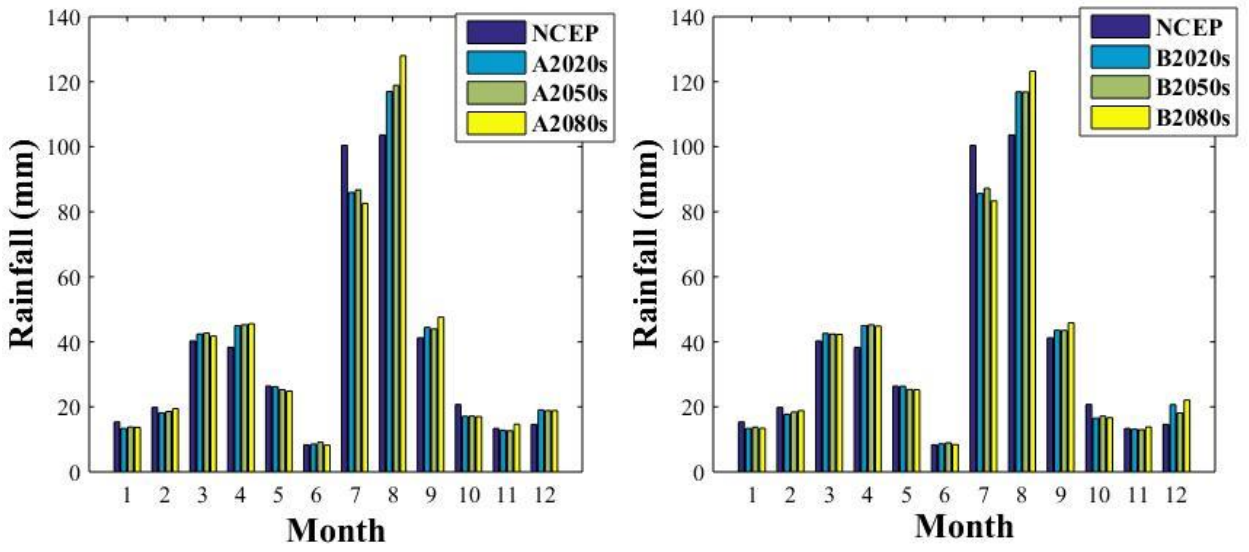

Figure 5.1 Projected rainfall for A2 and B2 scenarios

The mean rainfall projection of the main season (June-September) which shows increasing for the two emission scenarios except for July. Whereas the mean rainfall during the small rainy season (February-May) projection shows increasing for A2 and B2 scenarios except February. The mean rainfall during the dry season Bega (October-January) projection shows increasing for the two emission scenarios except for October and January. Generally, the projected mean rainfall in two scenarios is within the range projected by IPCC which reported that rainfall is predicted to increase December- February and Decrease June-August in parts of East Africa under intermediate warming scenarios (Adem et al., 2016). According to IPCC (2014), there will likely be more heavy rainfall over the east Africa with high certainty and more extremely wet days by the mid-21st century.

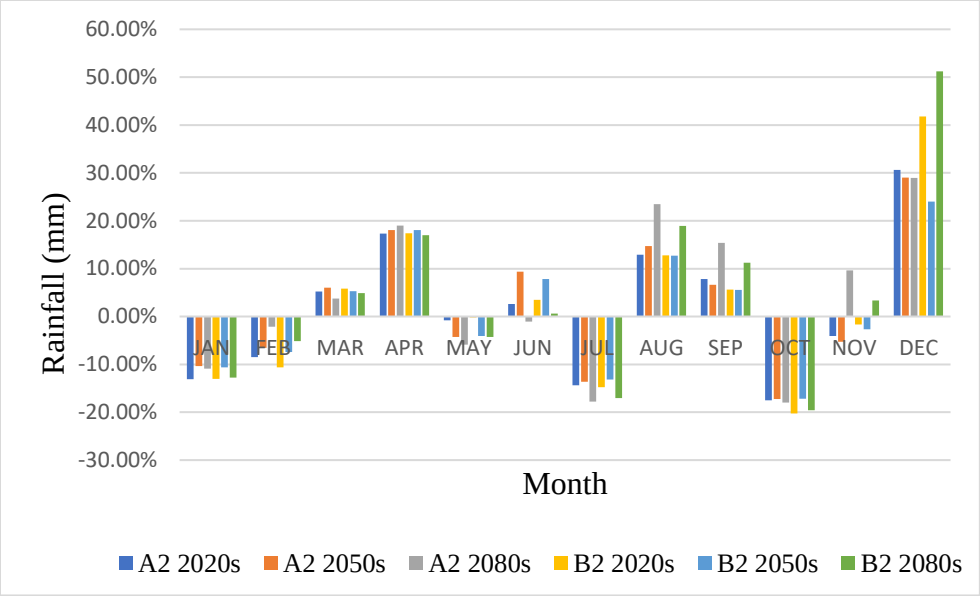

Figure 5.2 Percentage change in Rainfall for A2 and B2 scenarios

5.1.2. Change in Temperature

The output generated by the hydrological model based on the HadCM3 model input has projected temperature increases for Lower Awash Sub Bain. The models predict the annual maximum temperature to increase by 1.25%, 2.40%, 4.79%, for 2020s, 2050s and 2080s respectively in A2 scenarios and 1.34%, 2.11%, 3.44%, for 2020s, 2050s and 2080s respectively in B2 scenarios compared to the baseline maximum temperature at Lower Awash Sub Basin. Likewise, the models predict the annual minimum temperature to increase by 1.66%, 3.14%, 5.94%, for 2020s, 2050s and 2080s respectively in A2 scenarios and 1.82%, 2.60%, 4.19%, for 2020s, 2050s and 2080s respectively in B2 scenarios compared to the baseline minimum temperature. Generally, the projected minimum and maximum temperatures in two scenarios is within the range projected by IPCC which reported average temperature will rise by 1.4-5.8°C towards the end of century (Adem et al., 2016). According to IPCC (2014), maximum and minimum temperatures over equatorial East Africa will rise and that there will be more warmer days compared to the baseline by the middle and end of this century.

The annual mean temperature in the Lower Awash Sub Basin varies between 26.92°C to 33.07°C for 2020s, 26.52°C to 33.72°C for 2050s and 26.32°C to 34.56°C for 2080s from A2

scenarios whereas for B2 scenarios, the annual mean temperature varies between 26.93°C - 33.09°C, 26.59°C - 33.51°C and 26.63°C - 34.07°C for 2020s, 2050s and 2080s respectively.

Seasonal variation of temperature throughout the study area was also estimated. The highest maximum temperature of the seasons occurred on June whose temperature is 41.08 °C,41.89°C, 43.08°C for 2020s, 2050s and 2080s respectively in A2 scenarios and 41.1 °C,41.67°C, 42.41°C for 2020s, 2050s and 2080s respectively in B2 scenarios. The lowest maximum temperature was occurred in December and January reaches about 34.14°C, 33.22°C, 33.12°C for 2020s, 2050s and 2080s respectively in A2 scenarios and about 34.03°C, 33.8°C, 33.34°C for 2020s, 2050s and 2080s respectively in B2 scenarios.

The highest minimum temperature of the seasons occurred on September and July whose temperature value 26.15°C, 27.06°C, 28.75°C by 2020s, 2050s and 2080s respectively for A2 scenarios and about 26.12°C, 26.79°C, 26.15°C by 2020s, 2050s and 2080s respectively for B2 scenarios. The lowest minimum temperature was occurred in February reaches about 19.58°C, 18.97°C, 18.69°C for 2020s, 2050s and 2080s respectively in A2 scenarios whereas about 19.54°C, 18.97°C, 18.69°C by 2020s, 2050s and 2080s respectively for B2 scenarios.

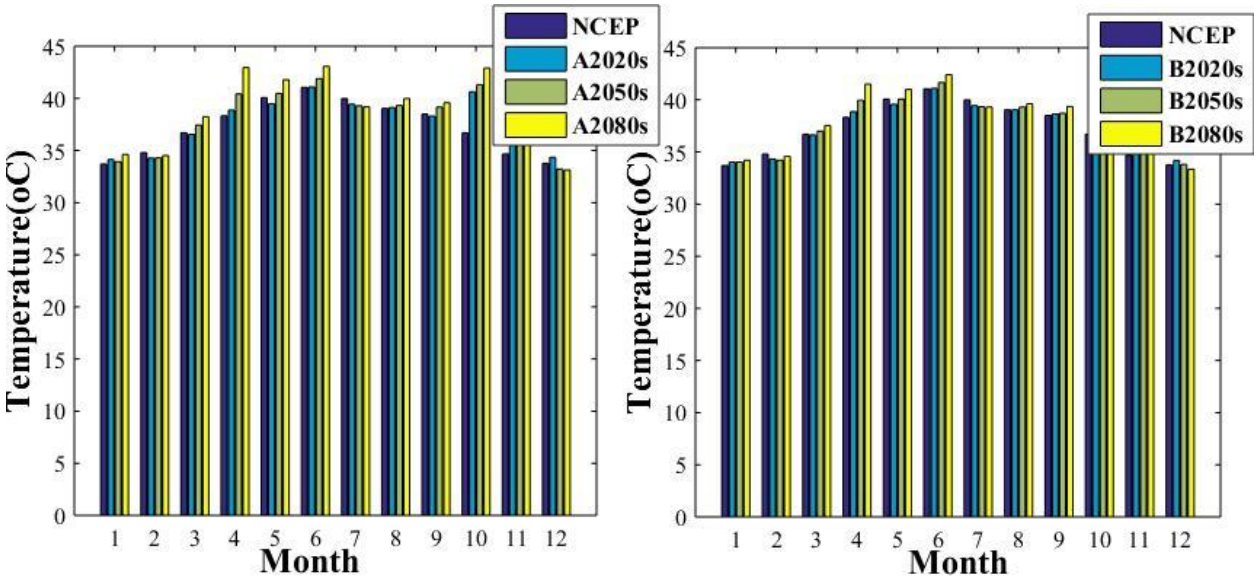

Figure 5.3 Projected maximum temperature for A2 and B2 scenarios

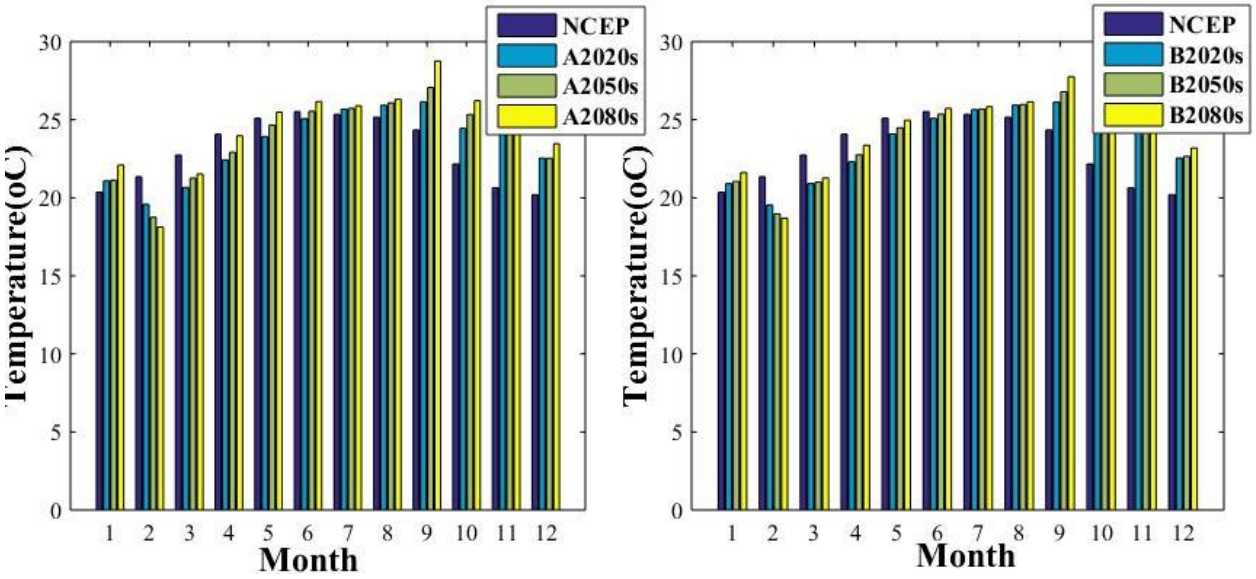

Figure 5.4 Projected minimum temperature for A2 and B2 scenarios

There is an increase percentage change maximum temperature throughout the year except in February, July and December for the future period under A2 and B2 scenarios. Whereas the minimum temperature projection shows increasing throughout the year except for the months February, March, April and May for both A2 and B2 scenarios.

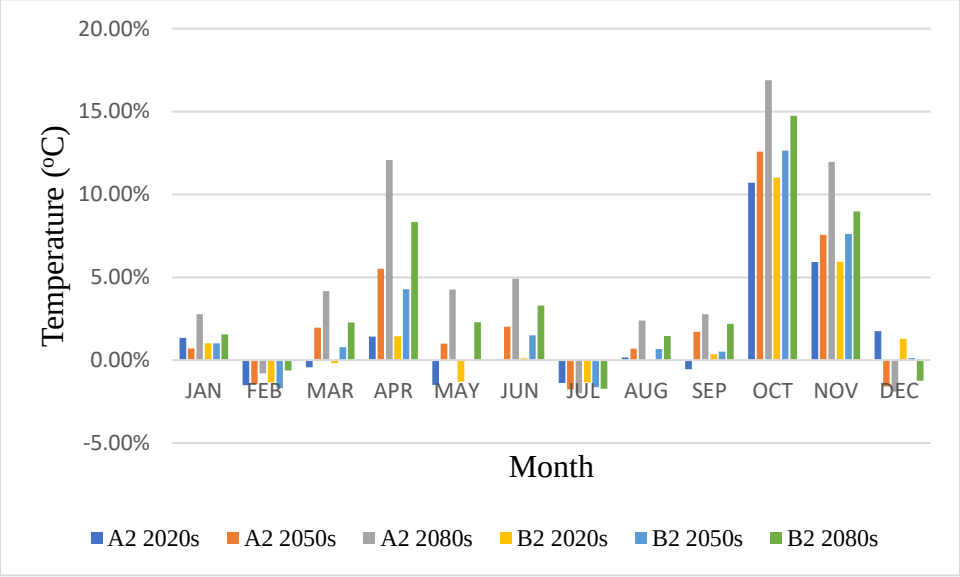

Figure 5.5 Percentage change in maximin temperature for A2 and B2 scenarios

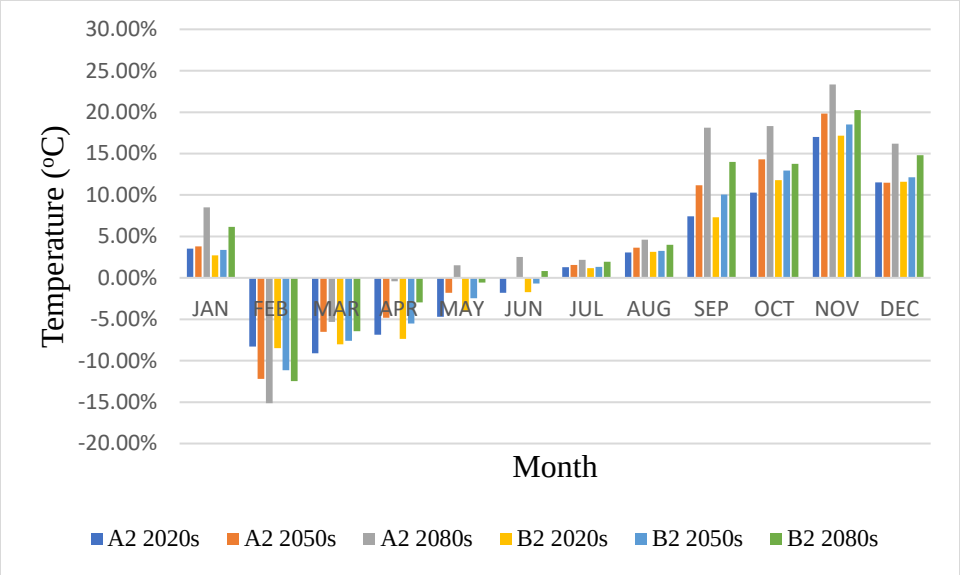

Figure 5.6 Percentage change in minimum temperature for A2 and B2 scenarios

5.1.3. Change in Evapotranspiration

Evaporation is the process by which water from an open water surface, on the soil surface and water on the leaves and branch of a plant escapes as vapor to the atmosphere through the transfer of heat energy. On the other hand, transpiration is also the process by which water (moisture) in the plant escapes to the atmosphere as vapor through the plant's leaves and stem. Transpiration happens mainly during the daytime (ADSWE, 2012) .

The Evapotranspiration (ET) for this study area was calculated for the three-time period slice 2020s, 2050s and 2080s by using the Hargreaves method depend on the maximum and minimum temperatures. The projected annual mean ET value increase by 5.10, 6.24 and 9.01% for 2020s, 2050s and 2080s respectively for A2 scenario similarly for B2 scenario, increased by 5.15, 5.72 and 7.71% for 2020s, 2050s and 2080s respectively. The annual ET value is expected to 346.19, 349.96 and 359.8 mm under A2 scenario in 2020s, 2050s and 2080s respectively while the value estimated to 346.35, 348.23 and 354.8mm in 2020s, 2050s and 2080s respectively under B2 scenario.

The most ET value is expected in August for both A2 and B2scenario. For the months of August, ET value is projected to increase by 7.47, 10.87 and 16.08% for 2020s, 2050s and 2080s

respectively for A2 scenario similarly for B2 scenario, increase by 8.67, 10.32 and 14.78% for 2020s, 2050s and 2080s respectively.

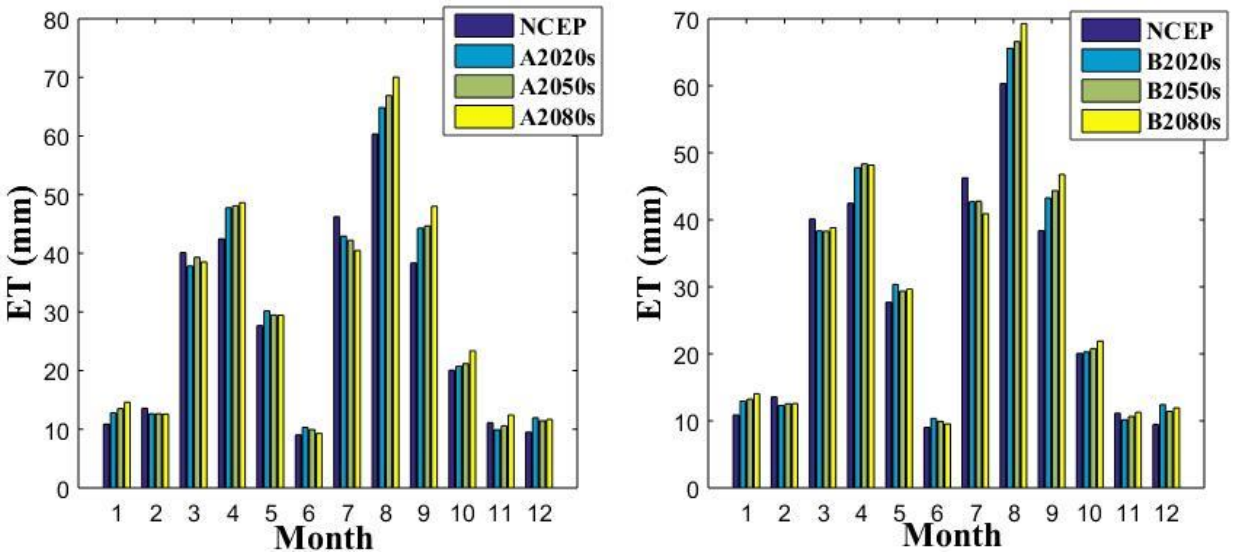

Figure 5.7 Projected evapotranspiration for A2 and B2 scenarios

There is an increase percentage change ET throughout the year except in February, March, July and November for the future period under A2 and B2 scenarios.

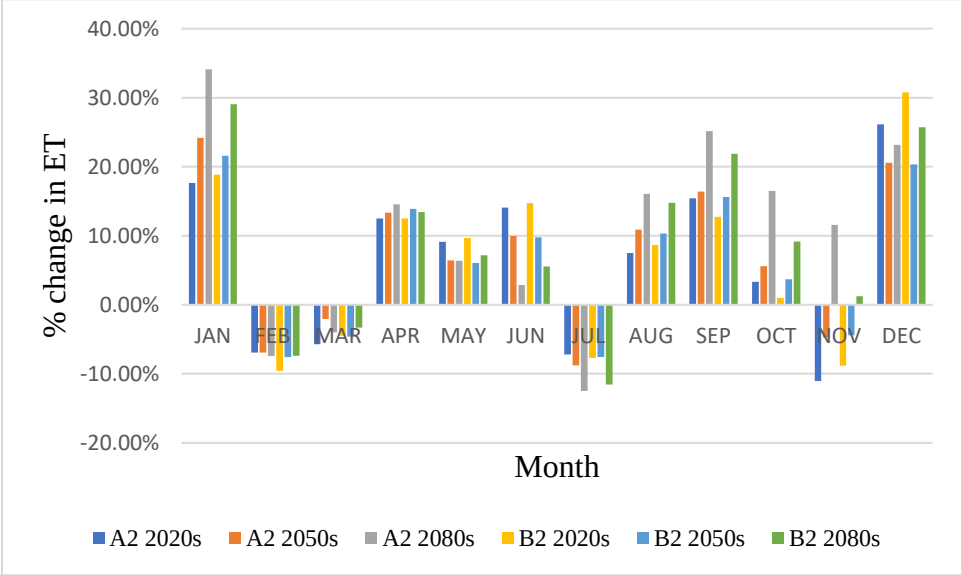

Figure 5.8 Percentage change in evapotranspiration for A2 and B2 scenarios

5.1.4. Change in Lateral Flow

Mean annual lateral flow projection increased by 2.37, 4.27 and 11.37% for 2020s, 2050s and 2080s respectively for A2 scenario similarly for B2 scenario, the model shows increased by 2.37, 2.84 and 6.16% for 2020s, 2050s and 2080s respectively. The annual lateral flow is expected to 3.91 m^3/s, 3.98 m^3/s and 4.25 m^3/s under A2 scenario in 2020s, 2050s and 2080s respectively while the value estimated to 3.91 m^3/s, 3.92 m^3/s and 4.05 m^3/s in 2020s, 2050s and 2080s respectively under B2 scenario.

The projected average monthly change of lateral flow shows the main rainy season which may be impacted highly with climate change. The most lateral flow value is expected in August and September and impacted highly for both A2 and B2scenario. For the months of August, lateral flow is projected to increase by 10.42, 14.58 and 25.0% for 2020s, 2050s and 2080s respectively for A2 scenario similarly for B2 scenario, the model shows increase by 8.33, 12.5 and 16.67% for 2020s, 2050s and 2080s respectively. For the months of September, lateral flow is projected to increase by 9.37, 12.5 and 31.25% for 2020s, 2050s and 2080s respectively for A2 scenario likewise for B2 scenario, the model shows increase by 9.37, 9.37 and 18.7% for 2020s, 2050s and 2080s respectively.

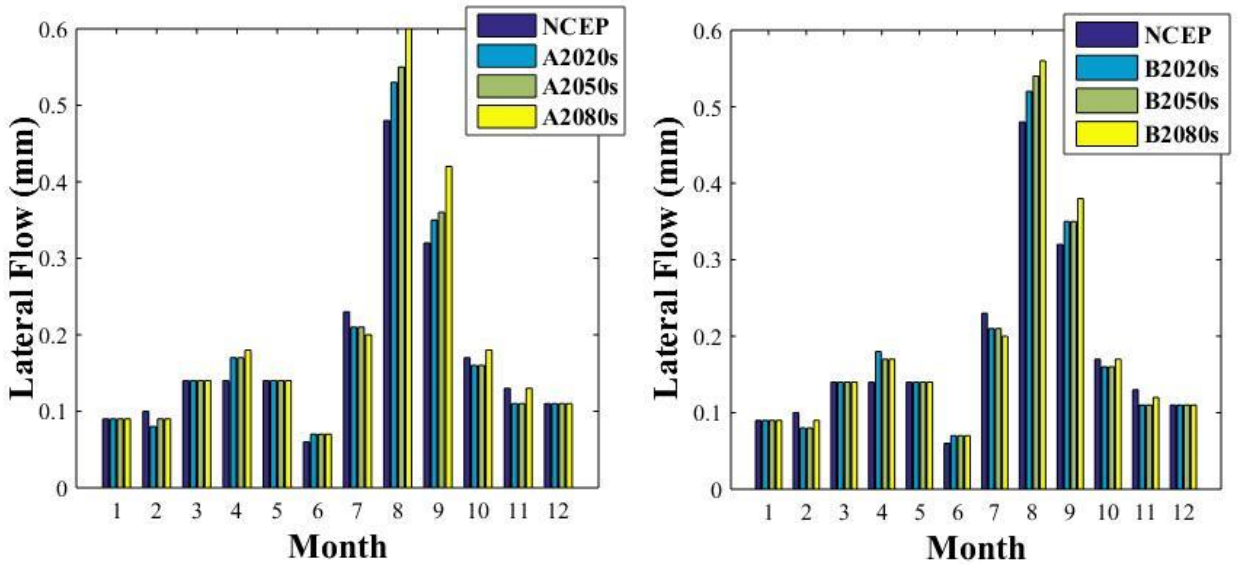

Figure 5.9 Projected lateral flow for A2 and B2 scenarios

5.1.5. Change in Surface Runoff

Mean annual surface runoff projection decreased by 6.85, 7.86 and 7.73% for 2020s, 2050s and 2080s respectively for A2 scenario also for B2 scenario, the model shows decrease by 6.66, 8.25 and 5.29% for 2020s, 2050s and 2080s respectively. The annual surface runoff is expected to 51.64 m^3/s, 51.08 m^3/s and 51.15 m^3/s under A2 scenario in 2020s, 2050s and 2080s respectively while the value estimated to 51.75 m^3/s, 50.86 m^3/s and 52.51 m^3/s in 2020s, 2050s and 2080s respectively under B2 scenario.

Mean monthly change of surface runoff clearly shows the season which may be impacted highly with climate change. The high surface runoff months of July and August impacted highly for both A2 and B2scenario. For the months of July, surface runoff is projected to decrease by 35.12, 26.43 and 34.05% for 2020s, 2050s and 2080s respectively for A2 scenario likewise for B2 scenario, the model shows decrease by 35.12, 26.67 and 34.88% for 2020s, 2050s and 2080s respectively. For the months of August, surface runoff is projected to increase by 20.55, 12.33 and 21.3% for 2020s, 2050s and 2080s respectively for A2 scenario likewise for B2 scenario, the model shows increase by 19.18, 11.46 and 19.18% for 2020s, 2050s and 2080s respectively. Percentage change of low surface runoff season is higher than that of high flow season but the volumetric change as compared to the high flow season is very low.

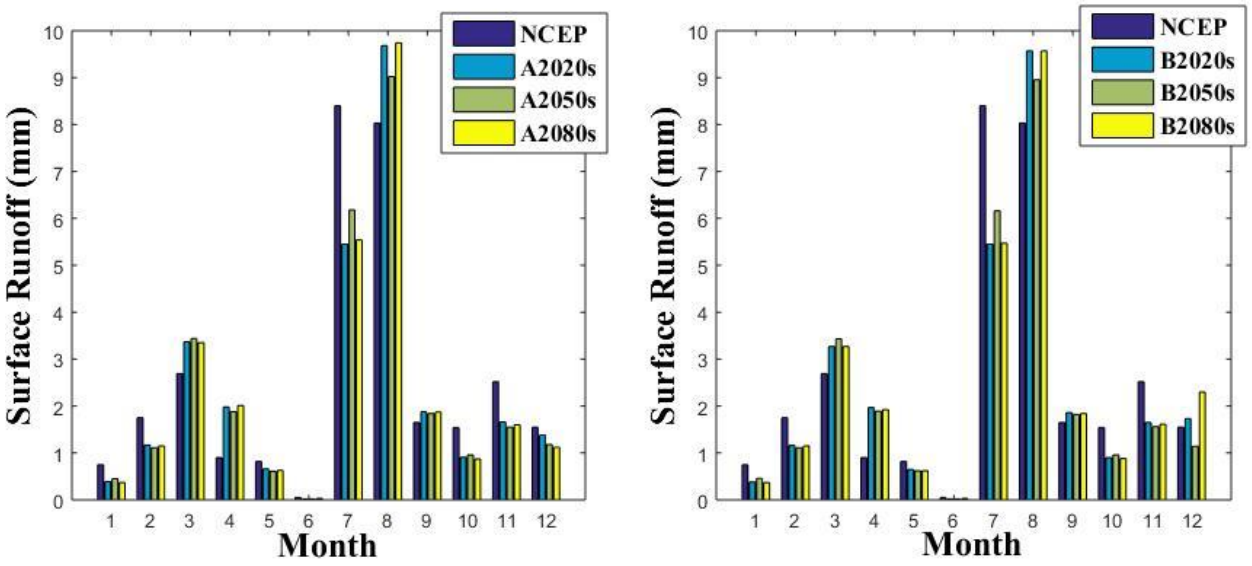

Figure 5.10 Projected surface runoff for A2 and B2 scenarios

There is a decrease percentage change surface runoff throughout the year except in March, April, August and September for the future period under A2 and B2 scenarios.

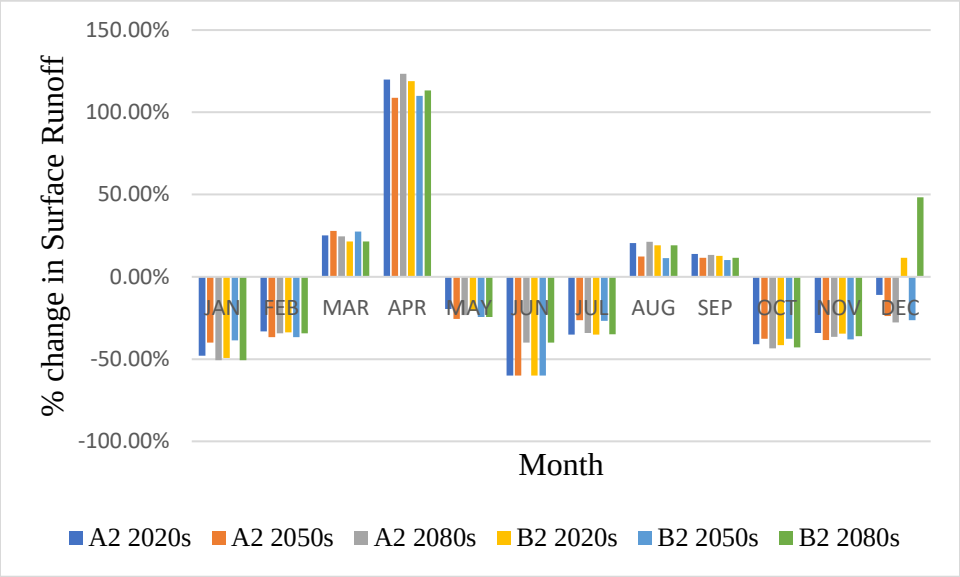

Figure 5.11 Percentage change in surface runoff for A2 and B2 scenarios

5.1.6. Change in Water Yield

The projected annual average water yield decreases by 5.95, 6.72 and 6.36% for 2020s, 2050s and 2080s respectively for A2 scenario likewise for B2 scenario, decrease by 6.09, 7.47 and 6.24% for 2020s, 2050s and 2080s respectively. The annual water yield is expected to 6811.81 Mm^3, 6756.47 $Mm^3$and 6782.14 Mm^3 under A2 scenario in 2020s, 2050s and 2080s respectively while the value estimated to 6802.11 Mm^3, 6701.72 m^3/s and 6791.27 Mm^3in 2020s, 2050s and 2080s respectively under B2 scenario.

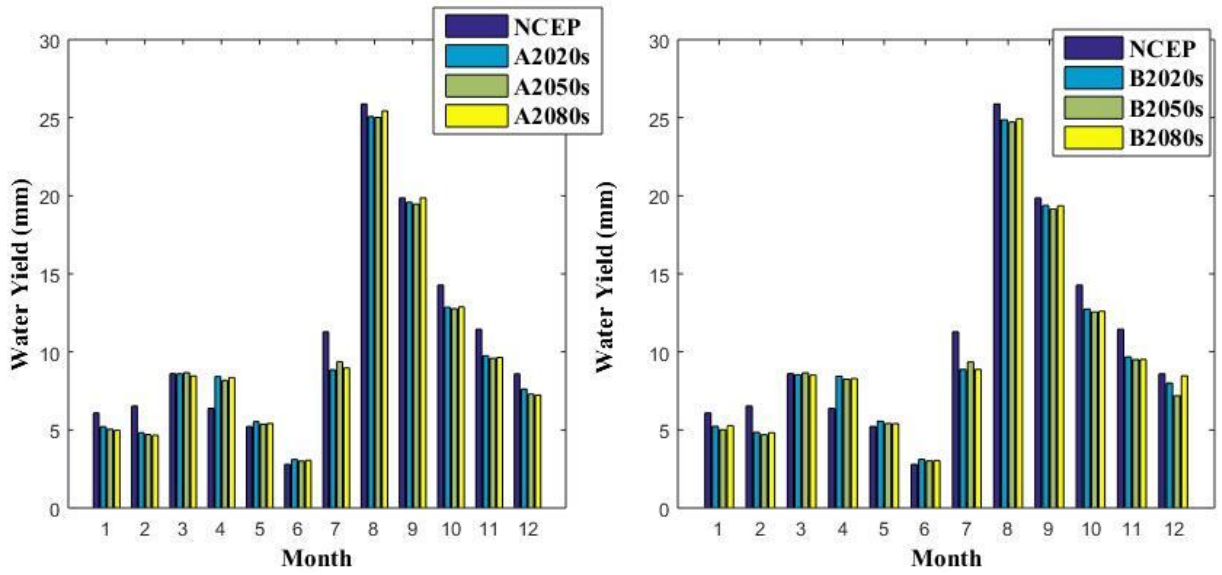

Figure 5.12 Projected water yield for A2 and B2 scenarios

The water yield projection of the main season (June-September) which shows decreasing for the two emission scenarios except for months of June for both A2 and B2 scenarios. Whereas the water yield during the small rainy season (February-May) projection shows increasing for future time period except for the months of February for both A2 and B2 scenarios. The water yield during the dry season (October-January) projection shows decreasing for the two emission scenarios.

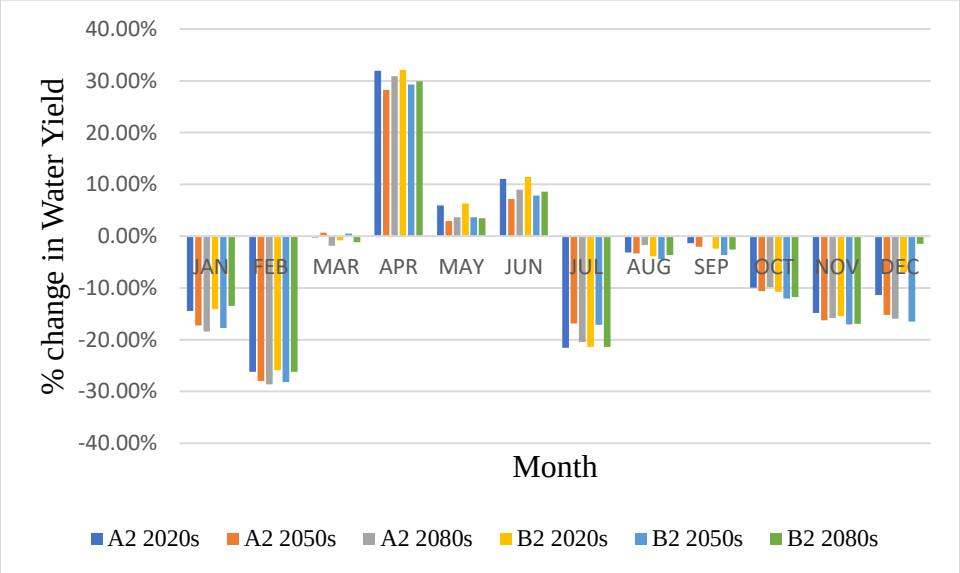

Figure 5.13 Percentage change in water yield for A2 and B2 scenarios

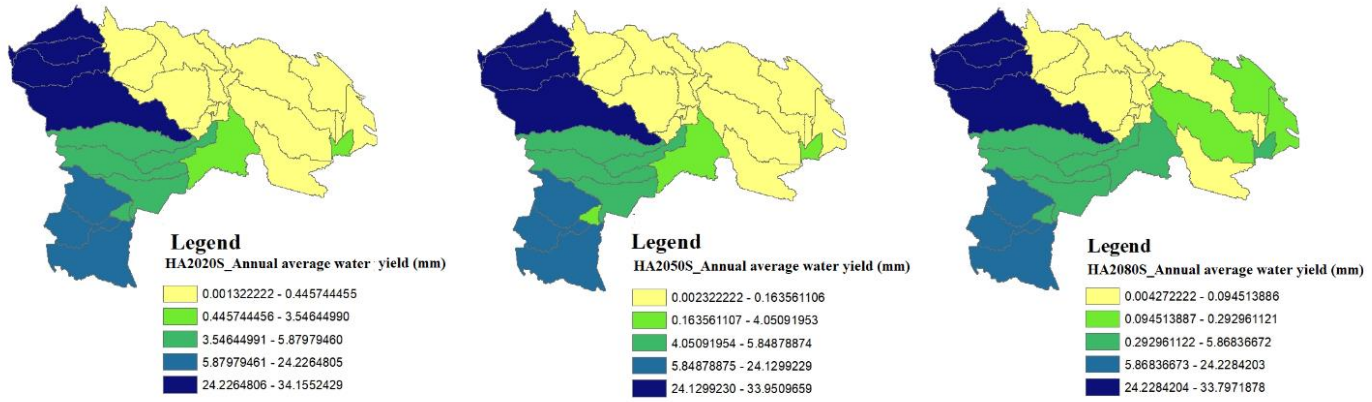

Figure 5.14 Spatial variability of average annual water yield in lower awash basin (mm) for A2 scenarios

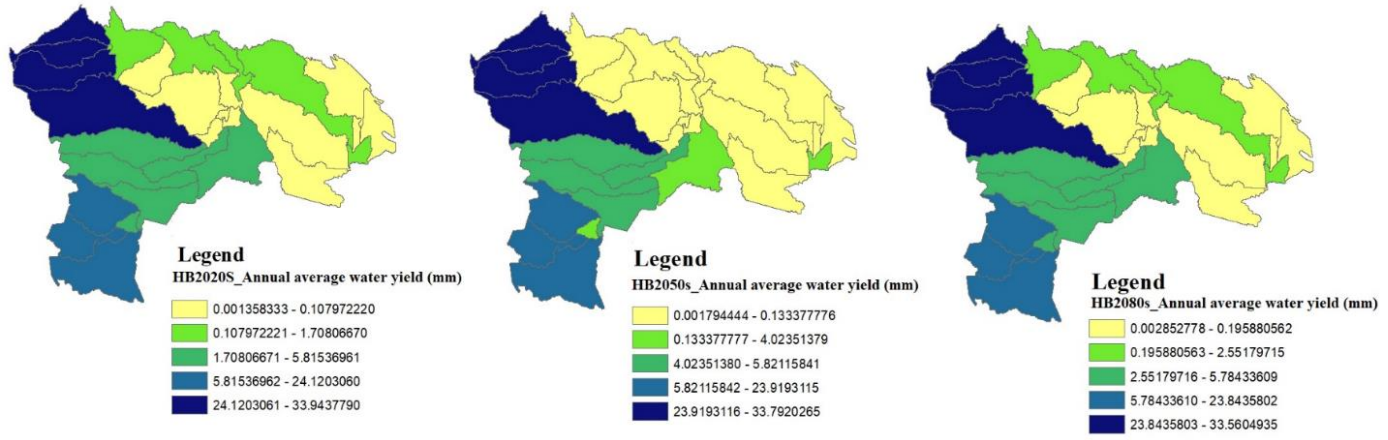

Figure 5.15 Spatial variability of average annual water yield in lower awash basin (mm) for B2 scenarios

CONCLUSION

This thesis research assessed the impact of climate change on hydrology over Lower Awash Sub Basin using downscaled climate projection from GCM product outputs of HadCM3. The Statistical Down Scaling Model (SDSM) was used to downscale the GCM data from A2 and B2 emissions scenarios for future climate predictions. The output generated from the statistical downscale model (precipitation and temperature) were used to derive a hydrological model (Soil and Water Assessment Tool, SWAT). SWAT was calibrated and was used to assess the hydrological response over Lower Awash Sub Basin due to climate change.

The results of downscaled GCM data for baseline period showed a satisfactory agreement between simulation data and observed data for maximum and minimum temperature at all station. However, the downscaled precipitation value at the all stations could not replicate the observed value compared to maximum and minimum temperature. Given the fact that, daily precipitation amounts at individual sites are relatively poorly resolved by regional scale predictions.

The results of downscaled GCM data for future period showed increasing tendency towards the end of century for maximum and minimum temperature value under A2 and B2 scenarios in all stations. Correspondingly, the projection of precipitation showed increasing trend towards end of century at Assaita and Dubti stations and declining rainfall trend observed at Logia stations under A2 and B2 scenarios.

SWAT hydrological model simulation was run for the baseline and three future scenarios (2020s, 2050s, and 2080s) to understand climate change impact on hydrological climate variable by keeping constant calibrated non-climate variables of soil and land use and some climate variables such as windspeed, sunshine hour and relative humidity. The average water balance components of the A2 and B2 scenario for three period time slices 2020s, 2050s and 2080s were compared with the baseline hydrological variable.

The performance of SWAT model in simulating the stream flow was shown to be good with a coefficient of determination (R^2) 0.92 and 0.77 and the Nash and Sutcliffe efficiency (NSE) of 0.88 and 0.75 for calibration and validation periods, respectively.

The projected annual maximum temperature shows to increase by 1.25%, 2.40%, 4.79%, for 2020s, 2050s and 2080s respectively in A2 scenarios and 1.34%, 2.11%, 3.44%, for 2020s, 2050s and 2080s respectively in B2 scenarios. Likewise, the models predict the annual minimum temperature to increase by 1.66%, 3.14%, 5.94%, for 2020s, 2050s and 2080s respectively in A2 scenarios and 1.82%, 2.60%, 4.19%, for 2020s, 2050s and 2080s respectively in B2 scenarios.

The rainfall expected to experience a mean annual increase by 1.69% ,2.34% and 4.45 % by 2020s, 2050s and 2080s respectively for A2 scenario and 1.70%, 1.67%, 3.49%, for 2020s, 2050s and 2080s respectively in B2 scenarios.

The projected annual mean ET increase by 5.10, 6.24 and 9.01% for 2020s, 2050s and 2080s respectively for A2 scenario similarly for B2 scenario, increased by 5.15, 5.72 and 7.71% for 2020s, 2050s and 2080s respectively.

The average annual lateral flow increased by 2.37, 4.27 and 11.37% for 2020s, 2050s and 2080s respectively for A2 scenario similarly for B2 scenario, increased by 2.37, 2.84 and 6.16% for 2020s, 2050s and 2080s respectively.

The average annual water yield decreased by 5.95, 6.72 and 6.36% for 2020s, 2050s and 2080s respectively for A2 scenario also for B2 scenario, decrease by 6.09, 7.47 and 6.24% for 2020s, 2050s and 2080s respectively.

The average annual surface runoff decreased by 6.85, 7.86 and 7.73% for 2020s, 2050s and 2080s respectively for A2 scenario also for B2 scenario, decrease by 6.66, 8.25 and 5.29% for 2020s, 2050s and 2080s respectively.

Increasing temperature decreased the surface runoff, water yield and increased evapotranspiration over the study area. The basin is less sensitive to precipitation as compared to temperature changes. Generally, the projected minimum and maximum temperatures in two scenarios is within the range projected by IPCC which reported average temperature will increase in future. Correspondingly the projected precipitation in two scenarios support by IPCC, which reported there will likely be more heavy rainfall over the east Africa with high certainty.

RECOMMENDATION

This study used various models and model outputs where each influenced a certain level of uncertainty. The SDSM downscaled due to the uncertainty assumption of predictor-predictand relationship under the current condition remain valid for future climate condition which might not be true all the time. The hydrological modeling approached due to the uncertainty assumptions that the climate variables such as windspeed, sunshine hour and relative humidity and non-climatic variables land use /land cover remain constant for future which also might not be true. Meanwhile, this study should be extended by considering changes in climatic and non-climatic variables and continuing studies should also consider the wide range of uncertainties associated with models and trying different GCM outputs, downscaling techniques and emission scenarios.

In this study, the result from SDSM on the application of GCM (HadCM3) reveals the uncertainties due to the downscaling method. For precipitation, the result shows significant difference where the GCM are not reliable in simulating precipitation at the local-scale. The result not well represented by the relationship used in the local-large scale model's predictors. For temperature, the downscaling shows the same trend. Hence, given such source of uncertainties the further use of the downscaled outputs in hydrological models needs to be handled with carefulness.

The lower awash sub basin in afar region is vulnerable and strongly impacted by climate change. The lack of precipitation and high temperature is the primary cause of a drought for this study area. A lack of precipitation results in water shortages for some activity such as fodder production for pastoralists in this study area. To mitigate the dire consequences of such extreme events, adaptation strategies should be designed. Agricultural water management such as soil and water conservation, run-off diversion and spreading, using various irrigation technologies, soil management and fertility improvement in both rain fed and irrigated agriculture are amongst the adaptation initiatives. The author recommends, further studies on vulnerability and adaptation using the result of this study.

REFERENCES

Abbaspour, K. C. (2015). *SWAT-CUP: SWAT Caliberation and Uncertainity Programs-A User Manual.* Swiss: Eawag aquatic research.

Abera, F. (2011). *Assessment of Climate Change Impact on the Hydrology of Upper Guder Catchment, Upper Blue Nile. Msc. Thesis.* Addis Ababa: Addis Ababa Institute of Technology.

Adem et al. (2016). Climate Change Impact on Stream Flow in the Upper Gilgel Abay Catchment, Blue Nile Basin, Ethiopia. *Springer International Publishing, Switzerland*, pp 645-673. DOI 10.1007/978-3-319-18787-7_29.

ADSWE, A. D. (2012). *Afar National Regional State, Lower Awash Sub-basin Integrated Land Use Planning and Environmental Impact Study Project;Technical Report: Hydrology and Water Resource Study (Afar LUPESP/LASB: V/2012).* Bahir Dar.

Akker, E. v. (2015). Reversing Natural Degradation into Resilience: The Afar Case. *Conference on International Research on Food Security, Natural Resource Management and Rural Development.* Berlin, Germany: Humboldt-Universität zu Berlin and the Leibniz Centre for Agricultural Landscape Research (ZALF).

Alemu, A. (2011). *Evaluation of Climate Change Impact on Extreme Hydrological Event, Case Study: Addis Ababa and Surrounding Catchment. Msc. Thesis.* Addis Ababa: Addis Ababa Institute of Technology .

Amorim, P. B. (2014). *Development of Regional Climate Change Projections For Hydrological Impact Asessments In Distrito Federal, Brazil. MSc. Thesis.* Dresden: Technische Universitat Dresden.

ARCC. (2014). *A Review of Downscaling Methods for Climate Change Projections.* Burligton, Vermont: Tetra Tech ARD.

Balcha, B. G. (2001). Environmental Degradation and Conflict in Borkena Area. *International Conference on African Development Archives*, paper 51.

Belete Berhanu, S. A. (2013). *Part 3: Hydro-Metrological Trend Analysis, Coping with the Water Scarcity -The Role of Agriculture Developing a National water Audit for Awash Basin (Ethiopia).* Addis Ababa: Ministry of Water and Energy.

Berhane, F. G. (2011). *Model Based Assessment of Potential Impact of Climate Change on The Flow of The Main Headwaters of The Nile River: Equatorial Lakes Region and Blue Nile Basins. MSc. Thesis.* University of Connecticut Graduate School.

Bjornaes, C. (2014). *A Guide to Representative Concentration Pathways.* Oslo: CICERO Center fior.

Carter, T. (2007). *General Guidelines on the Use of Scenario Data for Climate Impact and Adaptation Assessment.* Helsinki, Finland: Finnish Environmental Institute.

Choux, M. (2005). *Delopment of New Predictor Climate Variables For Statistical Downscaling of Daily Precipitiation Process. MSc. Thesis.* Monetreal, Canada: McGill University.

Fasil et al. (2001). *Traditional Coping Strategies of the Afar and Borana Pastoralists in Response to Drought.* Dry lands Coordination Group Report No. 17.

Gautam, B. (2012). *Modelling Stream Flow From Forested Watersheds on The Canadian Boreal Shield Using The Soil and Water Assessment Tool (SWAT).* Saskatoon: Masters Thesis,University of Saskatchewan.

Hailemariam, K. (1999). Impact of climate cahnge on the water resources of Awash River Basin, Ethiopia. *Climate Research*, Vol. 12:91-96.

Hare, F. (1983). Climate and desertification. pp5-20.revised analysis (WMO-UNDP) WCP-44.

IPCC. (2007). *General Guidelines on The Use of Scenario Data For Climate Impact and Adaptation Assessment. Version 2.* Prepared by T.R. Carter on behaif of the Intergovernmental Panel Climate Change,Task Group on Data and Scenario Support for Impact and Climate Assessment.

Kabiri, R. (2014). *Assessment of Climate Change Impact on Runoff and Peak Flow: A Case Study on Klang Watershed in West Malaysia. PhD Thesis.* University of Nottingham.

Kevin, M. (2012). *Assessment of Climate Change Impacts on Stream Flow Trending Using A Water Balance Model.* Florida: Florida Atlantic University.

Matthews, K. (2012). *Assessment of Climate Change Impacts on Stream Flow Trending Using A Water Balance Model.* Florida: Florida Atlantic University.

NAPA. (2007). *Climate Change National Adaptation Programme of Action (NAPA) of Ethiopia.* Addis Ababa: Ethiopia National Metrological Agency.

Neitsch et al. (2005). *Soil and water wssesmmnt tool input/output file documentation.* Temple,Texas: Blackland Researc Center, USDA Agriculture Research Service.

Pharasi, S. (2006). *Development of Statistical Downscaling Methods For The Daily Precipitation Process at A Local Site. MSc. Thesis.* Monetreal, Canada: McGill University.

Reza, K. (2014). *Assessment of Climate Chnage Impact on Runoff and Peak Flow-A Case Study on Klang Watershed in west Malaysia.* United Kingdom: University of Nottingham.

Sawyer, L. M. (2010). *Comparison of a watershed model (SWAT) and a groundwater flow model (GFLOW) to simulate the hydrology of two agricultural watersheds in Iowa.* Iowa: Iowa State University.

SDR-ASAL. (2014). *Capacity development for strengthening the drought resilience of the pastoral and agro-pastoral population in the lowlands of Ethiopia.* Addis Ababa, Ethiopia: Afar GIZ SDR ASAL program.

Tessema, S. M. (2011). *Hydrological modeling as a tool for sustainable water resources management: a case study of the Awash River basin.* Sweden: TRITA LWR.LIC 2056.

Wilby & Dawson. (2007). *Statistical DownScaling Model SDSM, Virsion 4.2 User Manual.* UK.

ANNEXES

Appendix A: SDSM Model Calibration Generated Parameter Files

[1] The number of predictors

[2] The season code (12 = months, 4 = seasons, 1 = annual model)

[3] The year length indicator (366, 365, or 360)

[4] Record start date

[5] Record length (days)

[6] Model fitting start date

[7] Number of days used in the model fitting

[8] Whether the model is conditional (true) or unconditional (false)

[9] Transformation (1 = none, 2 = fourth root, 3 = natural log, 4 = log normal)

[10] Ensemble size

[11] Auto regression indicator (True or false)

[12] Predictand file name

[13-18] predictor files

[19-30] Model Parameters; the first six columns are the parameters (including the intercept), the last two Columns are the SE and r2 statics

[31] The root directory of the predictand file

1. Precipitation

3
12
366
01/01/1983
6940
01/01/1983
6940
#TRUE#
2
1
False
Dubity_PCP_1_1_1983-03_28_2015.dat
ncepp__zaf.dat
ncepp5_faf.dat
ncepp5_uaf.dat

0.044	-0.011	0.010	-0.015	0.000	0.012	
-0.028	0.049	-0.022	0.025	0.000	0.023	
0.078	-0.005	-0.020	-0.003	0.000	0.004	
0.068	0.034	0.014	0.002	0.000	0.010	
0.049	-0.004	0.014	0.012	0.000	0.002	
0.016	-0.002	0.000	-0.003	0.000	0.000	
0.067	-0.043	0.013	-0.006	0.000	0.006	
0.078	-0.128	0.074	0.111	0.000	0.020	
0.019	-0.044	-0.011	-0.023	0.000	0.004	
0.019	-0.013	0.004	-0.009	0.000	0.006	
-0.003	0.013	0.000	0.001	0.000	0.006	
0.008	-0.002	-0.005	-0.001	0.000	0.003	
1.488	1.000	0.051	-0.693	0.202	0.324	0.561
1.255	1.000	0.125	0.101	0.097	0.490	0.057
1.606	1.000	-0.045	0.099	0.161	0.495	0.093
1.674	1.000	0.009	0.050	0.042	0.622	0.007
1.417	1.000	-0.038	0.048	0.085	0.407	0.032
1.797	1.000	0.262	0.516	0.809	0.227	0.284
1.573	1.000	0.057	-0.094	-0.068	0.477	0.019
1.390	1.000	0.160	-0.346	-0.662	0.424	0.084
0.808	1.000	-0.142	-0.583	-1.113	0.347	0.174
1.261	1.000	-0.394	-0.258	-0.501	0.501	0.080
7.506	1.000	-0.094	5.475	0.697	4.902	0.966
2.137	1.000	-0.702	0.406	-0.137	0.006	1.000

C:\Users\Babi\Desktop\SDSM_pcp\Dubity_PCP_observed\Dubity_PCP_1_1_1983-03_28_2015.dat

2. Maximum Temperature File

9
12
360
01/01/1983
6940
01/01/1983
6940
#FALSE#
1
1
False
Dubity_TempMax_1_1_1983-03_31_2015.dat
ncepmslpaf.dat
ncepp__zaf.dat
ncepp500af.dat
ncepp5thaf.dat
ncepp8_vaf.dat
ncepp8zhaf.dat
ncepr500af.dat
ncepshumaf.dat
nceptempaf.dat
35.904 -0.512 -1.996 0.076 0.002 -0.031 -0.389 -0.258 0.992 0.070 2.411 0.180
35.990 -0.774 -1.685 0.281 0.000 0.567 -0.071 -0.209 1.229 -0.161 2.373 0.201
35.054 -1.015 -1.219 0.141 -0.001 0.892 0.554 0.036 0.585 0.193 2.499 0.273
34.917 -0.937 -0.736 0.521 0.002 3.875 3.867 0.307 0.804 0.373 2.664 0.316
37.150 0.083 -1.739 0.086 -0.001 0.092 0.478 0.069 0.232 0.935 2.407 0.214
37.638 0.528 -0.717 -0.205 0.002 -1.693 -0.713 -0.154 0.733 0.932 2.415 0.148
38.726 1.280 -0.784 -0.792 0.003 0.915 1.800 -0.180 -0.190 1.270 2.360 0.153
40.429 1.057 -0.469 -0.878 0.000 -1.215 -1.375 -0.392 0.859 1.673 2.542 0.138
39.009 0.679 -1.834 -1.245 0.005 -0.584 -0.414 -0.530 -0.326 3.277 2.655 0.211
40.352 -0.550 -1.286 0.063 0.000 0.017 -0.210 0.462 -0.870 2.156 2.857 0.091
37.070 -0.692 -0.413 0.111 0.000 1.482 1.408 0.758 0.559 -0.719 2.368 0.271
36.787 -0.728 -1.311 0.221 -0.002 0.261 0.099 -0.201 2.122 -1.279 1.888 0.575
G:\SDSM DATA\11x_30y\Dubti \Dubti_TempMax_1_1_1983-03_31_2015.dat

3. Minimum Temperature File

4

12

360

12/11/1987

5135

12/11/1987

5135

#FALSE#

1

1

False

Dubity_TempMin_12_11_87-03_31_2015.dat

ncepp__zaf.dat

ncepp5thaf.dat

ncepp8_uaf.dat

ncepshumaf.dat

21.037	-0.381	-0.007	0.216	-0.303	3.335	0.014
20.372	-1.231	0.002	-0.451	0.268	3.403	0.003
19.884	0.803	0.001	0.507	0.689	3.613	0.011
22.026	-0.385	0.002	0.088	0.399	3.389	0.054
24.178	-0.533	-0.001	0.246	-0.774	2.451	0.034
24.174	0.178	0.001	0.137	1.091	2.230	0.139
25.126	-0.846	0.000	-0.154	0.258	2.091	0.062
25.280	-0.193	0.001	0.450	-0.005	2.095	0.025
24.416	0.015	-0.001	0.348	1.752	2.050	0.065
22.858	-1.686	0.004	-0.019	-0.471	2.145	0.115
22.634	-2.988	0.001	-0.786	0.603	2.970	0.262
21.569	-3.160	0.004	-0.702	-0.594	3.334	0.183

G:\SDSM DATA\11x_30y\Dubti \Dubti_TempMin_12_11_87-03_31_2015.dat

Appendix B: Water Balance Components on Annual Average Basis Over the Lower Awash Sub Basin.

B.1: Water balance components for Baseline

Month	Rain(mm)	Surface Runoff Q(mm)	Lateral Flow Q(mm)	Water Yield (mm)	ET (mm)	PET(mm)
1	15.4	0.75	0.09	6.09	10.88	129.26
2	19.86	1.75	0.1	6.53	13.58	132.14
3	40.27	2.69	0.14	8.61	40.13	169.47
4	38.32	0.9	0.14	6.38	42.46	206.6
5	26.41	0.82	0.14	5.22	27.68	221.43
6	8.32	0.05	0.06	2.8	9.03	211.45
7	100.42	8.4	0.23	11.28	46.25	206.59
8	103.61	8.03	0.48	25.88	60.34	198.54
9	41.22	1.65	0.32	19.86	38.37	191.07
10	20.72	1.54	0.17	14.28	20.06	174.19
11	13.35	2.52	0.13	11.45	11.13	144.74
12	14.6	1.55	0.11	8.6	9.49	137.28

B.2: Water balance components for A2_2020s

Month	Rain(mm)	Surface Runoff Q(mm)	Lateral Flow Q(mm)	Water Yield (mm)	ET (mm)	PET(mm)
1	13.38	0.39	0.09	5.21	12.8	154.07
2	18.18	1.17	0.08	4.82	12.64	121.88
3	42.37	3.37	0.14	8.59	37.83	165.41
4	44.96	1.98	0.17	8.42	47.77	211.69
5	26.2	0.66	0.14	5.53	30.2	243.1
6	8.54	0.02	0.07	3.11	10.3	220.13
7	85.96	5.45	0.21	8.85	42.92	219.4
8	116.97	9.68	0.53	25.07	64.85	211.9
9	44.44	1.88	0.35	19.59	44.28	222.5
10	17.09	0.91	0.16	12.86	20.73	235.51
11	12.81	1.66	0.11	9.75	9.9	177.74
12	19.07	1.38	0.11	7.62	11.97	151.32

B.3: Water balance components for A2_2050s

Month	Rain(mm)	Surface Runoff Q(mm)	Lateral Flow Q(mm)	Water Yield (mm)	ET (mm)	PET(mm)
1	13.8	0.45	0.09	5.04	13.51	162.57
2	18.56	1.11	0.09	4.7	12.64	109.38
3	42.7	3.44	0.14	8.67	39.31	180.54
4	45.23	1.88	0.17	8.18	48.12	215.83
5	25.28	0.61	0.14	5.37	29.46	250.28
6	9.1	0.02	0.07	3	9.93	216.07
7	86.73	6.18	0.21	9.38	42.2	220.92
8	118.87	9.02	0.55	25.01	66.9	212.33
9	43.94	1.84	0.36	19.46	44.67	226.18
10	17.15	0.96	0.16	12.76	21.18	250.19
11	12.65	1.55	0.11	9.59	10.6	202.92
12	18.84	1.18	0.11	7.29	11.44	144.59

B.3: Water balance components for A2_2080s

Month	Rain(mm)	Surface Runoff Q(mm)	Lateral Flow Q(mm)	Water Yield (mm)	ET (mm)	PET(mm)
1	13.72	0.37	0.09	4.97	14.59	180.39
2	19.44	1.15	0.09	4.66	12.57	103.18
3	41.79	3.35	0.14	8.45	38.52	196.15
4	45.59	2.01	0.18	8.35	48.64	222.91
5	24.85	0.63	0.14	5.41	29.45	277.04
6	8.23	0.03	0.07	3.05	9.29	212.93
7	82.56	5.54	0.2	8.97	40.48	230.52
8	127.96	9.74	0.6	25.43	70.04	212.52
9	47.56	1.87	0.42	19.86	48.02	234.39
10	17	0.87	0.18	12.88	23.37	271.97
11	14.64	1.6	0.13	9.64	12.42	218.81
12	18.83	1.12	0.11	7.23	11.69	137.82

B.3: Water balance components for B2_2020s

Month	Rain(mm)	Surface Runoff Q(mm)	Lateral Flow Q(mm)	Water Yield (mm)	ET (mm)	PET(mm)
1	13.39	0.38	0.09	5.23	12.93	152.84
2	17.75	1.16	0.08	4.84	12.28	120.44
3	42.62	3.27	0.14	8.54	38.34	166.04
4	44.98	1.97	0.18	8.43	47.76	210.37
5	26.35	0.65	0.14	5.55	30.36	242.49
6	8.61	0.02	0.07	3.12	10.36	221.68
7	85.6	5.45	0.21	8.87	42.68	217.61
8	116.86	9.57	0.52	24.87	65.57	217.42
9	43.53	1.86	0.35	19.38	43.25	221.88
10	16.52	0.9	0.16	12.74	20.26	239.38
11	13.13	1.65	0.11	9.68	10.15	182.83
12	20.7	1.73	0.11	8	12.41	150.86

B.3: Water balance components for B2_2050s

Month	Rain(mm)	Surface Runoff Q(mm)	Lateral Flow Q(mm)	Water Yield (mm)	ET (mm)	PET(mm)
1	13.76	0.46	0.09	5.01	13.23	156.54
2	18.39	1.11	0.08	4.69	12.55	114.14
3	42.39	3.43	0.14	8.65	38.29	175.34
4	45.25	1.89	0.17	8.25	48.35	216.65
5	25.34	0.62	0.14	5.41	29.36	249.94
6	8.97	0.02	0.07	3.02	9.91	214.01
7	87.23	6.16	0.21	9.35	42.76	220.26
8	116.81	8.95	0.54	24.73	66.57	218.95
9	43.51	1.82	0.35	19.14	44.35	227.38
10	17.16	0.96	0.16	12.56	20.8	251.31
11	12.99	1.56	0.11	9.5	10.64	191.79
12	18.11	1.14	0.11	7.18	11.42	145.11

B.3: Water balance components for B2_2080s

Month	Rain(mm)	Surface Runoff Q(mm)	Lateral Flow Q(mm)	Water Yield (mm)	ET (mm)	PET(mm)
1	13.43	0.37	0.09	5.27	14.04	164.88
2	18.84	1.15	0.09	4.82	12.58	109.54
3	42.25	3.27	0.14	8.51	38.81	183.41
4	44.82	1.92	0.17	8.29	48.16	219.12
5	25.28	0.62	0.14	5.4	29.66	263.42
6	8.37	0.03	0.07	3.04	9.53	213.25
7	83.31	5.47	0.2	8.87	40.9	226.62
8	123.24	9.57	0.56	24.93	69.26	219.95
9	45.85	1.84	0.38	19.35	46.76	235.12
10	16.66	0.88	0.17	12.6	21.9	263.82
11	13.8	1.61	0.12	9.51	11.27	210.34
12	22.08	2.3	0.11	8.47	11.93	141.05